

ESD-TR-81-100

12

AD A113936

**DEPARTMENT OF DEFENSE  
Electromagnetic Compatibility Analysis Center  
Annapolis, Maryland 21402**

**A SIMPLIFIED METHOD FOR CALCULATING THE BOUNDS  
ON THE EMISSION SPECTRA OF CHIRP RADARS  
(REVISED EDITION)**

Prepared for

DEPARTMENT OF DEFENSE  
Electromagnetic Compatibility Analysis Center  
Annapolis, Maryland 21402



AUGUST 1982

FINAL REPORT

Prepared by

Paul D. Newhouse

**IIT Research Institute  
Under Contract to  
Department of Defense**

**DTIC  
ELECTE  
SEP 7 1982  
S D D**

DTIC FILE COPY

Approved for public release; distribution unlimited.

ESD-TR-81-100

This report was prepared by the IIT Research Institute under Contract F-19628-80-C-0042 with the Electronic Systems Division of the Air Force Systems Command in support of the DoD Electromagnetic Compatibility Analysis Center, Annapolis, Maryland.

Reviewed by:

*Paul D. Newhouse*

PAUL D. NEWHOUSE  
Scientific Advisor, IITRI

*Alan W. Cook*  
for

JAMES H. COOK  
Assistant Director  
Contractor Operations

Approved by:

*Charles L. Flinn*  
for

CHARLES L. FLINN  
Colonel, USAF  
Director

*A. M. Messer*

A. M. MESSER  
Chief, Plans & Resources  
Management

ELECTROMAGNETIC COMPATIBILITY ANALYSIS CENTER  
North Severn, Annapolis, Maryland 21402



REPLY TO  
ATTN OF:

XM-924 (J. R. Janoski)

27 AUG 1982

SUBJECT:

Forwarding of ESD-TR-81-100, "A Simplified Method for Calculating the Bounds of the Emission Spectra of Chirp Radars (Revised Edition)", by Paul Newhouse

TO:

DISTRIBUTION

1. Calculation of emission spectra is one of the steps in making electromagnetic compatibility (EMC) analyses of radar systems. For ordinary radars, the calculation is easy to accomplish, but in the case of chirp radars, it is difficult if the conventional equation for describing the spectra of linear frequency-modulated (LFM) pulses is used. The conventional equation involves Fresnel integrals and requires that a large number of high-precision computations be performed. In doing an EMC analysis, an upper bound on the spectrum rather than the spectrum itself is used. It is the purpose of this technical report to provide EMC analysts with simple equations and procedures for calculating the approximate bounds on the spectra of LFM pulses. This revised edition presents in greater detail the derivations of the equations and included an additional section consisting of numerical examples that illustrate the application of the procedures.

\* 2. This report supercedes ESD-TR-70-273 published in 1971, the title and author of the previous report are the same as above.

3. Any questions on this document should be addressed to Miss Jacqueline R. Janoski, AUTOVON 281-2354, Commercial 301-267-2354, FTS 930-2354.

*A. M. Messer*  
A. M. MESSER

Chief, Plans & Resource Mgt.



## EXECUTIVE SUMMARY

Simple equations and procedures were developed that permit rapid hand-calculation and plotting of approximations of strong upper bounds on the spectra of linear frequency-modulated RF pulses that have a trapezoidal envelope.<sup>a</sup> The plots of the approximate bounds consist of segments of straight lines on semilogarithmic graph paper, and are very easy to draw.

The approach used in deriving the model involved the use of an asymptotic expansion instead of the usual Fresnel integrals to describe the skirts of the voltage-density spectrum.

The approximate bounds are within about 1 dB of the spectrum determined using the Fresnel integrals at the center of the central lobe and within a fraction of a dB at the centers of the minor lobes that occur at frequencies well above and below the central lobe. The approximation is the least accurate in a relatively narrow frequency interval at the edges of the central lobe, where it may underestimate the spectrum by about 5-10 dB.

Accession For	
NTIS GRA&I	<input checked="" type="checkbox"/>
DTIC TAB	<input type="checkbox"/>
Unannounced	<input type="checkbox"/>
Justification	
By _____	
Distribution/ _____	
Availability Codes	
Dist	Avail and/or Special
A	



<sup>a</sup>An upper bound, in this application, is defined as a function that is never less than the actual spectrum. A strong bound is close to the spectrum at various points. See Figure 6 on page 12.

PREFACE

The Electromagnetic Compatibility Analysis Center (ECAC) is a Department of Defense facility, established to provide advice and assistance on electromagnetic compatibility matters to the Secretary of Defense, the Joint Chiefs of Staff, the military departments and other DoD components. The center, located at North Severn, Annapolis, Maryland 21402, is under the policy control of the Assistant Secretary of Defense for Communications, Command, Control, and Intelligence and the Chairman, Joint Chiefs of Staff, or their designees, who jointly provide policy guidance, assign projects, and establish priorities. ECAC functions under the executive direction of the Secretary of the Air Force and the management and technical direction of the Center are provided by military and civil service personnel. The technical support function is provided through an Air Force-sponsored contract with the IIT Research Institute (IITRI).

To the extent possible, all abbreviations and symbols used in this report are taken from American National Standard ANSI Y10.19 (1969) "Letter Symbols for Units Used in Science and Technology" issued by the American National Standards Institute, Inc.

Users of this report are invited to submit comments that would be useful in revising or adding to this material to the Director, ECAC, North Severn, Annapolis, Maryland 21402, Attention: XM.

## TABLE OF CONTENTS

<u>Subsection</u>	<u>Page</u>
SECTION 1	
INTRODUCTION	
BACKGROUND.....	1
OBJECTIVE.....	1
APPROACH.....	2
SECTION 2	
DEVELOPMENT OF EQUATIONS AND PROCEDURES	3
SECTION 3	
DESCRIPTION OF PARAMETERS AND APPLICATION OF MODEL	
PULSE PARAMETERS USED IN THE MODEL.....	5
EFFECT OF PARAMETERS ON SHAPE OF SPECTRUM.....	7
Pulse Without Frequency Modulation (FM).....	7
Pulse with FM.....	8
PROCEDURE FOR PLOTTING THE BOUNDS OF THE SPECTRUM.....	9
Calculation of Bounds on Ordinary Radar Emission Spectrum.....	10
Calculation of Bounds on Chirp (LFM) Spectrum.....	16
Spectrum Bounds.....	21
Sample Calculations of Radar Emission Spectrum Bounds.....	22
Fit of the Approximate Bounds to the Spectrum.....	28
SECTION 4	
DERIVATION OF THE MODEL	
APPROACH TO DEVELOPING THE MODEL.....	29
DESCRIPTION OF THE CHIRP SIGNAL.....	29
VOLTAGE-DENSITY SPECTRUM.....	33

## TABLE OF CONTENTS (Continued)

<u>Subsection</u>	<u>Page</u>
SECTION 4 (Continued)	
BOUNDS ON THE VOLTAGE-DENSITY SPECTRUM.....	36
BOUNDS ON IN-BAND REGION OF SPECTRUM.....	37
BOUNDS ON THE SKIRTS OF THE SPECTRUM.....	39
For the Case When $\beta < 1/\pi\delta$ .....	40
For the Case When $\beta > 1/\pi\delta$ .....	43
BOUNDS ON ENERGY-DENSITY SPECTRUM.....	45
RELATIVE ENERGY DENSITY.....	47
METHOD FOR HANDLING NEGATIVE DEVIATION.....	48
DISPLACEMENT BETWEEN $f_o$ AND $f_c$ .....	53

## SECTION 5

NUMERICAL EXAMPLES OF THE BOUNDS ON CHIRP SPECTRA	57
---	----

## LIST OF ILLUSTRATIONS

<u>Figure</u>	<u>Page</u>
1 Parameters used to describe a chirp pulse.....	6
2 Bounds on spectrum of a trapezoidal pulse without FM.....	7
3 Bounds on spectrum of chirp pulse when $\delta_r = \delta_f$ .....	8
4 Bounds on spectrum of chirp pulse when $\delta_r < \delta_f$ and frequency deviation is positive.....	9
5 Idealized radar pulse (nonchirp).....	11
6 Ordinary radar pulse (nonchirp).....	12
7 Spectrum bounds for ordinary radar pulse (trapezoidal).....	13
8 Spectrum bounds for chirp radar pulse.....	18
9 The bounds on an ordinary radar pulse, Example 1.....	24
10 Bounds on the normalized energy-density spectrum of the chirp pulse in Example 2.....	27

## TABLE OF CONTENTS (Continued)

<u>Figure</u>		<u>Page</u>
LIST OF ILLUSTRATIONS (Continued)		
11	The simple expression derived for the spectral voltage-density function provides a very accurate approximation for points $a_-$ and $a_+$ (which are 6-dB down) and the portion of the function represented by the solid curve.....	30
12	Parameters describing a chirp pulse.....	31
13	The voltage-density spectrum $ F(\Delta f) $ and its bound $\hat{F}(\Delta f)$ . ...	37
14	The curves that approximate the bounds on the voltage-density spectrum, $\hat{F}(\Delta f)$ , when $\beta < 1/\pi\delta$ . ....	42
15	The curves that approximate the bounds on the voltage-density spectrum, $\hat{F}(\Delta f)$ , when $\beta > 1/\pi\delta$ . ....	46
16	The curves that approximately bound the energy-density spectrum, $\epsilon(\Delta f)$ , when $\beta\delta < 1/\pi$ .....	49
17	The curves that approximately bound the energy-density spectrum, $\epsilon(\Delta f)$ , when $\beta > 1/\pi\delta$ . ....	51
18	Relationship between $f_o$ and $f_c$ .....	55
19	A graph of the spectral bounds for Example 1.....	59
20	A graph of the spectral bounds for Example 2.....	60
21	A graph of the spectral bounds for Example 3.....	61
22	A graph of the spectral bounds for Example 4.....	62
23	A graph of the spectral bounds for Example 5.....	63
24	A graph of the spectral bounds for Example 6.....	64
25	A graph of the spectral bounds for Example 7.....	65
26	Graphs of the relative energy density function (solid line) and the bounds (dashed line) for Example 7; note that the frequency scale is linear.....	66
27	Expanded plots of the relative energy density function (solid line) and the bounds (dashed line) for Example 7....	67

## TABLE OF CONTENTS (Continued)

<u>Table</u>		<u>Page</u>
1	VALUES ASSIGNED TO M, N, AND Q.....	16
2	TABULATION OF THE GIVEN AND CALCULATED PARAMETER VALUES FOR THE EXAMPLES.....	58

## LIST OF APPENDIXES

APPENDIX

A	TREATMENT OF NEGATIVE FREQUENCIES.....	69
B	DERIVATION OF VOLTAGE-DENSITY FUNCTION.....	75
C	EXPRESSING THE COMPLEX FRESNEL INTEGRAL AS AN ASYMPTOTIC EXPANSION.....	81
D	APPROXIMATIONS OF $F(\Delta f)$ AND $E(\Delta f)$ USING ASYMPTOTIC EXPANSIONS.....	85
E	$F(\Delta f)$ FOR SKIRTS OF SPECTRUM.....	97
F	BOUNDS ON SKIRTS OF SPECTRUM WHEN $\beta < \frac{1}{\pi\delta}$ AND $\delta = \delta_r = \delta_f$ $< t_b, t_r \approx t_1 \approx t_2, t_f \approx t_3 \approx t_4$ .....	103
G	BOUNDS ON SKIRTS OF SPECTRUM WHEN $\beta > \frac{1}{\pi\delta}$ .....	109
H	CHOOSING A LOCATION FOR THE ORIGIN ON THE TIME SCALE.....	117
I	DISPLACEMENT BETWEEN $f_o$ AND $f_c$ .....	121

SECTION 1  
INTRODUCTION

BACKGROUND

Calculation of emission spectra is one of the steps in making electromagnetic compatibility (EMC) analyses of radar systems. For ordinary radars, the calculation is easy to accomplish, but in the case of chirp radars, it is difficult if the conventional equation for describing the spectra of linear frequency-modulated (LFM) pulses is used. The conventional equation involves Fresnel integrals and requires that a large number of high-precision computations be performed.

In making an EMC analysis, an upper bound on the spectrum rather than the spectrum itself is used. It is the purpose of this technical report to provide EMC analysts with simple equations and procedures for calculating the approximate bounds on the spectra of LFM pulses. The first edition was issued in February 1971.<sup>1</sup> This revised edition presents in greater detail the derivations of the equations and includes an additional section consisting of numerical examples that illustrate the application of the procedures.

OBJECTIVE

The objective of this project was to provide a simple method for calculating and plotting strong bounds, or a good approximation thereof, on the spectra of LFM radio frequency (RF) pulses that have trapezoidal envelopes.

---

<sup>1</sup>Newhouse, P.D., A Simplified Method for Calculating the Bounds on the Emission Spectra of Chirp Radars, ESD-TR-70-273, Electromagnetic Compatibility Analysis Center, Annapolis, MD, February 1971.

APPROACH

The conventional equation for the spectrum of a chirp pulse was replaced by two equations, one of which is convenient for describing the center region of the spectrum and the other for describing the skirts of the spectrum. Using these equations, simple expressions were derived that yield approximate bounds on the spectrum.

SECTION 2  
DEVELOPMENT OF EQUATIONS AND PROCEDURES

The simple equations and procedures developed permit rapid hand-calculation and plotting of an approximation of strong bounds on the spectra of LFM RF pulses that have a trapezoidal envelope. The plots of the approximate bounds consist of segments of straight lines on semilogarithmic graph paper; thus, they are very easy to draw.

By definition, a bounding function is never less than the bounded function. The functions derived here, however, may underestimate by several dB the actual spectrum in a few places, such as at the edges of the central lobe of the spectrum. Therefore, the functions are referred to here as approximate bounds on the spectrum.

The approximate bounds are within about 1 dB of the spectrum at the center of the central lobe and within a fraction of a dB at the centers of the minor lobes that occur at frequencies well above and below the central lobe. The approximation is the least accurate at the edges of the central lobe, where it may underestimate the spectrum by about 5-10 dB in a relatively narrow frequency interval, as illustrated in the numerical examples included in Sections 3 and 5 of this report.

## SECTION 3

## DESCRIPTION OF PARAMETERS AND APPLICATION OF MODEL

The approximate bounds on the spectrum of chirp pulses can be calculated and plotted within a few minutes using the model described in this section. A derivation of the model is presented in Section 4.

PULSE PARAMETERS USED IN THE MODEL

The following terms and their definitions specify the pulse parameters used in calculating critical frequencies for the model. Figure 1 shows the pulse parameters, graphically.

- $f_c$  = nominal carrier frequency, in Hz
  - $P$  = peak power, in watts
  - $\tau_b$  = pulse width at base, in seconds
  - $\delta_r$  = rise time, in seconds
  - $\delta_f$  = fall time, in seconds.
- } defined as the time interval from 0 to 100% of the voltage amplitude, as shown in Figure 1.

In addition to those terms, one of the following is needed:

- $\beta$  = frequency deviation, in Hz
- $D$  = compression ratio
- $\tau_c$  = compressed pulse width, in seconds.

When  $\beta$  is not given, it can be calculated using the relationship:

$$\beta = \frac{1}{\tau_c} = \frac{D}{\tau_b} \quad (1)$$

When the pulse is not symmetrical ( $\delta_r \neq \delta_f$ ), it is also necessary to know whether the deviation is positive or negative.

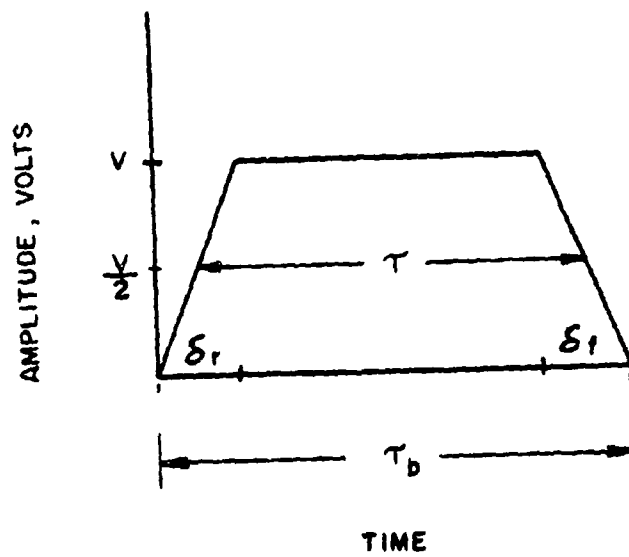
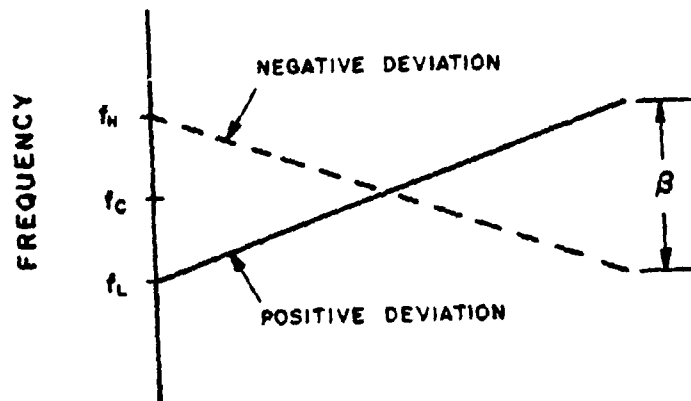


Figure 1. Parameters used to describe a chirp pulse.

EFFECT OF PARAMETERS ON SHAPE OF SPECTRUM

A brief discussion of the effect of the pulse parameters on the behavior of the spectrum will be helpful in understanding the model. The carrier frequency of the RF pulse,  $f_c$ , is assumed to be very large in comparison to the total frequency deviation,  $\beta$ . For that condition, the shape of the spectrum may be considered to be solely dependent on the shape of the envelope of the pulse and on the magnitude and polarity of the frequency deviation.

Pulse Without Frequency Modulation (FM)

When there is no FM, the spectrum of a pulse is symmetrical, as shown in Figure 2, regardless of whether the pulse shape is symmetrical.

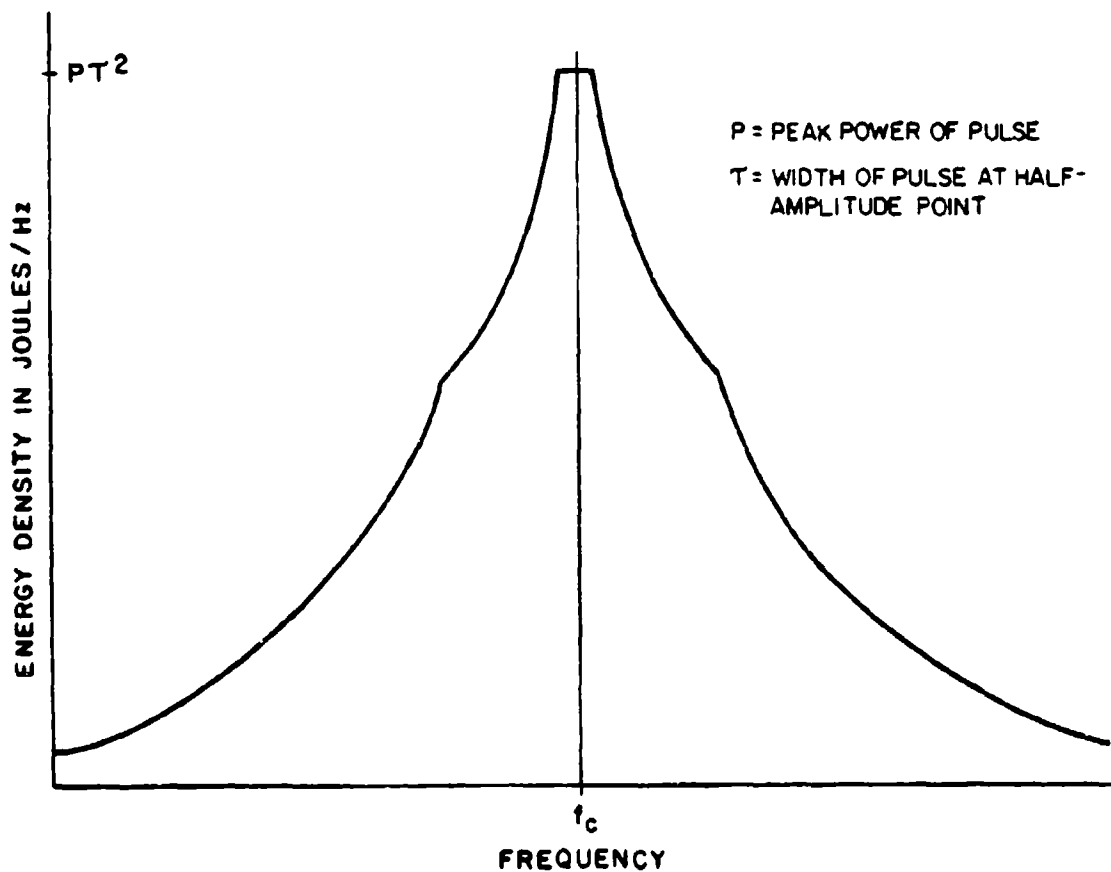


Figure 2. Bounds on spectrum of a trapezoidal pulse without FM.

Pulse with FM

FM reduces the peak of the spectrum; however, the bounds on the skirts of the spectrum are essentially unaffected by the FM, as shown in Figure 3. If the pulse shape were symmetrical, the spectrum would be symmetrical about  $f_c$ .

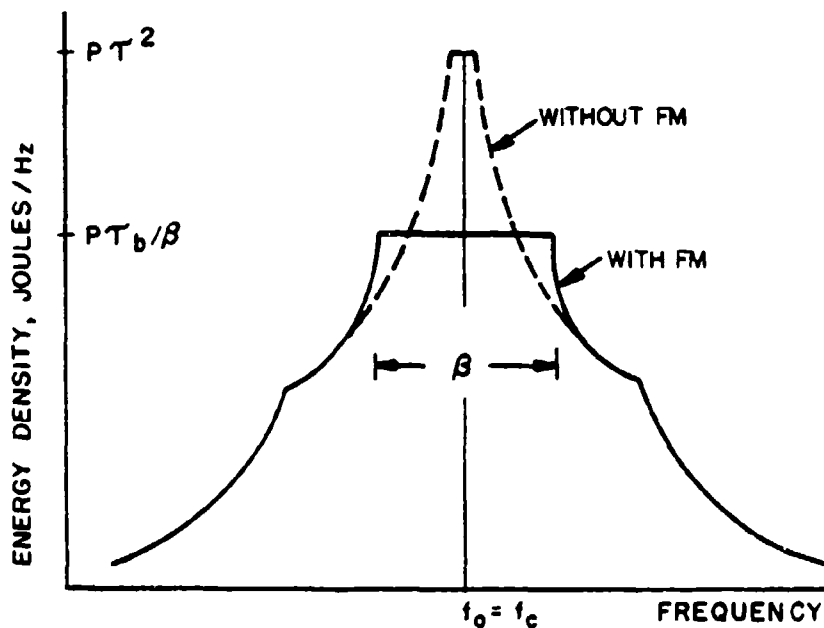


Figure 3. Bounds on spectrum of chirp pulse when  $\delta_r = \delta_f$ .

If the pulse shape were asymmetrical, i.e.,  $\delta_r \neq \delta_f$ , the central portion of the spectrum would be asymmetrical as indicated in Figure 4. The shape of the spectrum will depend upon whether the deviation is negative or positive, as indicated in the figure. The skirts of the spectrum, however, are symmetrical about a frequency,  $f_0$ , which is displaced from  $f_c$ , the nominal carrier frequency. The relationship between  $f_0$  and  $f_c$  is explained later in this section.

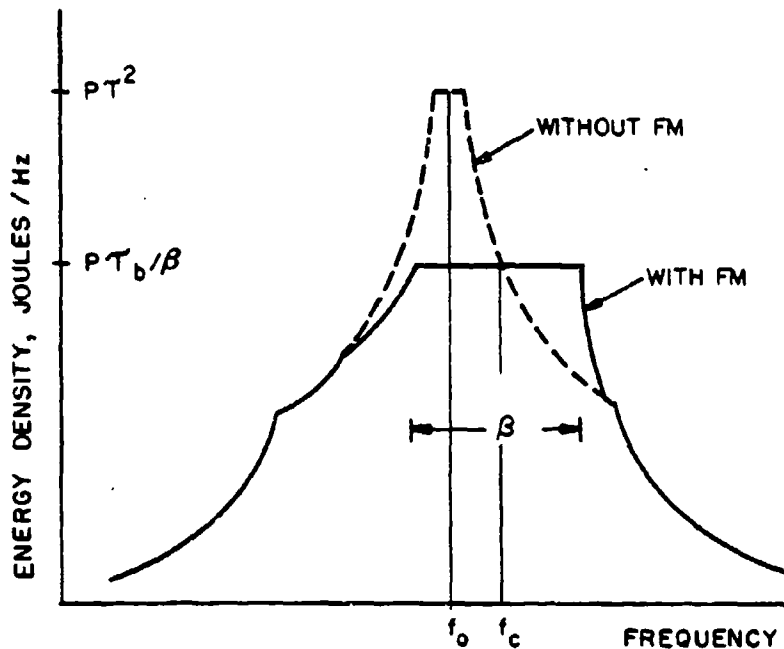


Figure 4. Bounds on spectrum of chirp pulse when  $\delta_r < \delta_f$  and frequency deviation is positive. If the deviation were negative, the bounds would be the mirror image with respect to  $f_0$ .

#### PROCEDURE FOR PLOTTING THE BOUNDS OF THE SPECTRUM

The chirp pulse considered in this report is LFM. When the frequency deviation is relatively small so that  $\beta\tau \leq 2/\pi$ , the bounds on the spectrum are not influenced by the frequency modulation. For that condition the spectral bounds can be obtained using the same procedures that are available for an ordinary radar pulse, i.e., one that is not frequency modulated. It is very unlikely that a chirp radar would be designed to have such a small amount of frequency deviation; however, procedures are given here for plotting the spectral bounds when  $\beta\tau \leq 2/\pi$ , as well as when  $\beta\tau > 2/\pi$ .

Calculation of Bounds on Ordinary Radar Emission Spectrum (Nonchirp or Chirp when  $\beta\tau \leq 2/\pi$ )

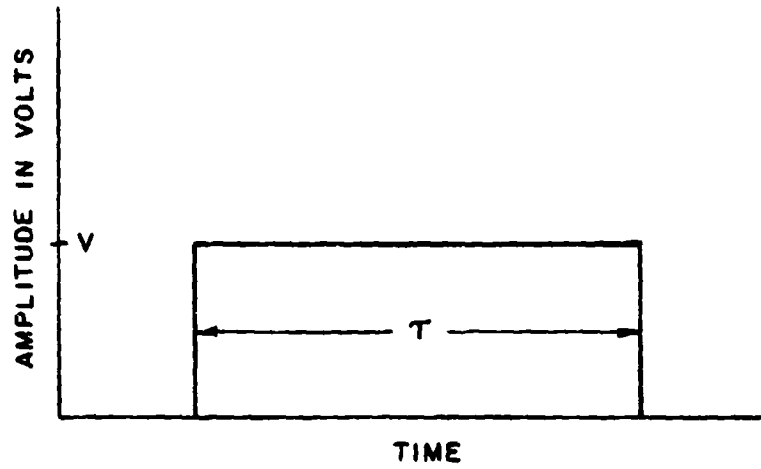
An ideal ordinary radar pulse has a rectangular waveform and a  $(\sin x/x)^2$  spectrum as shown in Figure 5. As a practical matter, however, a rectangular pulse is not attainable because the leading and trailing edges will have a finite slope due to practical circuit limitations. Therefore, radar pulses are assumed to be trapezoidal with the dimensions shown in Figure 6a. The spectrum takes the form shown by the solid curve in Figure 6b. Assuming a more intricate pulse shape (such as a trapezoid with rounded corners) in order to model an even more realistic radar pulse generally does not yield much practical benefit. Rounding the corners of a trapezoidal pulse, for example, has little or no significant effect on the bounds of the spectrum except for frequencies far from the center of the spectrum; at those frequencies, the spurious emissions of a radar transmitter usually determine the level of the spectrum.

In EMC analyses it is appropriate, as well as convenient, to represent the spectrum by a bound, such as the dotted curve in Figure 6b. It is common practice to normalize the graph of the spectral density by dividing by the peak value,  $P\tau^2$ , and expressing the ratio in decibels (dB). The normalized graph, which is referred to as the relative spectral density, is applicable to the energy-density and the power-density spectra as well as the envelope of the power spectrum, which is a line spectrum.

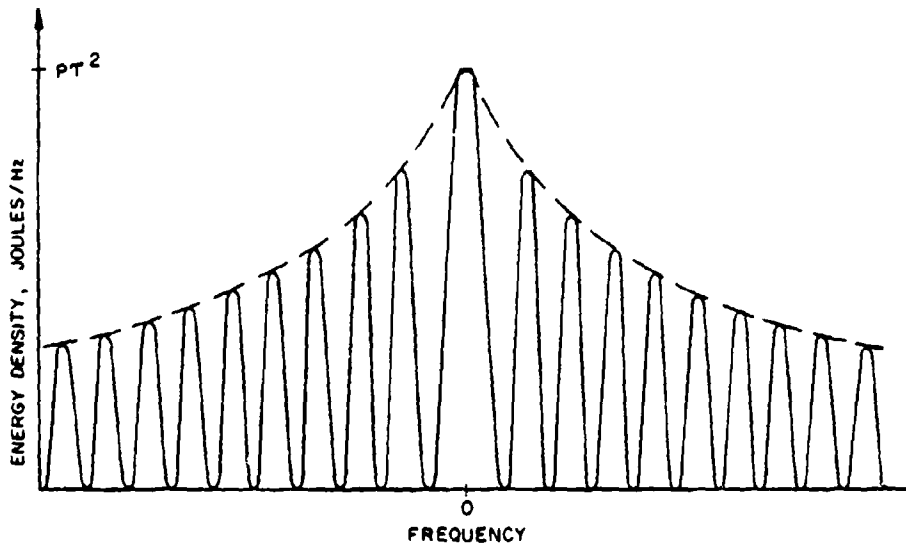
When a logarithmic scale is used for the abscissa (frequency) and a decibel (dB) scale is used for the ordinate, the curves that constitute the bounds in Figure 7a can be drawn as straight lines, as shown in Figure 7b.<sup>2</sup> The frequency is referenced to the carrier frequency,  $f_c$ , i.e.,  $\Delta f = f - f_c$ . To plot the spectrum bounds, the following steps are required.

---

<sup>2</sup>Mason, S.J., and Zimmermann, H.J., Electronic Circuits, Signals, and Systems, John Wiley & Sons, Inc., 1960, p. 237.

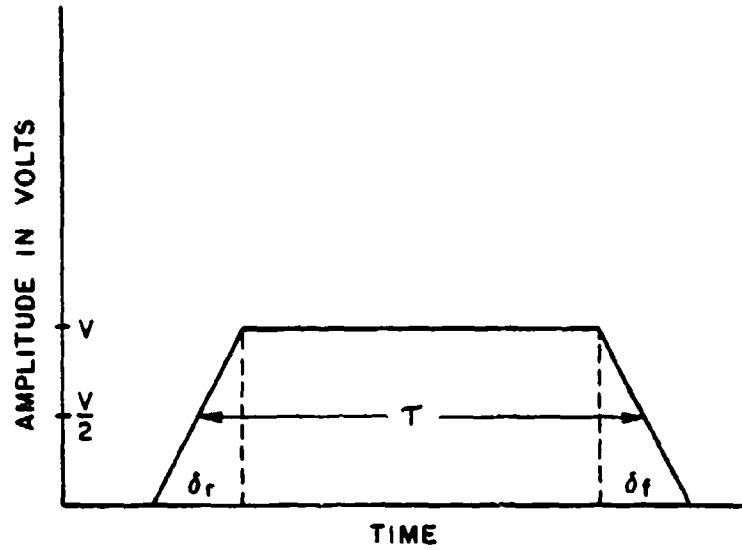


a. Rectangular pulse.

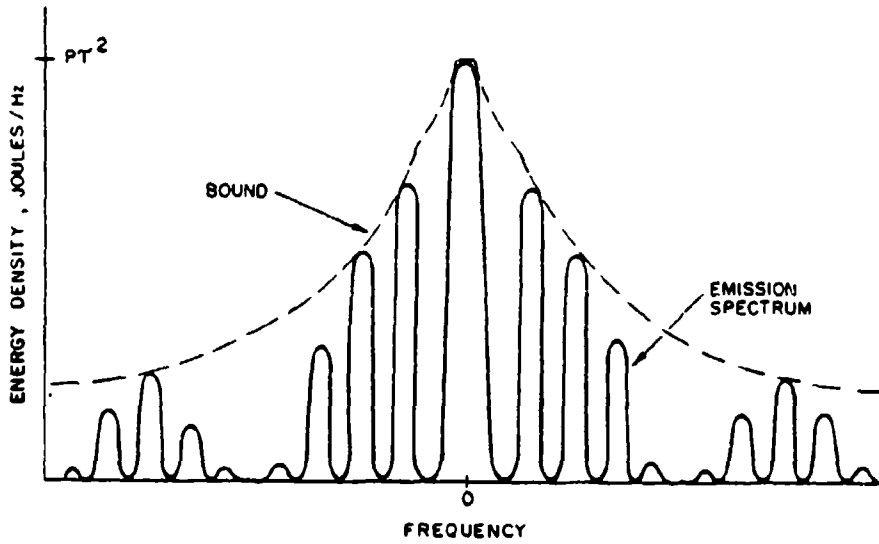


b. Energy density spectrum.

Figure 5. Idealized radar pulse (nonchirp).

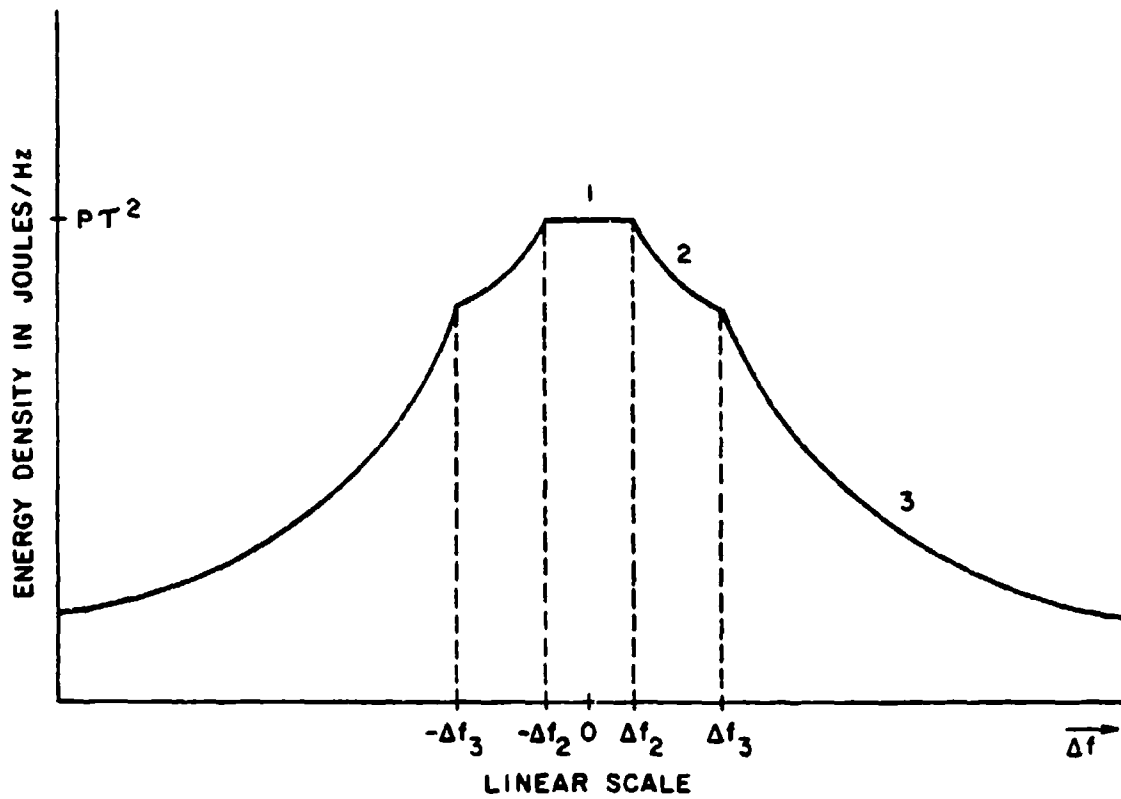


a. Trapezoidal pulse.



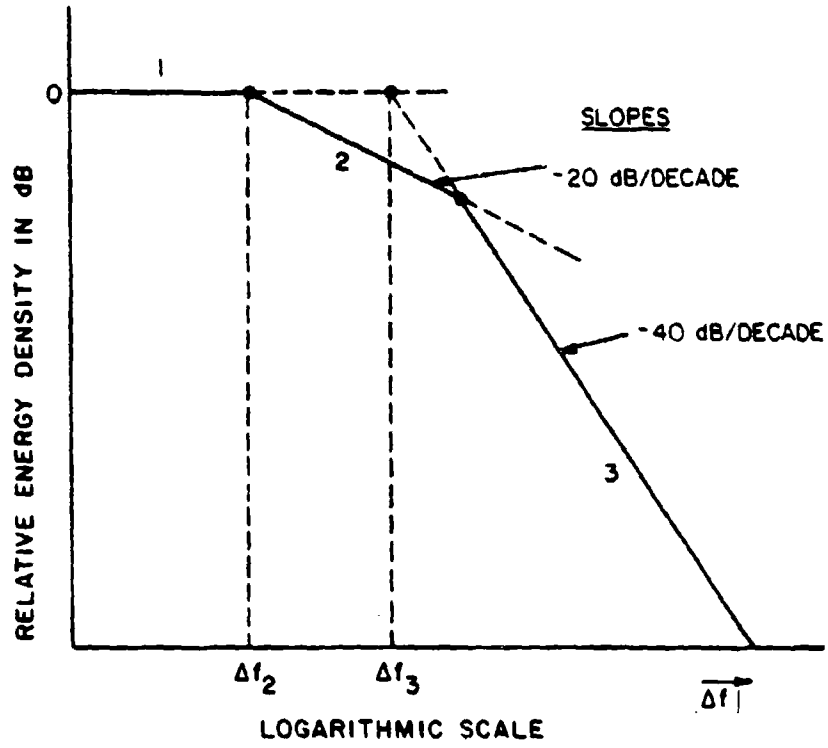
b. Energy density spectrum.

Figure 6. Ordinary radar pulse (nonchirp).



a. Linear frequency scale.

Figure 7. Spectrum bounds for ordinary radar pulse (trapezoidal).  
(Page 1 of 2).



b. Logarithmic frequency scale.

Figure 7. (Page 2 of 2).

Step 1 - Calculate the critical frequencies,  $\Delta f_2$  and  $\Delta f_3$ :

$$\Delta f_2 = \frac{1}{\pi\tau} \quad (2)$$

$$\Delta f_3 = \frac{1}{\pi\sqrt{\tau\delta}} \quad (3)$$

where

$$\frac{1}{\delta} = \frac{1}{2} \left( \frac{1}{\delta_r} + \frac{1}{\delta_f} \right)$$

$\tau$  = pulse duration between half amplitude points, in seconds  
 $\delta_r$  = rise time, in seconds } defined as the time interval from  
 $\delta_f$  = fall time, in seconds } 0 to 100% of the voltage amplitude.

Note - A pulse that is not frequency modulated has a spectrum that is symmetrical about the carrier frequency,  $f_c$ , whether or not the pulse is symmetrical.

Step 2 - On semilogarithmic paper, draw line 1 horizontally through 0 dB.

Step 3 - Starting on line 1 at  $\Delta f_2$ , draw line 2 with a slope of -20 dB/decade.

Step 4 - Starting on line 1 at  $\Delta f_3$ , draw line 3 with a slope of -40 dB/decade. The spectrum is bounded by lines 1, 2, and 3 of Figure 7b.

The peak energy density level,  $P_d$ , corresponding to the 0-dB level in Figure 7b, is obtained by:

$$P_d = P\tau^2 \quad \text{joules/Hz} \quad (4)$$

where

$P$  = peak pulse power level, in watts

Calculation of Bounds on Chirp (LFM) Spectrum (When  $\beta\tau > 2/\pi$ )

When linear frequency modulation is applied to the pulsed carrier frequency, the peak of the spectrum is reduced in amplitude from  $P\tau^2$  to  $P\tau/\beta$  and the central lobe of the spectrum is broadened, as shown in Figure 3, but the spectrum bounds further removed from the carrier frequency remain essentially unaffected by the frequency modulation. The energy-density spectrum of the chirp pulse is normalized by dividing by  $P\tau/\beta$ .

If the pulse is a symmetrical trapeziod, the spectrum will be symmetrical about the nominal carrier frequency,  $f_c$ , as shown in Figure 3. If the pulse shape is asymmetrical, the spectrum will be asymmetrical, as shown in Figure 4. The direction in which the spectrum is shifted will depend on whether the deviation is negative or positive, with respect to time. The spectrum boundaries further removed from the carrier frequency will be symmetrical about a frequency,  $f_o$ , which is displaced from  $f_c$ , as shown below:

$$f_o = f_c + Q \frac{\beta(\delta_r - \delta_f)}{2(\delta_r + \delta_f)} \quad (5)$$

where  $Q$  is defined in TABLE 1.

TABLE 1  
VALUES ASSIGNED TO M, N, AND Q

Constants	Positive Frequency Shift	Negative Frequency Shift
M	$\delta_f$	$\delta_r$
N	$\delta_r$	$\delta_f$
Q	+1	-1

The plots of the bounds on the chirp pulse spectrum are referenced to  $f_0$ :

$$\Delta f = f - f_0 \quad (6)$$

The procedure for plotting the bounds on the chirp pulse when the product  $\beta\tau > 2/\pi$  is illustrated in Figure 8 and entails the following steps. Several numerical examples are presented in Section 5. Step 1 (A) is used when the pulse is symmetrical, whereas Step 1 (B) is used when the pulse is asymmetrical.

Step 1 (A) - If the pulse is symmetrical ( $\delta_r = \delta_f$ ), calculate the critical frequencies,  $\Delta f_2$ ,  $\Delta f_3$ ,  $\Delta f_{a+}$ ,  $\Delta f_{a-}$ ,  $\Delta f_{b+}$ , and  $\Delta f_{b-}$  as:

$$\Delta f_2 = \frac{1}{\pi} \left( \frac{\beta}{\tau_b} \right)^{1/2} \quad (7)$$

$$\Delta f_3 = \frac{1}{\pi} \left( \frac{\beta}{\tau_b} \right)^{1/4} \left( \frac{1}{\delta} \right)^{1/2} \quad (8)$$

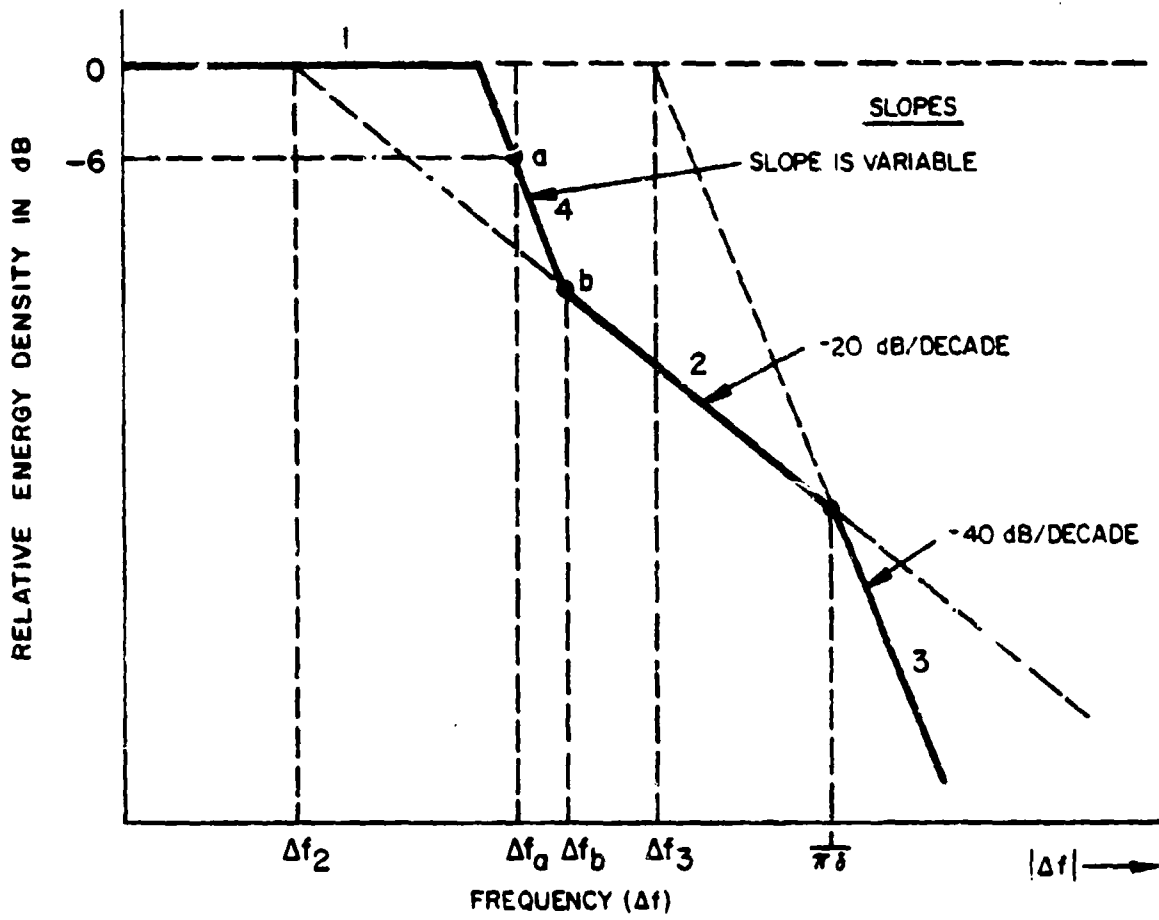
where

$$\frac{1}{\delta} = \frac{1}{2} \left( \frac{1}{\delta_r} + \frac{1}{\delta_f} \right)$$

$$\Delta f_{a+} = \frac{\beta}{2} \left( 1 - \frac{\delta}{\tau_b} \right) \quad \Delta f_{a-} = -\Delta f_{a+} \quad (9)$$

$$\Delta f_{b+} = 2\Delta f_{a+} \quad \Delta f_{b-} = -\Delta f_{b+} \quad (10)$$

The spectrum is symmetrical about  $f_0$ , so the same plot can be used for positive and negative values of  $\Delta f$ .

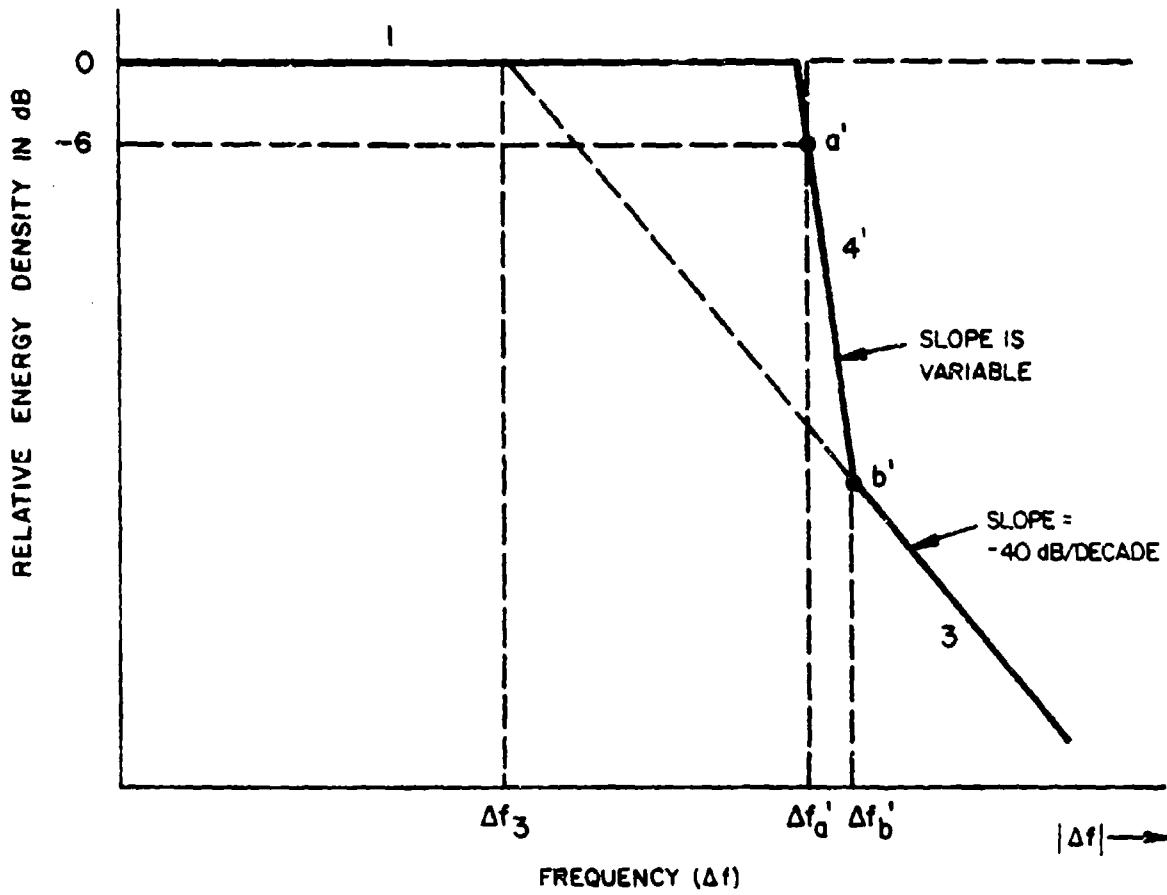


(LOGARITHMIC SCALE)

a. When  $\Delta f_b < 1/\pi\delta$ .

Figure 8. Spectrum bounds for chirp radar pulse. (Page 1 of 2).

Note: This figure depicts the bounds for positive values of  $\Delta f$  based on Equations 13 and 14. The bounds for negative values of  $\Delta f$  are plotted in a similar manner based on Equations 15 and 16.



(LOGARITHMIC SCALE)

b. When  $\Delta f_b > 1/\pi\delta$ .

Figure 8. (Page 2 of 2).

Step 1 (B) - When the pulse is asymmetrical and  $\beta\tau > 2/\pi$ , critical frequencies may be calculated using the equations:

$$\Delta f_2 = \frac{1}{\pi} \left( \frac{\beta}{\tau_b} \right)^{1/2} \quad (11)$$

$$\Delta f_3 = \frac{1}{\pi} \left( \frac{\beta}{\tau_b} \right)^{1/4} \left( \frac{1}{\delta} \right)^{1/2} \quad (12)$$

where

$$\frac{1}{\delta} = \frac{1}{2} \left( \frac{1}{\delta_r} + \frac{1}{\delta_f} \right)$$

When the spectrum is asymmetrical, positive and negative halves must be plotted separately because  $f_o \neq f_c$ , as shown in Equations 7, 8, 9, and 10.

For positive  $\Delta f$ :

$$\Delta f_{a+} = \frac{M\beta}{\delta_r + \delta_f} \left( 1 - \frac{\delta_r + \delta_f}{2\tau_b} \right) \quad (13)$$

$$\Delta f_{b+} = \begin{cases} 2\Delta f_{a+} & (\text{when } \beta \leq 1/\pi) \\ \frac{M\beta}{\delta_r + \delta_f} \left( \frac{1}{1 - \frac{N}{\sqrt{2(\delta_r + \delta_f)}}} \right) & (\text{when } \beta\delta > 1/\pi) \end{cases} \quad (14)$$

For negative  $\Delta f$ :

$$\Delta f_{a-} = \frac{-N\beta}{\delta_r + \delta_f} \left( 1 - \frac{\delta_r + \delta_f}{2\tau_b} \right) \quad (15)$$

$$\Delta f_b = \begin{cases} 2\Delta f_{a-} & (\text{when } \beta\delta \leq 1/\pi) \\ \frac{-N\beta}{\delta_r + \delta_f} \left( \frac{1}{1 - \frac{M}{\sqrt{2(\delta_r + \delta_f)}}} \right) & (\text{when } \beta\delta > 1/\pi) \end{cases} \quad (16)$$

For the M and N values used here, see TABLE 1.

Step 2 - Draw line 1 horizontally through 0 dB (see Figures 8a and 8b).

Step 3 - If  $\Delta f_b$  is less than  $1/(\pi\delta)$ , use Figure 8a and draw line 2 with a slope of -20 dB/decade starting on line 1 at  $\Delta f_2$ .

If  $\Delta f_b$  is equal to or greater than  $1/(\pi\delta)$ , skip this step and use Figure 8b for the next step.

Step 4 - Draw line 3 with a slope of -40 dB/decade starting on line 1 at  $\Delta f_3$  in Figure 8a or 8b.

Step 5 - Locate point "a" or "a'" at 6 dB down from 0 dB at  $\Delta f_a$  or  $\Delta f_a'$  in Figure 8a or 8b, respectively.

Step 6 - Locate point "b" or "b'" at  $\Delta f_b$  on line 2 in Figure 8a, or on line 3 in Figure 8b, respectively.

Step 7 - Draw line 4 or line 4' through points "a" and "b" in Figure 8a, or through points "a'" and "b'" in Figure 8b.

#### Spectrum Bounds

For the situation where  $\Delta f_b < 1/(\pi\delta)$ , the spectrum is bounded by a curve as described by lines 1, 4, 2, and 3 in Figure 8a. If  $\Delta f_b \geq 1/(\pi\delta)$ , the

spectrum would be bounded by a curve, as described by lines 1, 4, and 3 in Figure 8b.

The peak energy-density level,  $P_d$ , corresponding to the 0 dB level in Figure 8a or 8b is calculated as follows:

$$P_d = (P\tau_b/\beta) \quad \text{joules/Hz} \quad (17)$$

where

$$\begin{aligned} \beta &= \text{frequency deviation during pulse, in Hz} \\ \tau_b &= \text{pulse width at the base of the pulse, in seconds.} \end{aligned}$$

#### Sample Calculations of Radar Emission Spectrum Bounds

##### Example 1. Ordinary (nonchirp) trapezoidal pulse

$$\begin{aligned} \tau &= 6 \times 10^{-6} \text{ s} \\ \delta_r &= 0.2 \times 10^{-6} \text{ s} \\ \delta_f &= 0.35 \times 10^{-6} \text{ s} \end{aligned}$$

Step 1 - Calculate critical frequencies  $\Delta f_2$  and  $\Delta f_3$  using Equations 2 and 3:

$$\Delta f_2 = \frac{1}{\pi\tau} = \frac{1}{\pi(6 \times 10^{-6})} = 53.1 \text{ kHz}$$

$$\frac{1}{\delta} = \frac{1}{2} \left( \frac{1}{\delta_r} + \frac{1}{\delta_f} \right) = \frac{10^6}{2} \left( \frac{1}{0.2} + \frac{1}{0.35} \right) = \frac{1}{0.25 \times 10^{-6} \text{ s}}$$

$$\Delta f_3 = \frac{1}{\pi(\tau\delta)^{1/2}} = \frac{1}{\pi[(6 \times 10^{-6})(0.25 \times 10^{-6})]^{1/2}} = 259.9 \text{ kHz}$$

Step 2 - Using Figure 9, draw line 1 horizontally through 0 dB on the ordinate representing the peak energy-density level.

Step 3 - Starting on line 1 at  $\Delta f_2$ , draw line 2 with a slope of -20 dB/decade.

Step 4 - Starting on line 1 at  $\Delta f_3$ , draw line 3 with a slope of -40 dB/decade.

The spectrum bounds are described by lines 1, 2, and 3. To indicate the accuracy of this approximation technique, portions of the energy-density function are plotted in Figure 9.

The peak energy-density level corresponding to the 0 dB point is calculated as follows:

Assume: Peak power (P) =  $1 \times 10^6$  watts

From Equation 4,

$$\begin{aligned} P_d &= (P\tau^2) \\ &= (1 \times 10^6)(6 \times 10^{-6})^2 \\ &= 3.6 \times 10^{-5} \text{ joules/Hz.} \end{aligned}$$

#### Example 2. Linear chirp pulse

To illustrate the procedure for determining the approximate bounds on the spectrum of a typical chirp pulse, the following example is considered where the pulse parameters are:

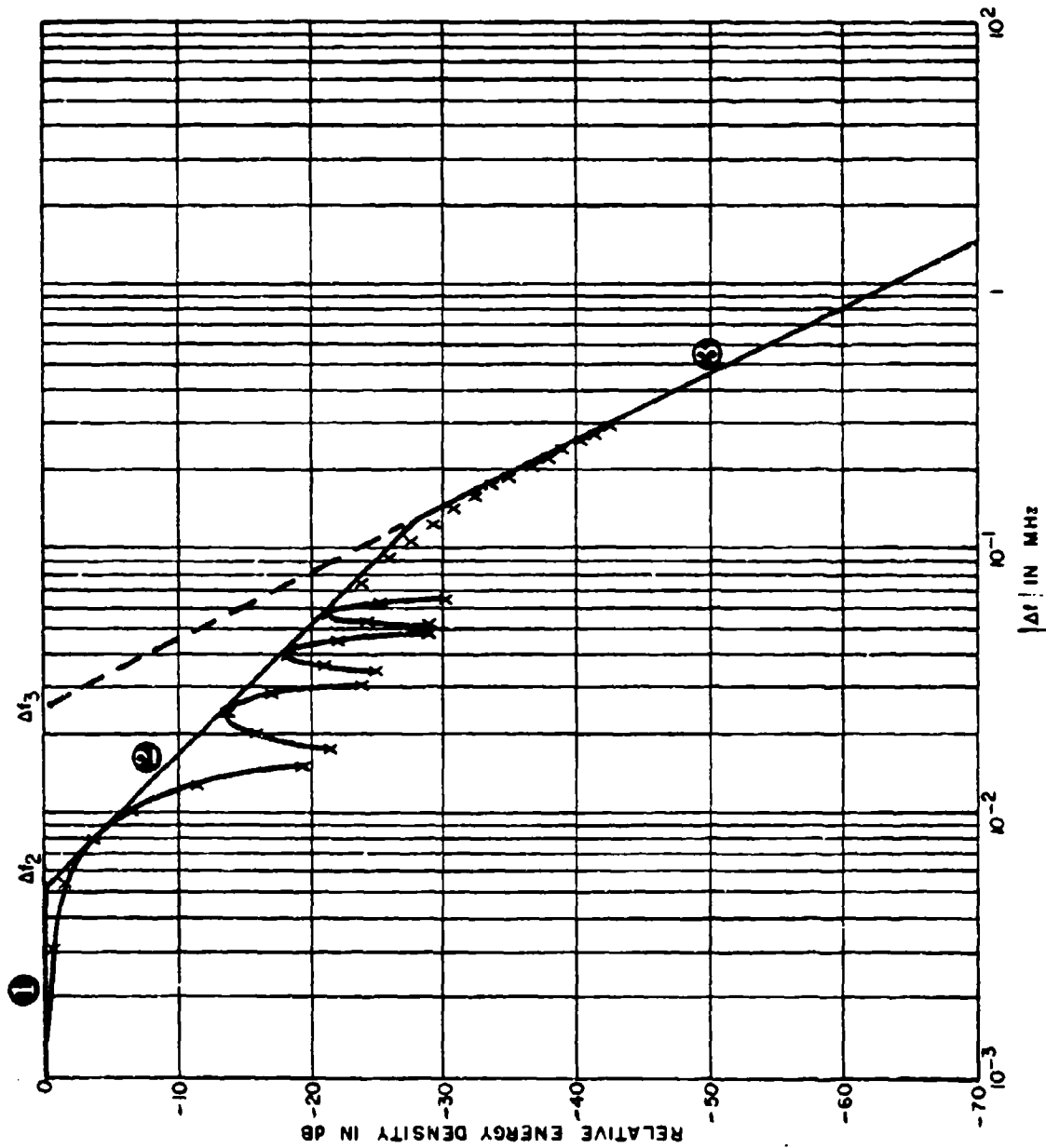


Figure 9. The bounds on an ordinary radar pulse, Example 1.

$$\begin{aligned}\beta &= 1 \times 10^6 \text{ Hz, positive deviation} \\ \tau_b &= 102 \times 10^{-6} \text{ s} \\ \delta_r &= \delta_f = 1 \times 10^{-6} \text{ s} \\ \tau &= 101 \times 10^{-6} \text{ s}.\end{aligned}$$

Step 1 - Determine if  $\beta > 2/(\pi\tau)$  and if the pulse is symmetrical.  
 $2/(\pi\tau) = 0.0063 \times 10^6$ , which is less than  $\beta$ ,

$$\delta_r = \delta_f \text{ and therefore the pulse is symmetrical.}$$

Since the pulse meets these conditions, calculate  $\Delta f_2$ ,  $\Delta f_3$ ,  $\Delta f_{a+}$ ,  $\Delta f_{a-}$ ,  $\Delta f_{b+}$ , and  $\Delta f_{b-}$  according to Step 1 (A).

Step 1 (A):

$$\Delta f_2 = \frac{1}{\pi} \left[ 1 \times 10^6 / (102 \times 10^{-6}) \right]^{1/2} = 0.032 \times 10^6 \text{ Hz}$$

$$1/\delta = 1/2 \left( \frac{1}{10^{-6}} + \frac{1}{10^{-6}} \right) = (10^6) \text{ s}^{-1}$$

$$\Delta f_3 = \frac{1}{\pi} \left[ 1 \times 10^6 / (102 \times 10^{-6}) \right]^{1/4} (1 \times 10^6)^{1/2} = 0.10 \times 10^6 \text{ Hz}$$

$$\Delta f_{a+} = \frac{10^6}{2} \left( 1 - \frac{10^{-6}}{102 \times 10^{-6}} \right) = 0.50 \times 10^6 \text{ Hz}$$

$$\Delta f_{a-} = -\Delta f_{a+} = -0.50 \times 10^6 \text{ Hz}$$

$$\Delta f_{b+} = 2\Delta f_{a+} = 1.0 \times 10^6 \text{ Hz}$$

$$\Delta f_{b-} = 2\Delta f_{a-} = -1.0 \times 10^6 \text{ Hz}$$

Now, plot the spectrum bounds as follows and as shown in Figure 10.

Step 2: Draw line 1 horizontally through 0 dB.

Step 3: Is  $\Delta f_b > 1/(\pi\delta)$ ?

$1/(\pi\delta) = \frac{10^6}{\pi} = 0.32 \times 10^6 \text{ Hz}$ , which is less than  $\Delta f_b$ . Therefore, line 2 is not used in the approximation of the spectrum bounds. Proceed to Step 4.

Step 4: Starting on line 1 in Figure 10, at  $\Delta f = \Delta f_3$ , draw line 3 with a slope of -40 dB/decade.

Step 5: Locate point "a" 6 dB down at  $\Delta f = \Delta f_{a+}$ .

Step 6: Since  $\Delta f_{b+} > 1/(\pi\delta)$ , for this example, locate point b at  $\Delta f = \Delta f_{b+}$  on line 3.

Step 7: Draw line 4 through points a and b.

The approximate bounds of the spectrum are formed by the solid lines 1, 4, and 3 on Figure 10. Line 2 is not used in this particular example because  $\Delta f_b > 1/(\pi\delta)$ . The pulse is symmetrical, therefore the spectrum is also symmetrical and the plot can be used for either positive or negative values of  $\Delta f$ .

The peak energy-density level corresponding to the 0 dB is calculated as follows:

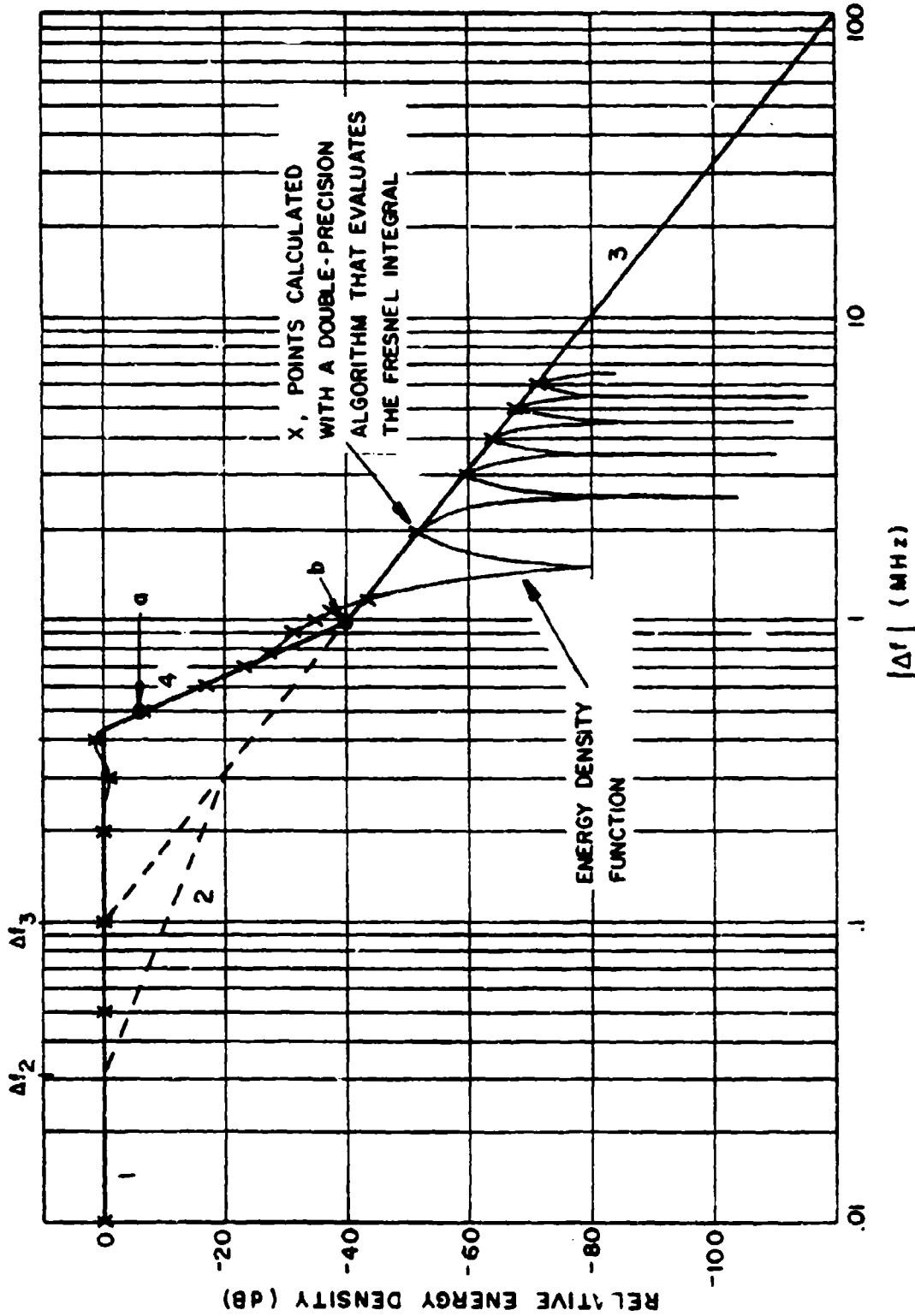


Figure 10. Bounds on the normalized energy-density spectrum of the chirp pulse in Example 2. (The normalized energy-density function calculated with a double precision algorithm is also shown for comparison.)

Assume: peak power (P) =  $1 \times 10^6$  watts

From Equation 17:

$$\begin{aligned} P_d &= P\tau_b/\beta \\ &= (1 \times 10^6) (102 \times 10^{-6})/1 \times 10^6 \\ &= 10.2 \times 10^{-5} \text{ joules/Hz.} \end{aligned}$$

To indicate the accuracy attained in the above example, the spectral power-density function, calculated using a double precision algorithm, also is plotted in Figure 10 using the symbol "x" to designate representative points on the energy-density function.

Additional numerical examples are given in Section 5.

#### Fit of the Approximate Bounds to the Spectrum

The fit of the approximate bounds obtained with the method described varies over the spectrum, and is best for values of  $\Delta f$  greater than 38. At about  $\Delta f = 38$ , the difference between the approximate bound and the peaks of the lobes in the spectrum are less than 1 dB. As  $\Delta f$  is increased further, the difference rapidly approaches zero. In the region represented by line 1, the difference usually is in the order of 1 dB.

The largest difference occurs in the region represented by line 4 at Point b. For long symmetrical pulses, the approximate bound here usually underestimates the spectrum by less than 6 dB, but for asymmetrical pulses, especially when  $\tau_b$  is not much larger than either  $\delta_r$  or  $\delta_f$ , the approximate difference may be as much as about 10 dB. Because line 4 is used to represent only a small part of the overall spectrum, this difference is acceptable for most spectrum analyses.

SECTION 4  
DERIVATION OF THE MODEL

This section and the appendixes present derivations of the formulas used in procedures given in Section 3. Since all of the information required to apply the procedures is given in Section 3, Section 4 can be skipped by the reader who is not interested in the derivations.

APPROACH TO DEVELOPING THE MODEL

The equation of the spectrum of a chirp pulse involves Fresnel integrals and thus is cumbersome to evaluate.<sup>3</sup> By expressing the Fresnel integral in the form of an asymptotic expansion and using only the first few terms, a simple expression was obtained that yields a very accurate approximation of the spectral voltage-density function, except for frequencies within two relatively narrow intervals,  $\Omega_1$  to  $\Omega_2$  and  $\Omega_3$  to  $\Omega_4$ , as indicated in Figure 11. The simple expression also yields an accurate approximation at the center of each of those intervals, namely at points  $a_-$  and  $a_+$ , so that even within those intervals a good estimate of the spectral voltage-density can be obtained. Using the expression derived for the spectral voltage-density function, formulas were derived for functions that bound the chirp spectrum.

DESCRIPTION OF THE CHIRP SIGNAL

The parameters that describe a LFM or chirp pulse are shown in Figure 12. A trapezoidal envelope is used because the skirts of the spectrum are very sensitive to the slopes of the edges of the pulse. A rectangular envelope is adequate if only the in-band region of the spectrum is of interest; however, in electromagnetic compatibility analyses the skirts of the spectrum are of primary concern. Therefore, the skirts must be represented realistically.

---

<sup>3</sup>Cook, C.E., "Pulse Compression -- Key to More Efficient Radar Transmission," Proc. IRE, Vol. 48, March 1960, pp. 310-316.

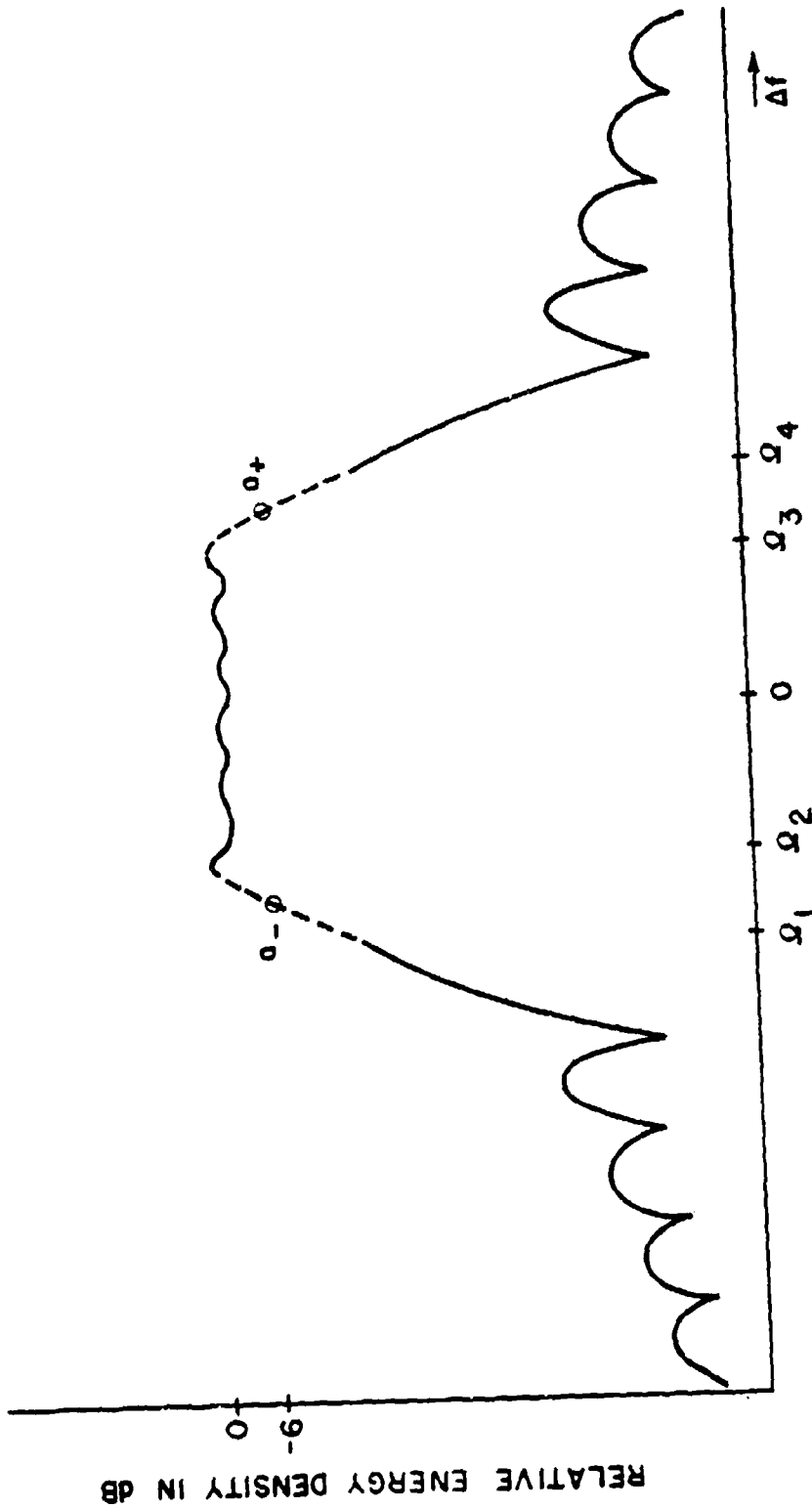


Figure 11. The simple expression derived for the spectral voltage-density function provides a very accurate approximation for points  $a_-$  and  $a_+$  (which are 6 dB down) and the portion of the function represented by the solid curve.

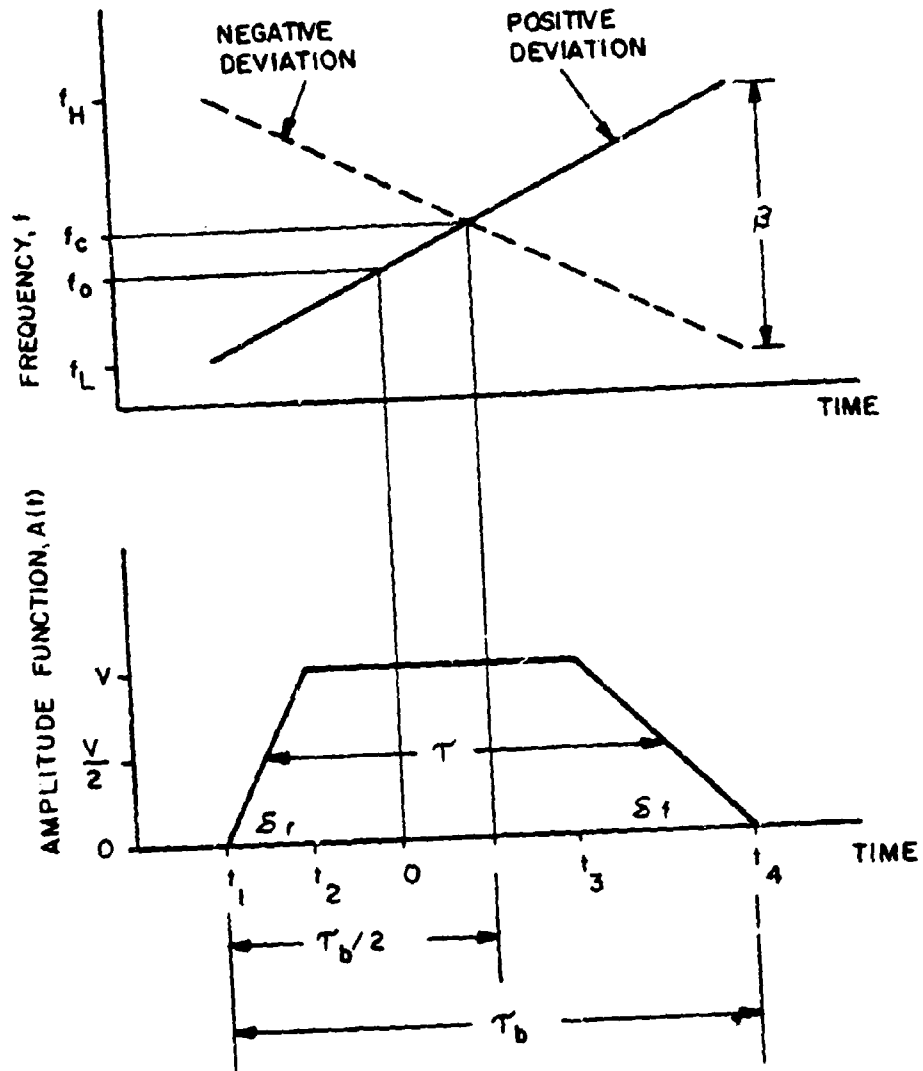


Figure 12. Parameters describing a chirp pulse.

The time waveform of the pulse can be expressed by (see Reference 2):

$$v(t) = A(t) \cos \left[ 2\pi \left( f_0 t + \frac{kt^2}{2} \right) \right] \quad (18)$$

where

$f_0$  is the reference frequency used here for a chirp pulse

$$A(t) = \begin{cases} v(t - t_1)/\delta_r, & t_1 \leq t \leq t_2 \\ v, & t_2 \leq t \leq t_3 \\ v(t_4 - t)/\delta_f, & t_3 \leq t \leq t_4 \\ 0, & t_4 < t < t_1 \end{cases} \quad (18a)$$

$$k = \beta/\tau_b \quad (18b)$$

The derivation will be made assuming that the deviation is positive, i.e., the frequency is shifted upward during the pulse. The model developed can also handle negative deviation using a procedure that is explained at the end of this section.

As explained in APPENDIX H, the location of the origin of the chirp signal on the time scale, relative to  $t_1$ ,  $t_2$ , etc., affects the closeness of the fit of the approximate bounds to the spectrum. Studying the appendix will be more meaningful if the reader goes through this section first. The origin of the signal is located so that:

$$t_1 = -\delta_r \tau_b / (\delta_r + \delta_f) \quad (19)$$

$$t_2 = t_1 + \delta_r \quad (20)$$

$$t_3 = t_4 - \delta_f \quad (21)$$

$$t_4 = \delta_f \tau_b / (\delta_r + \delta_f) \quad (22)$$

With this time scale, the instantaneous frequency is equal to  $f_0$  when  $t = 0$ . Other time parameters used in the derivation are:

$$t_r = (t_1 + t_2)/2 \quad (23)$$

$$t_f = (t_3 + t_4)/2 \quad (24)$$

$$\tau = t_f - t_r \quad (25)$$

$$\tau_b = t_4 - t_1 \quad (26)$$

$$\frac{1}{\delta} = \frac{1}{2} \left( \frac{1}{\delta_r} + \frac{1}{\delta_f} \right) \quad (27)$$

#### VOLTAGE-DENSITY SPECTRUM

The basic expression for the voltage-density spectrum,  $V(f)$ , is:

$$V(f) = \int_{-\infty}^{\infty} v(t) e^{-j2\pi ft} dt \quad (28)$$

The spectrum for the time waveform described by Equation 18 is:

$$V(f) = F(f) + G(f) \quad (29)$$

where

$$F(f) = \frac{1}{2} \int_{t_1}^{t_4} A(t) e^{j2\pi [kt^2/2 + (f_0 - f)t]} dt \quad (30)$$

$$G(f) = \frac{1}{2} \int_{t_1}^{t_4} A(t) e^{-j2\pi [kt^2/2 + (f_0 + f)t]} dt \quad (31)$$

The spectrum  $F(f)$  is centered on  $+f_0$ , and the spectrum  $G(f)$  on  $-f_0$ . Determining the energy-density spectrum,  $E(f)$ , one of the steps in deriving the model can be accomplished by using either  $F(f)$  or  $G(f)$ , as explained in APPENDIX A. In the derivation that follows  $F(f)$  will be used.

By performing the mathematical manipulations shown in APPENDIX B,  $F(\Delta f)$  can be expressed in the form:

$$F(\Delta f) = \frac{V}{4k} e^{-j\pi\Delta f^2/k} \sum_{i=1}^4 \frac{1}{\delta_i} [\chi_i Z(\chi_i) - \phi(\chi_i)] \quad (32)$$

where

$$\Delta f = f - f_0 \quad (33)$$

$$\delta_1 = \delta_r \quad \delta_2 = -\delta_r \quad \delta_3 = -\delta_f \quad \delta_4 = \delta_f \quad (34)$$

$$X_i = \sqrt{2k} t_i - \sqrt{2/k} \Delta f \quad (35)$$

$$Z(X_i) = \int_0^{X_i} \cos(\pi t^2/2) dt + j \int_0^{X_i} \sin(\pi t^2/2) dt \quad (36)$$

$$\Phi(X_i) = \frac{1}{\pi} e^{-j \frac{\pi}{2} (1 - X_i^2)} \quad (37)$$

$$i = 1, 2, 3, 4$$

Equation 36 is called the complex Fresnel integral. APPENDIX C presents some asymptotic expansions that can be used to evaluate the integral. Using the asymptotic expansions, approximations that can be used in place of Equation 32 were derived in APPENDIX D. These approximations are as follows:

$$F(\Delta f) \approx \frac{V e^{j\pi/4}}{2 \sqrt{k}}, \quad \Omega_2 < \Delta f < \Omega_3 \quad (38)$$

$$F(\Delta f) \approx -\frac{V}{8\pi} \sum_{i=1}^4 \frac{e^{j2\pi t_i (\frac{kt_i}{2} - \Delta f)}}{\delta_i (kt_i - \Delta f)^2}, \quad \Delta f < \Omega_1 \text{ or } \Delta f > \Omega_4 \quad (39)$$

$$F(0) = \frac{V e^{j\pi(\frac{1}{4})^2}}{2 \sqrt{k}} \quad (40)$$

$$F(\Delta f_r) \approx \frac{1}{2} F(0) \quad (41)$$

$$F(\Delta f_f) \approx \frac{1}{2} F(0) \quad (42)$$

where

$$\Omega_1 = -\frac{\beta\delta_r}{\delta_r + \delta_f} - \sqrt{\frac{\beta}{2\tau_b}} \quad (43)$$

$$\Omega_2 = -\beta\left(\frac{\delta_r}{\delta_r + \delta_f} - \frac{\delta_r}{\tau_b}\right) + \sqrt{\frac{\beta}{2\tau_b}} \quad (44)$$

$$\Omega_3 = \beta\left(\frac{\delta_f}{\delta_r + \delta_f} - \frac{\delta_f}{\tau_b}\right) - \sqrt{\frac{\beta}{2\tau_b}} \quad (45)$$

$$\Omega_4 = \frac{\beta\delta_f}{\delta_r + \delta_f} + \sqrt{\frac{\beta}{2\tau_b}} \quad (46)$$

$$\Delta f_r = kt_r \quad (47)$$

$$\Delta f_f = kt_f \quad (48)$$

Figure D-1 in APPENDIX D shows the frequency bands that are defined by  $\Omega_1$ ,  $\Omega_2$ ,  $\Omega_3$ , and  $\Omega_4$ . As explained in that appendix, the approximations that yield Equations 38 and 39 are not valid when  $\Omega_1 < \Delta f < \Omega_2$  or  $\Omega_3 < \Delta f < \Omega_4$ .

#### BOUNDS ON THE VOLTAGE-DENSITY SPECTRUM

The function  $|F(\Delta f)|$ , which describes the magnitude of the spectrum, contains lobes, as shown in Figure 13. To simplify mathematical modeling, the usual practice in making EMC analyses is to represent the spectrum with a set of smooth curves that bound the spectrum. The functions used as the bound should satisfy two requirements -- simplicity of expression and production of a close-fitting bound or a good approximation thereof.

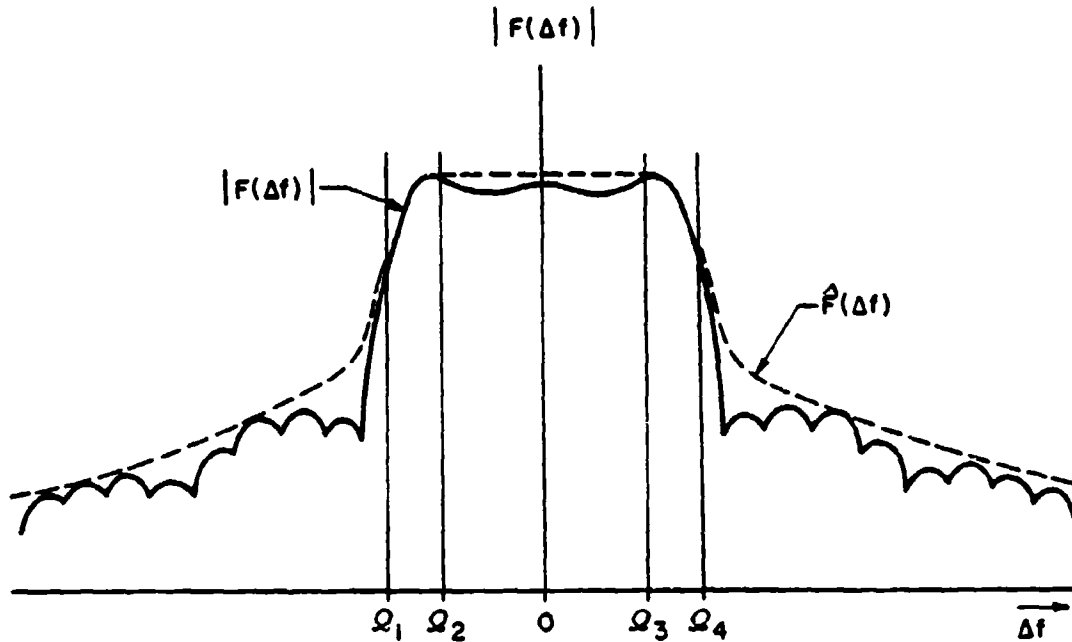


Figure 13. The voltage-density spectrum  $|F(\Delta f)|$  and its bound  $\hat{F}(\Delta f)$ .

The function that we will use as a bound on the spectrum is denoted by  $\hat{F}(\Delta f)$ . By definition the bound should satisfy the condition:

$$\hat{F}(\Delta f) \geq |F(\Delta f)| \quad (49)$$

Expressions for  $\hat{F}(\Delta f)$ , which has the general characteristics indicated in Figure 13, will be derived using Equations 38 through 42.

#### BOUNDS ON IN-BAND REGION OF SPECTRUM

For the interval between  $\Omega_2$  and  $\Omega_3$ , which we refer to as the in-band region, Equation 38 will be used to describe  $F(\Delta f)$ . As indicated in Figure 13,

the amplitude of the voltage-density spectrum is nearly constant in this region:

$$|F(\Delta f)| = \frac{V}{2\sqrt{k}}, \quad \Omega_2 < \Delta f < \Omega_3 \quad (50)$$

It follows that:

$$\hat{F}(0) = \frac{V}{2\sqrt{k}} = \frac{V}{2} \sqrt{\frac{\tau_b}{B}} \quad (51)$$

Near the lower end of this spectral region, where:

$$\Delta f = \Delta f_r = kt_r \quad (52)$$

Equation 41 is used to obtain:

$$\hat{F}(\Delta f_r) = \frac{\hat{F}(0)}{2} = \frac{V}{4\sqrt{k}} \quad (53)$$

Therefore, at  $\Delta f = kt_r$ ,  $\hat{F}(\Delta f)$  is approximately 6 dB down with respect to  $\hat{F}(0)$  when:

$$\Delta f = \Delta f_f = kt_f \quad (54)$$

Equation 42 is used to obtain:

$$\hat{F}(\Delta f) = \frac{\hat{F}(0)}{2} = \frac{V}{4\sqrt{k}} \quad (55)$$

Thus at  $\Delta f = kt_f$ ,  $\hat{F}(\Delta f)$  is approximately 6 dB down with respect to  $\hat{F}(0)$ .

#### BOUNDS ON THE SKIRTS OF THE SPECTRUM

When

$$\Delta f < \Omega_1 = -\frac{\beta\delta_r}{\delta_r + \delta_f} - \sqrt{\frac{\beta}{2\tau_b}} \quad (56)$$

or

$$\Delta f > \Omega_4 = \frac{\beta\delta_f}{\delta_r + \delta_f} + \sqrt{\frac{\beta}{2\tau_b}} \quad (57)$$

the variable  $|x_1|$  or  $|x_4| \geq 1$  and the voltage-density spectrum can be expressed in the form of an asymptotic expansion, as explained in APPENDIX D. Although it is not apparent at this point in the derivation, two frequencies critical in determining the bounds are  $\Delta f = \pm 1/(\pi\delta)$ . Therefore, the asymptotic expansion is expressed in two ways. When  $1/\pi\delta < \beta < |\Delta f|$ , it is convenient to use:

$$F(\Delta f) = -\frac{V}{8\pi} \sum_{i=1}^4 \frac{e^{j2\pi t (kt_i/2 - \Delta f)}}{\delta_i (kt_i - \Delta f)^2} \quad (58)$$

where

$$\delta_1 = \delta_r \quad \delta_2 = -\delta_r \quad \delta_3 = -\delta_f \quad \delta_4 = \delta_f$$

When  $\beta < |\Delta f| < 1/(\pi\delta)$  it is convenient to use:

$$F(\Delta f) = \frac{V e^{j\pi/2}}{4\pi} \quad (59)$$

$$\cdot \left\{ \left[ e^{j\pi k(t_r^2 + \delta_r^2/4)} \frac{e^{-j2\pi t_r \Delta f}}{(k t_r - \Delta f)} \frac{\sin \pi \delta_r (k t_r - \Delta f)}{\pi \delta_r (k t_r - \Delta f)} \right] \right. \\ \left. - \left[ e^{j\pi k(t_f^2 + \delta_f^2/4)} \frac{e^{-j2\pi t_f \Delta f}}{(k t_f - \Delta f)} \frac{\sin \pi \delta_f (k t_f - \Delta f)}{\pi \delta_f (k t_f - \Delta f)} \right] \right\}$$

The derivations for these equations are given in APPENDIX E.

First we consider the case where  $\beta < 1/\pi\delta$  and then the case where  $\beta > 1/\pi\delta$ .

For the Case When  $\beta < 1/\pi\delta$

When  $\beta < 1/\pi\delta$  the bound on the skirts of the spectrum is found by using Equation 59, as explained in APPENDIX F.

When  $\beta < |\Delta f| < 1/\pi\delta$ :

$$\hat{F}(\Delta f) = \frac{V}{4\pi} \left( \left| \frac{1}{(k t_r - \Delta f)} \right| + \left| \frac{1}{(k t_f - \Delta f)} \right| \right) \quad (60)$$

When  $\Delta f$  is slightly more negative than  $kt_f$ :

$$\hat{F}(\Delta f) = \left| \frac{V}{4\pi (kt_f - \Delta f)} \right| \quad (61)$$

When  $\Delta f$  is slightly more positive than  $kt_f$ :

$$\hat{F}(\Delta f) = \left| \frac{V}{4\pi (kt_f + \Delta f)} \right| \quad (62)$$

When  $-1/(\pi\delta_f) < \Delta f \ll kt_f$ :

$$\hat{F}(\Delta f) = \frac{V}{-2\pi\Delta f} \quad (63)$$

When  $kt_f \ll \Delta f < 1/(\pi\delta_f)$ :

$$\hat{F}(\Delta f) = \frac{V}{2\pi\Delta f} \quad (64)$$

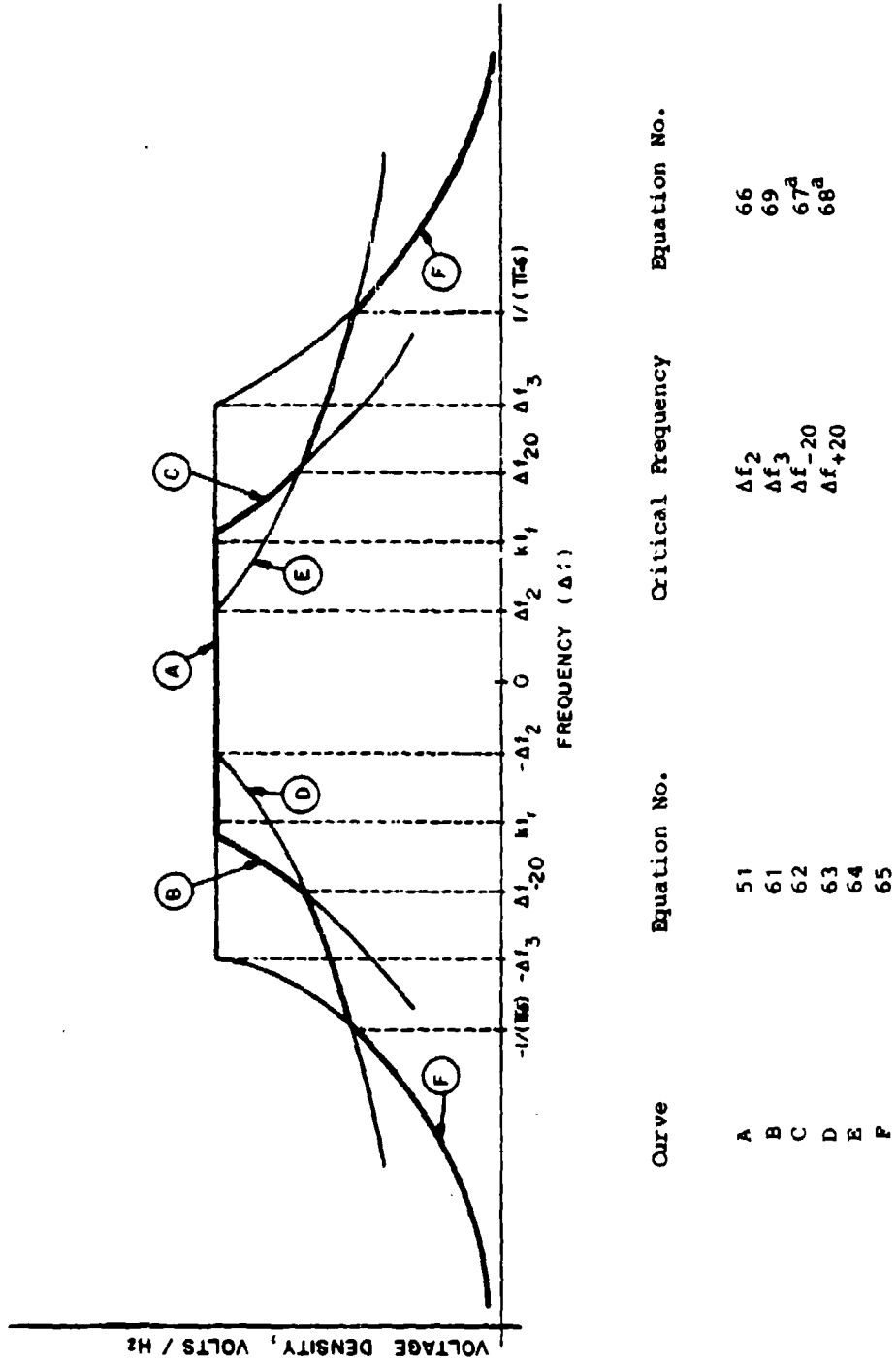
When  $\Delta f < -1/(\pi\delta_f)$ , or  $\Delta f > 1/(\pi\delta_f)$ :

$$\hat{F}(\Delta f) = \frac{V}{2\delta(\pi\Delta f)^2} \quad (65)$$

The curves described by these equations are shown in Figure 14.

Critical Frequencies. The critical frequencies at which the above curves intersect are as follows. Equating the curves given by Equations 51 and 64, gives:

$$\Delta f_2 = \frac{1}{\pi} \sqrt{\frac{\beta}{\tau_b}} \quad (66)$$



<sup>a</sup>The subscript 20 is used here because curves D and E have slopes of 20 dB per decade.

Figure 14. The curves that approximate the bounds on the voltage-density spectrum,  $F(\Delta f)$ , when  $\beta < 1/\pi\delta$ .

Equating the curves in Equations 61 and 53 gives:

$$\Delta f_{-20} = \frac{-2\beta\delta_r}{(\delta_r + \delta_f)} \left( 1 - \frac{\delta_r + \delta_f}{2\tau_b} \right) \quad (67)$$

Equating the curves in Equations 62 and 64 gives:

$$\Delta f_{+20} = \frac{2\beta\delta_f}{(\delta_r + \delta_f)} \left( 1 - \frac{\delta_r + \delta_f}{2\tau_b} \right) \quad (68)$$

Equating the curves in Equations 51 and 65 gives:

$$\Delta f_3 = \frac{1}{\pi} \left( \frac{\beta}{\tau_b} \right)^{1/4} \left( \frac{1}{\delta} \right)^{1/2} \quad (69)$$

where

$$\frac{1}{\delta} = \frac{1}{2} \left( \frac{1}{\delta_r} + \frac{1}{\delta_f} \right) \quad (70)$$

For the Case When  $\beta > 1/\pi\delta$

When  $\beta > 1/\pi\delta$ , the bound on the skirts of the spectrum is found by using Equation 58. As explained in APPENDIX G, the results are as follows:

$$\begin{aligned} \hat{F}(\Delta f) = & \frac{V}{8\pi^2} \left\{ \frac{1}{\delta_r} \left[ \frac{1}{(kt_1 - \Delta f)^2} + \frac{1}{(kt_2 - \Delta f)^2} \right] \right. \\ & \left. + \frac{1}{\delta_f} \left[ \frac{1}{(kt_3 - \Delta f)^2} + \frac{1}{(kt_4 - \Delta f)^2} \right] \right\} \quad (71) \end{aligned}$$

When  $\Delta f$  is slightly more negative than  $kt_1$ :

$$\hat{F}(\Delta f) = \frac{V}{8\pi^2} \frac{1}{\delta_r (kt_1 - \Delta f)^2} \quad (72)$$

The approximation given by Equation 72 will be used when  $\Delta f_{-40} < \Delta f < kt_1$ , where  $\Delta f_{-40}$  is given by Equation 76. For most chirp radar pulses, the approximation causes an error of about 5-6 dB at  $\Delta f = \Delta f_{-40}$ , which corresponds to point "b" in Figure 10. Because this error exists over a very small interval of frequency, it is acceptable for most EMC analyses.

Similarly, when  $kt_4 < \Delta f < \Delta f_{+40}$ , where  $\Delta f_{+40}$ :

$$\hat{F}(\Delta f) = \frac{V}{8\pi^2} \frac{1}{\delta_f (kt_4 - \Delta f)^2} \quad (73)$$

When  $\Delta f \ll kt_1$  or  $\Delta f \gg kt_4$ :

$$\hat{F}(\Delta f) = \frac{V}{(2\pi\Delta f)^2} \left( \frac{1}{\delta_r} + \frac{1}{\delta_f} \right) = \frac{V}{2\delta(\pi\Delta f)^2} \quad (74)$$

The parameter  $\delta$  is defined by Equation 27.

For the kinds of pulses used in most chirp radars, the approximation given by Equation 74 is in error by about 6 dB when  $|\Delta f| = \beta$ , and less than 1 dB when  $|\Delta f| \geq 3\beta$ . Equating 51 and 74 yields:

$$\Delta f_3 = \frac{1}{\pi} \left( \frac{\beta}{t_b} \right)^{1/4} \left( \frac{1}{\delta} \right)^{1/2} \quad (75)$$

Equating 72 and 74 yields:

$$\Delta f_{-40} = \frac{-\beta\delta_r}{\delta_r + \delta_f} \left( \frac{1}{1 - \sqrt{\frac{\delta_f}{2(\delta_r + \delta_f)}}} \right) \quad (76)$$

Equating 73 and 74 yields:

$$\Delta f_{+40} = \frac{\beta \delta_f}{(\delta_r + \delta_f)} \left( \frac{1}{1 - \frac{\delta_r}{2(\delta_r + \delta_f)}} \right) \quad (77)$$

The curves described by these equations are shown in Figure 15.

#### BOUNDS ON ENERGY-DENSITY SPECTRUM

Up to this point, the curves that approximate the bounds on the voltage-density spectrum have been derived. Next, we want to approximate the bounds on the single-sided energy-density spectrum  $E(f)$ . The relationship between these two functions, which is derived in APPENDIX A, is:

$$E(f) = 2 |V(f)|^2 = 2 |F(f)|^2, \quad f \geq 0 \quad (78)$$

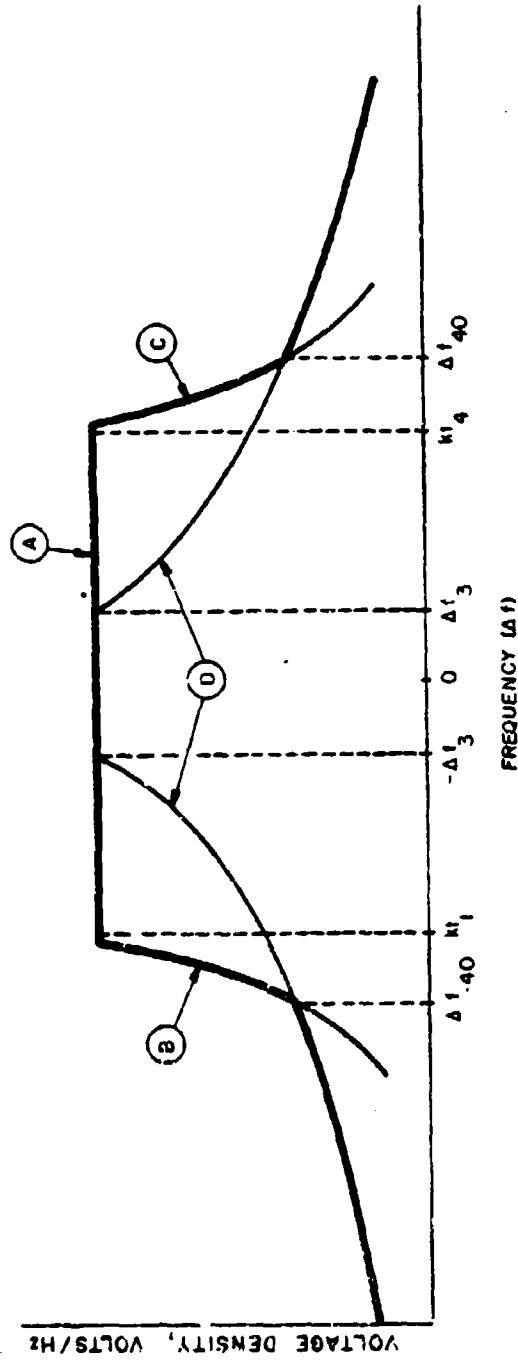
Note that we have defined the energy-density spectrum as being single sided, i.e., it exists for positive frequencies only. This is in contrast to the voltage-density spectrum, which exists for both negative and positive frequencies.

Using  $f_0$  as the reference frequency and letting  $\Delta f = f - f_0$ , we have:

$$E(\Delta f) = 2 |V(\Delta f)|^2 = 2 |F(\Delta f)|^2 \quad (79)$$

The bounds of  $E(\Delta f)$  are given by:

$$\hat{E}(\Delta f) = 2 |\hat{F}(\Delta f)|^2 \quad (80)$$



Curve	Equation No.	Critical Freq.	Equation No.
A	51	$\Delta f_3$	75
B	72	$\Delta f_{-40}$	76 <sup>a</sup>
C	73	$\Delta f_{+40}$	77 <sup>a</sup>
D	74		

<sup>a</sup>The subscript 40 is used here because both D curves have slopes of  $\pm 40$  dB per decade.

Figure 15. The curves that approximate the bounds on the voltage-density spectrum,  $\hat{F}(\Delta f)$ , when  $\beta > 1/\pi\delta$ .

With this relationship, we can express the approximate bounds for the various regions of the energy-density spectrum using Equations 51 through 77, which describe the bounds on the voltage-density spectrum.

Starting with Equation 51 we get:

$$\hat{E}(0) = 2[\hat{F}(0)]^2 = v^2 \tau_b / (2\beta) \quad (81)$$

Assuming a 1-ohm resistive load:

$$P = v^2 / 2 = v_{\text{rms}}^2 \quad (82)$$

where

$v$  is the peak instantaneous voltage, as indicated in Figure 12

$v_{\text{rms}}$  is the effective, or root-mean-square voltage

$P$  is defined as the average power over one cycle while the envelope of the pulse is at its maximum value, i.e., when  $t_2 \leq t \leq t_3$ .  $P$  is referred to as the peak power of the pulse.

Using Equations 81 and 82 gives the bounds at  $\Delta f = 0$ :

$$\hat{E}(0) = P \tau_b / \beta \text{ joules/Hz} \quad (83)$$

#### RELATIVE ENERGY DENSITY

For convenience, the bounds on the energy-density spectrum are normalized to the peak value and expressed in decibels. The normalized function, which is denoted by  $\epsilon(\Delta f)$  and is referred to as the relative energy-density spectrum, is obtained by.

$$\epsilon(\Delta f) = 10 \log[\hat{E}(\Delta f) / \hat{E}(0)] = 20 \log[\hat{F}(\Delta f) / \hat{F}(0)] \quad (84)$$

The various equations used to obtain  $\epsilon(\Delta f)$  are shown in Figures 16 and 17. A logarithmic scale is used for the abscissa and a dB scale is used for the ordinate so that the functions can be plotted as straight lines.

As indicated in these figures, the bounds on the relative energy-density spectrum in the vicinity of the -6 dB points are labeled  $a_-$  and  $a_+$  in the figures, and are more closely approximated by straight lines drawn through points  $a_-$  and  $b_-$  and through points  $a_+$  and  $b_+$ . Curves B and C in Figures 16 and 17 were useful for locating points  $b_-$  and  $b_+$ .

In the model described in Section 3:

$$\Delta f_{b-} = \begin{cases} \Delta f_{-40} & \text{when } \beta \delta \geq 1/\pi \\ \Delta f_{-20} & \text{when } \beta \delta < 1/\pi \end{cases} \quad (85)$$

$$\Delta f_{b+} = \begin{cases} \Delta f_{+40} & \text{when } \beta \delta \geq 1/\pi \\ \Delta f_{+20} & \text{when } \beta \delta < 1/\pi \end{cases} \quad (86)$$

#### METHOD FOR HANDLING NEGATIVE DEVIATION

As explained in the discussion associated with Equation 18b, defining  $k$ , the derivation assumes a positive frequency deviation during the pulse (frequency is shifted upward). With this condition the rise time tends to have the greatest influence on the negative region of the spectrum, and the fall time, on the positive region.

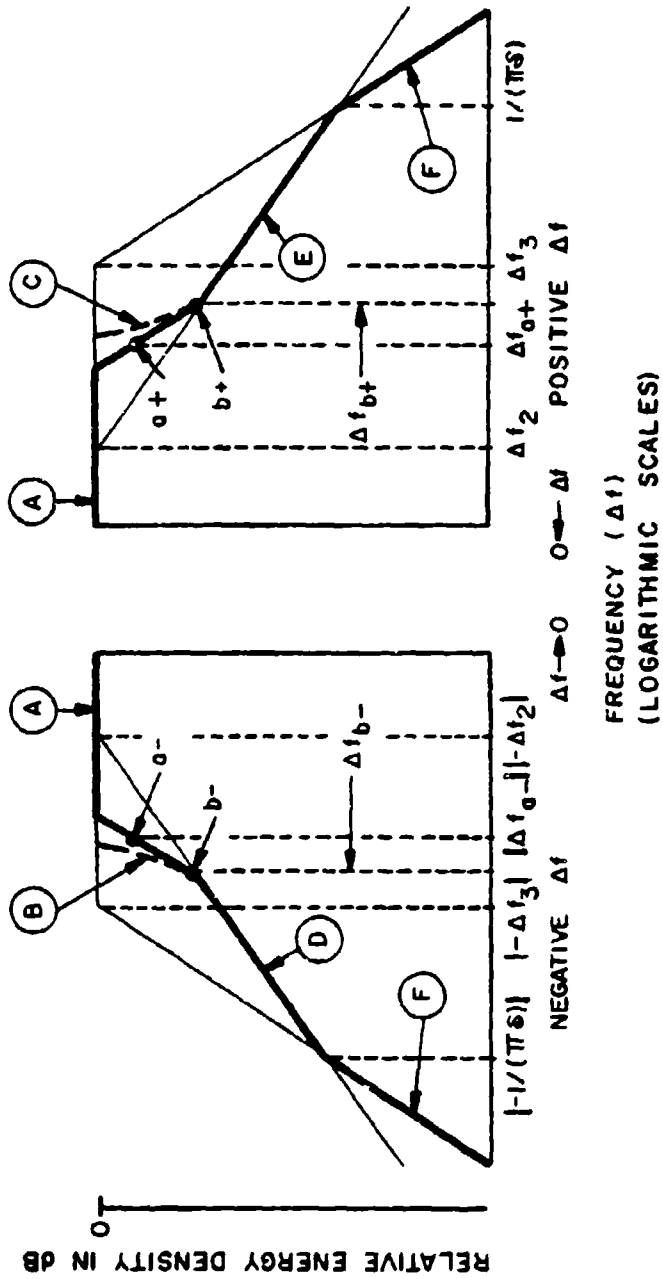


Figure 16. The curves that approximately bound the energy-density spectrum,  $\epsilon(\Delta f)$ , when  $\beta\delta < 1/\pi$ .  
(Page 1 of 2).

The labeled curves and lines correspond to the curves shown in Figure 14.

The relative amplitude is found by:

$$\text{Line A, } 20 \log \left[ \hat{F}(0)/\hat{F}(0) \right] = 0 \text{ dB}$$

Line through points a<sub>-</sub> and b<sub>-</sub>, is a better bound than Curve B. Point a<sub>-</sub> is located 6 dB down at  $\Delta f_{a-} = k\tau_r$  (see Equations 52 and 53) and point b<sub>-</sub> is located on line D at  $\Delta f_{b-} = \Delta f_{-20}$  (see Equation 74).

Line through points a<sub>+</sub> and b<sub>+</sub>, is a better bound than Curve C. Point a<sub>+</sub> is located 6 dB down at  $\Delta f_{a+} = k\tau_r$  (see Equations 54 and 55) and point b<sub>+</sub> is located on line D at  $\Delta f_{b+} = \Delta f_{+20}$  (see Equation 75).

Line D, found by using Equations 63, 78, 82, and 83, is:

$$10 \log \left[ \frac{P}{(\pi \Delta f)^2} \cdot \frac{\beta}{P\tau_b} \right] = 10 \log \left[ \frac{\beta}{\tau_b (\pi \Delta f)^2} \right]$$

Line E, found by using Equations 64, 78, 82, and 83, is:

$$10 \log \left[ \frac{\beta}{\tau_b (\pi \Delta f)^2} \right]$$

Line F, found by using Equations 65, 78, 82, and 83, is:

$$10 \log \left[ \frac{P}{\delta^2 (\pi \Delta f)^4} \cdot \frac{\beta}{P\tau_b} \right] = 10 \log \left[ \frac{\beta}{\tau_b \delta^2 (\pi \Delta f)^4} \right]$$

Figure 16. (Page 2 of 2).

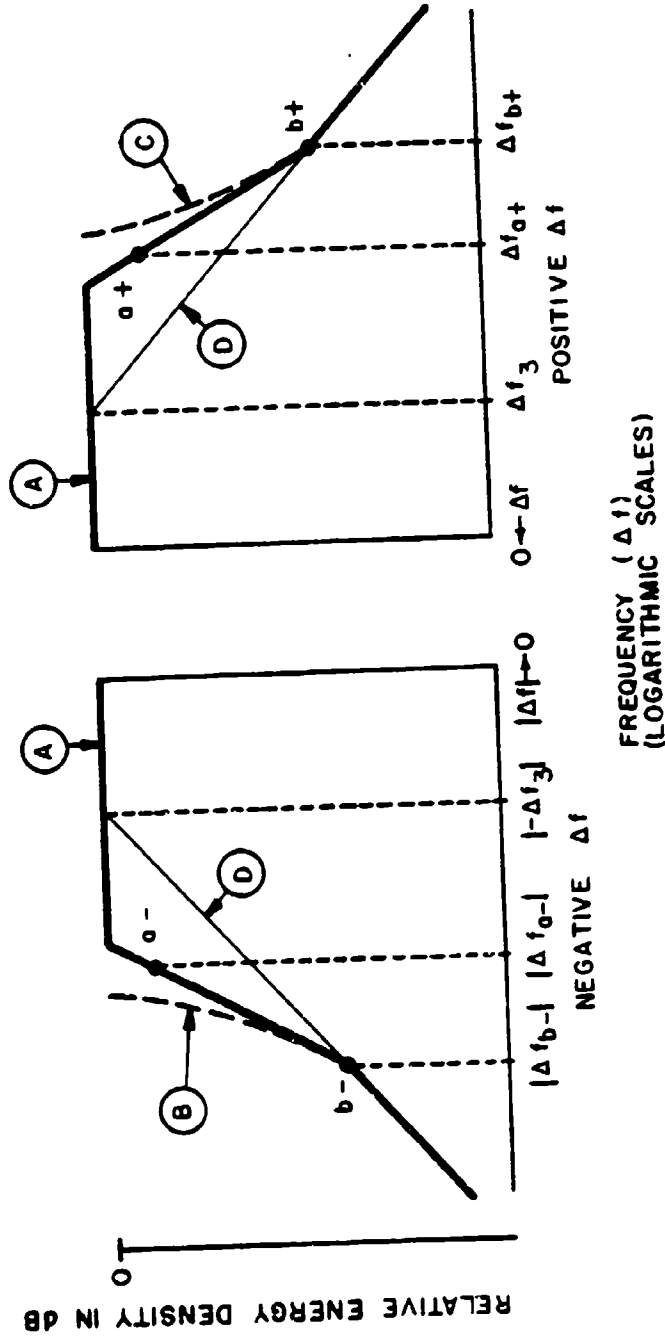


Figure 17. The curves that approximately bound the energy-density spectrum,  $\epsilon(\Delta f)$ , when  $\beta > 1/\pi\delta$ . (Page 1 of 2).

The labeled curves and lines correspond to the curves shown in Figure 15. The relative amplitude is found by:

$$10 \log [\hat{E}(f)/\hat{E}(0)] = 20 \log [\hat{F}(f)/\hat{F}(0)]$$

Line A is:  $20 \log [\hat{P}(0)/\hat{F}(0)] = 0 \text{ dB}$

Line through points a<sub>-</sub> and b<sub>-</sub>, is a better bound than curve B. Point a<sub>-</sub> is 6 dB down at  $\Delta f_{a-} = k\tau_T$  (see Equations 52 and 53) and point b<sub>-</sub> is located on line D at  $\Delta f_{b-} = \Delta f_{-40}$  (see Equation 71).

Line through points a<sub>+</sub> and b<sub>+</sub>, is a better bound than Curve C. Point a<sub>+</sub> is 6 dB down at  $\Delta f_{a+} = k\tau_f$  (see Equations 54 and 55) and point b<sub>+</sub> is located on line D at  $\Delta f_{b+} = \Delta f_{+40}$  (see Equation 72).

Line D, found using Equations 69, 78, 82, and 83, is:

$$10 \log \left[ \frac{P}{\delta^2 (\pi \Delta f)^4} \frac{\beta}{P\tau_b} \right] = 10 \log \left[ \frac{\beta}{\tau_b \delta^2 (\pi \Delta f)^4} \right]$$

Figure 17. (Page 2 of 2).

When the deviation is negative:

$$k = -\beta/\tau_b, \quad (87)$$

and the roles of  $\delta_r$  and  $\delta_f$  are interchanged; consequently,  $kt_1$  and  $kt_2$  are positive, and  $kt_3$  and  $kt_4$  are negative. In the model described in Section 3, the parameters Q, M, and N given in TABLE 1 enable the model to accommodate either positive or negative frequency deviation.

#### DISPLACEMENT BETWEEN $f_o$ AND $f_c$

Two key frequencies included among the parameters describing the chirp pulse are  $f_o$  and  $f_c$ , as shown in Figure 12.

$f_o$  = the instantaneous frequency at  $t = 0$ , the asymptotic frequency of the skirts of the spectrum.

$f_c$  = the instantaneous frequency that corresponds to the midpoint of the base of the pulse; the nominal center frequency.

When  $\delta_r = \delta_f$ ,  $f_o = f_c$ , but when  $\delta_r \neq \delta_f$ ,  $f_o$  and  $f_c$  are displaced from one another. Since  $f_o$  is not a given parameter it must be calculated.

When the deviation is positive:

$$f_o = f_c + \frac{\beta(\delta_r - \delta_f)}{2(\delta_r + \delta_f)} \quad (88)$$

When the deviation is negative:

$$f_o = f_c - \frac{\beta(\delta_r - \delta_f)}{2(\delta_r + \delta_f)} \quad (89)$$

Equations 88 and 89 are derived in APPENDIX I.

Consider the following example. Given:

$$\delta_r = .1\mu s \quad \delta_f = 1\mu s$$

$$\beta = 1 \text{ MHz, positive deviation}$$

$$f_c = 1100 \text{ MHz}$$

Calculate  $f_o$  using Equation 88:

$$\begin{aligned} f_o &= 1100 + \frac{1 (.1 - 1)}{2 (.1 + 1)} \\ &= (1100 - .41) \text{ MHz} \end{aligned}$$

Using  $f_o$  as the reference:

$$\Delta f_c = .41 \text{ MHz}$$

A plot of the bounds on the spectrum of this example would have the characteristics shown in Figure 18. Two numerical examples of asymmetrical pulses are also included in Section 5.

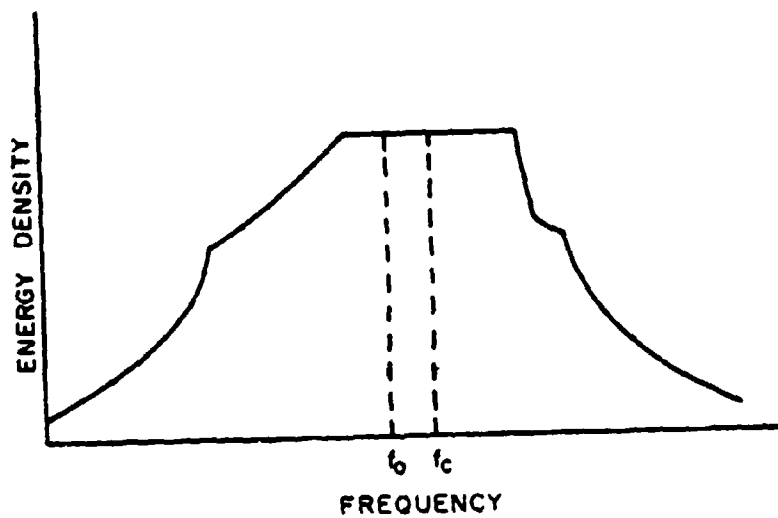


Figure 18. Relationship between  $f_0$  and  $f_c$  for the example on the preceding page.

SECTION 5  
 NUMERICAL EXAMPLES OF THE  
 BOUNDS ON CHIRP SPECTRA

To aid the reader in applying the procedures for plotting the spectral bounds on chirp pulses, seven numerical examples are presented here. The given parameter values that describe the chirp waveforms and calculated parameter values that are used in plotting the spectral bounds are listed in TABLE 2. The resulting graphs, which are shown in Figures 19 through 25, illustrate the effect of the pulse parameters on the overall shape of the spectrum.

In Examples 1 through 5, the pulse shapes are symmetrical, i.e.,  $\delta_r = \delta_f$ . For that condition, the spectrum and its bounds are symmetrical about the carrier frequency,  $f_c$ , so that  $f_0 = f_c$ .

In Examples 6 and 7, the pulses are asymmetrical. Plots of the bounds for these two examples are shown in Figures 24 and 25. The bounds for example 7 are also plotted in Figures 26 and 27, which have linear frequency scales. Each of these two figures includes a graph of the energy-density function (solid line) as well as the bounds (dashed line) to show how well the bounds fit the spectral-density function and to better show the effects of pulse asymmetry. Each graph shows the relative spectral density as a function of the variable  $\Delta f$  (scale along the bottom of the graph) and as a function of the variable  $\Delta f_c$  (scale along the top of the graph)

where

$$\Delta f = f - f_0$$

$$\Delta f_c = f - f_c$$

$$f = \text{frequency of interest}$$

TABLE 2  
 TABULATION OF THE GIVEN AND CALCULATED PARAMETER VALUES FOR THE EXAMPLES

Example Number	Given Parameter Values					Calculated Parameter Values <sup>a</sup>								Figure Number
	B (MHz)	$\tau_b$ ( $\mu$ s)	$\delta_r$ ( $\mu$ s)	$\delta_f$ ( $\mu$ s)		$\Delta f_3$ (MHz)	$\Delta f_{a+}$ (MHz)	$\Delta f_{b+}$ (MHz)	$\Delta f_{a-}$ (MHz)	$\Delta f_{b-}$ (MHz)	$f_o - f_c$ (MHz)			
1	0.35	100	1	1		0.077	0.173	0.347	-0.173	-0.347	0	19		
2	0.05	100	1	1		0.048	-0.250	0.050	0.025	-0.050	0	20		
3	10	10	0.1	0.1		1.010	4.950	9.900	-4.950	-9.900	0	21		
4	1	100	10	10		0.032	0.450	0.900	-0.450	-0.900	0	22		
5	0.2	100	1	1		0.067	0.099	0.198	-0.099	-0.198	0	23		
6	1	102	10	1		0.135	0.086	0.279	-0.086	-1.155	0.409	24		
7	1	111	1	10		0.073	0.864	1.156	-0.086	-0.279	-0.409	25		

<sup>a</sup> These parameter values were calculated using the procedures given in Section 3.

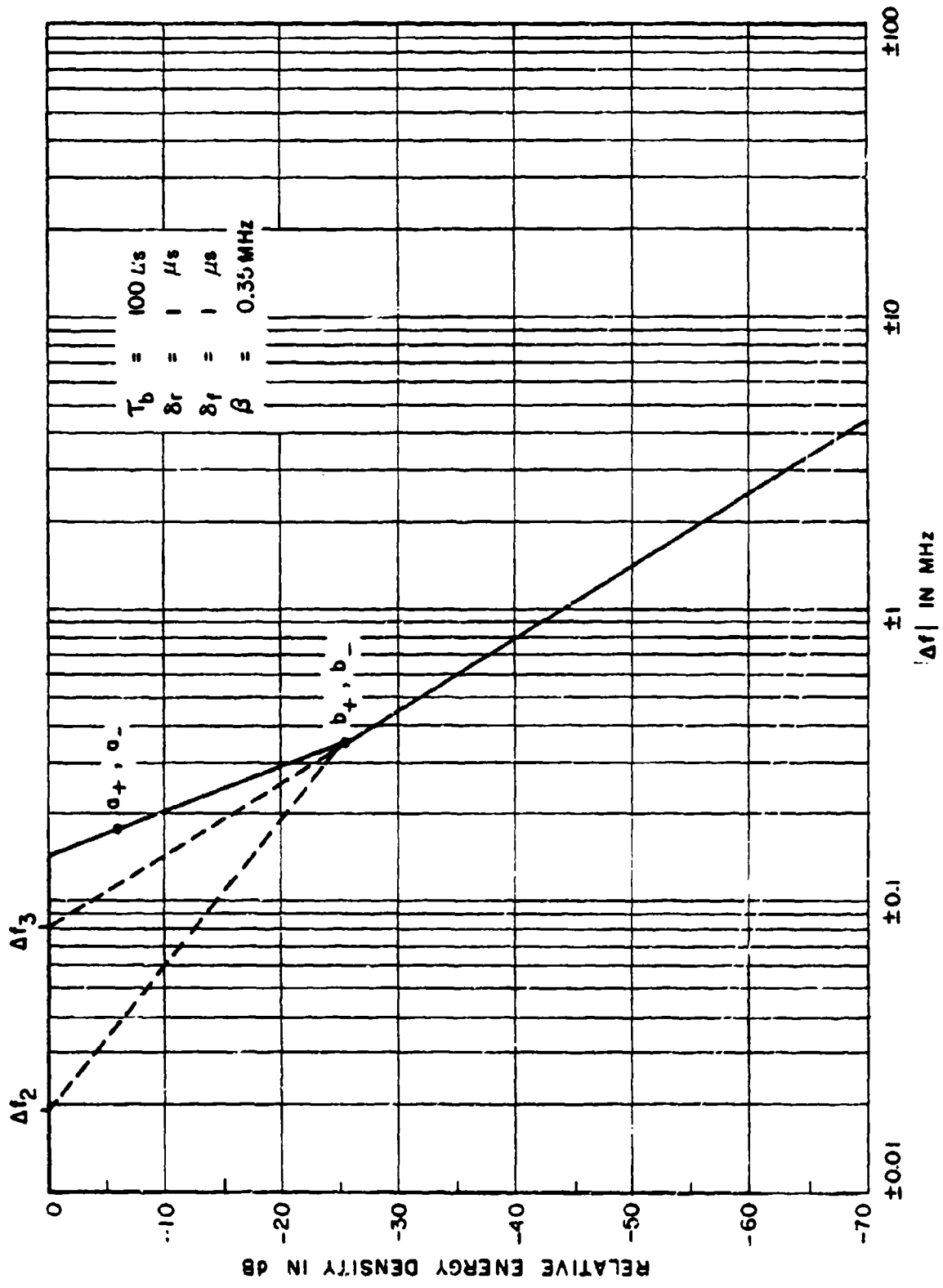


Figure 19. A graph of the spectral bounds for Example 1.

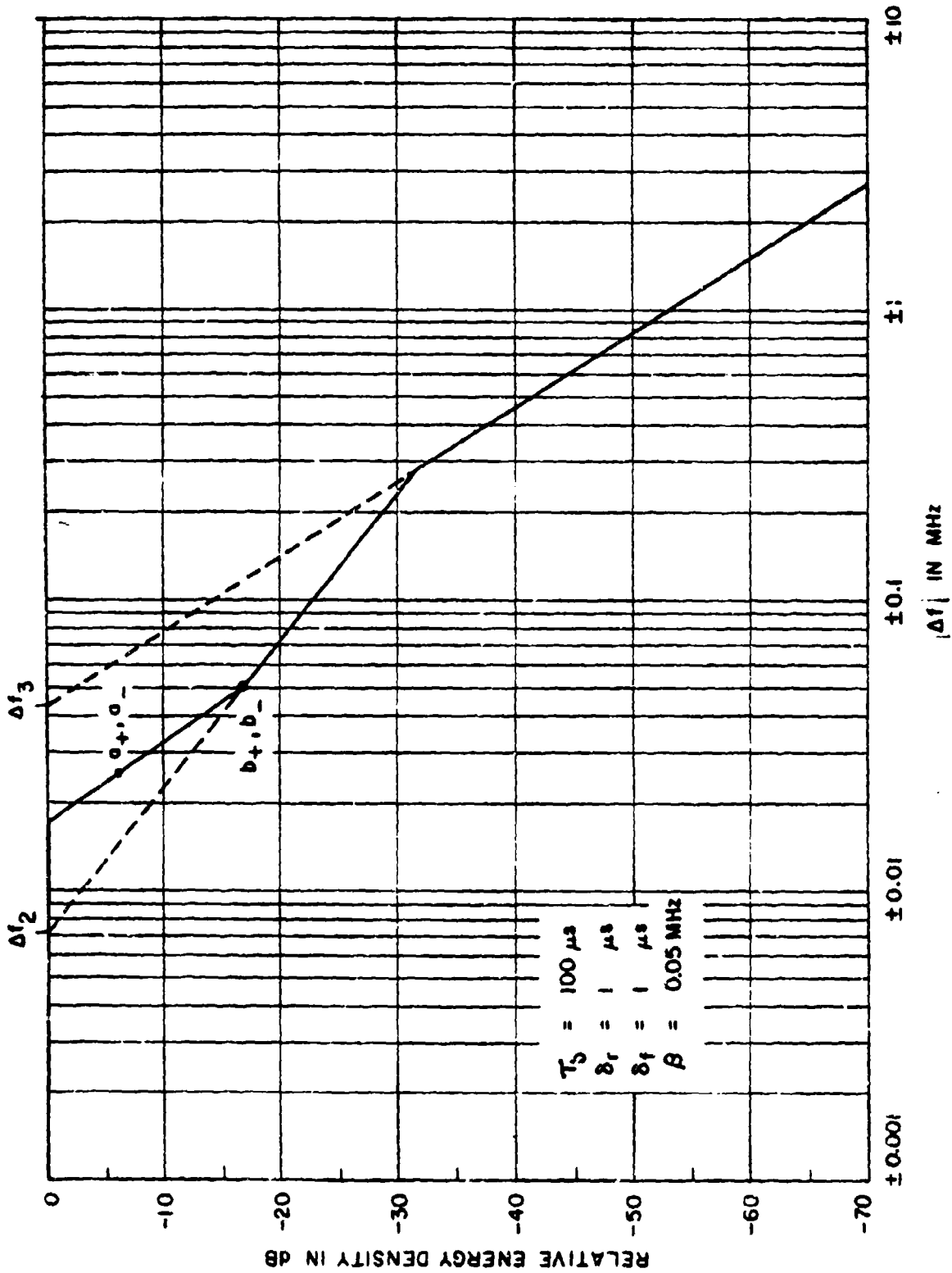


Figure 20. A graph of the spectral bounds for Example 2.

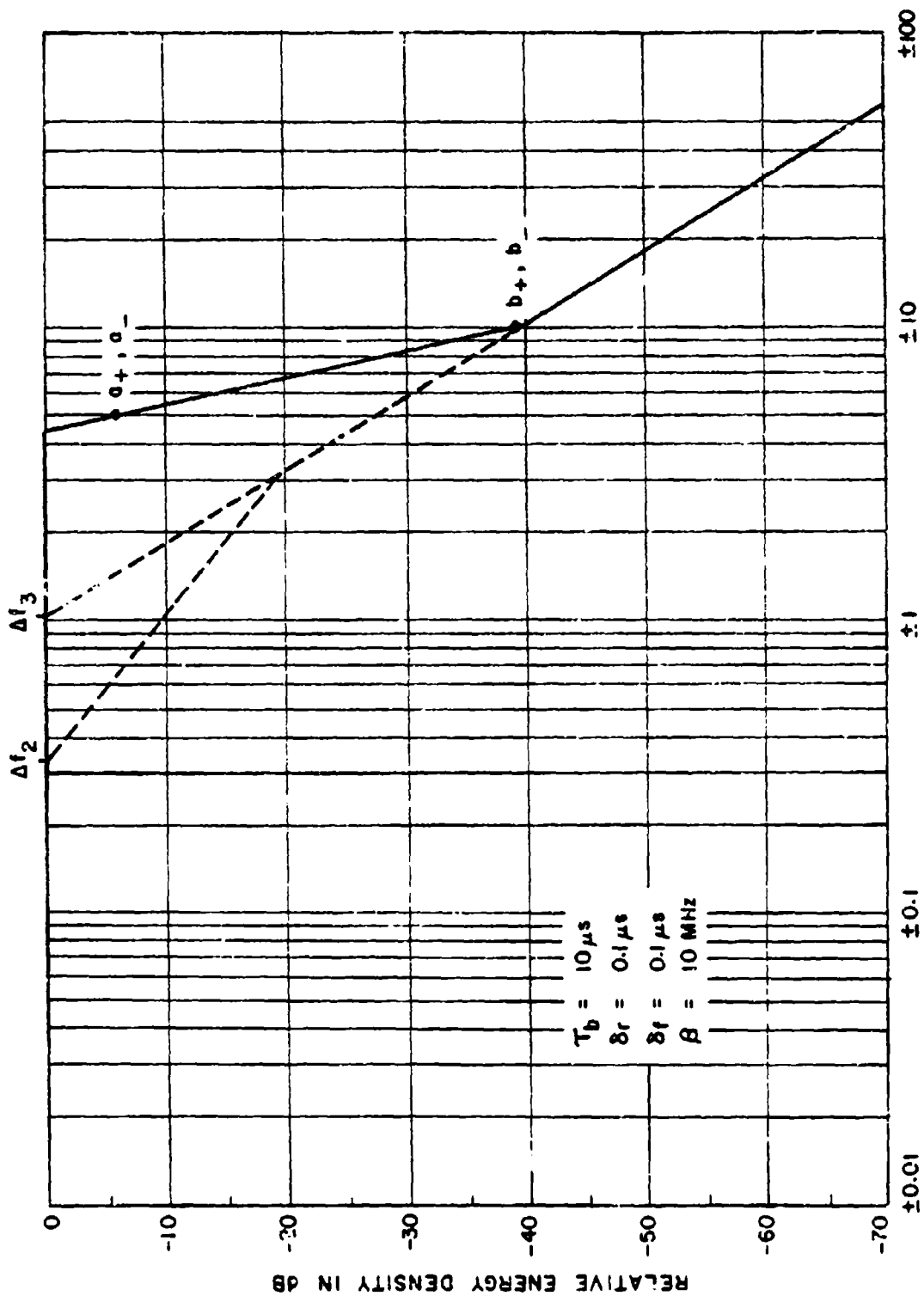


Figure 21. A graph of the spectral bounds for Example 3.

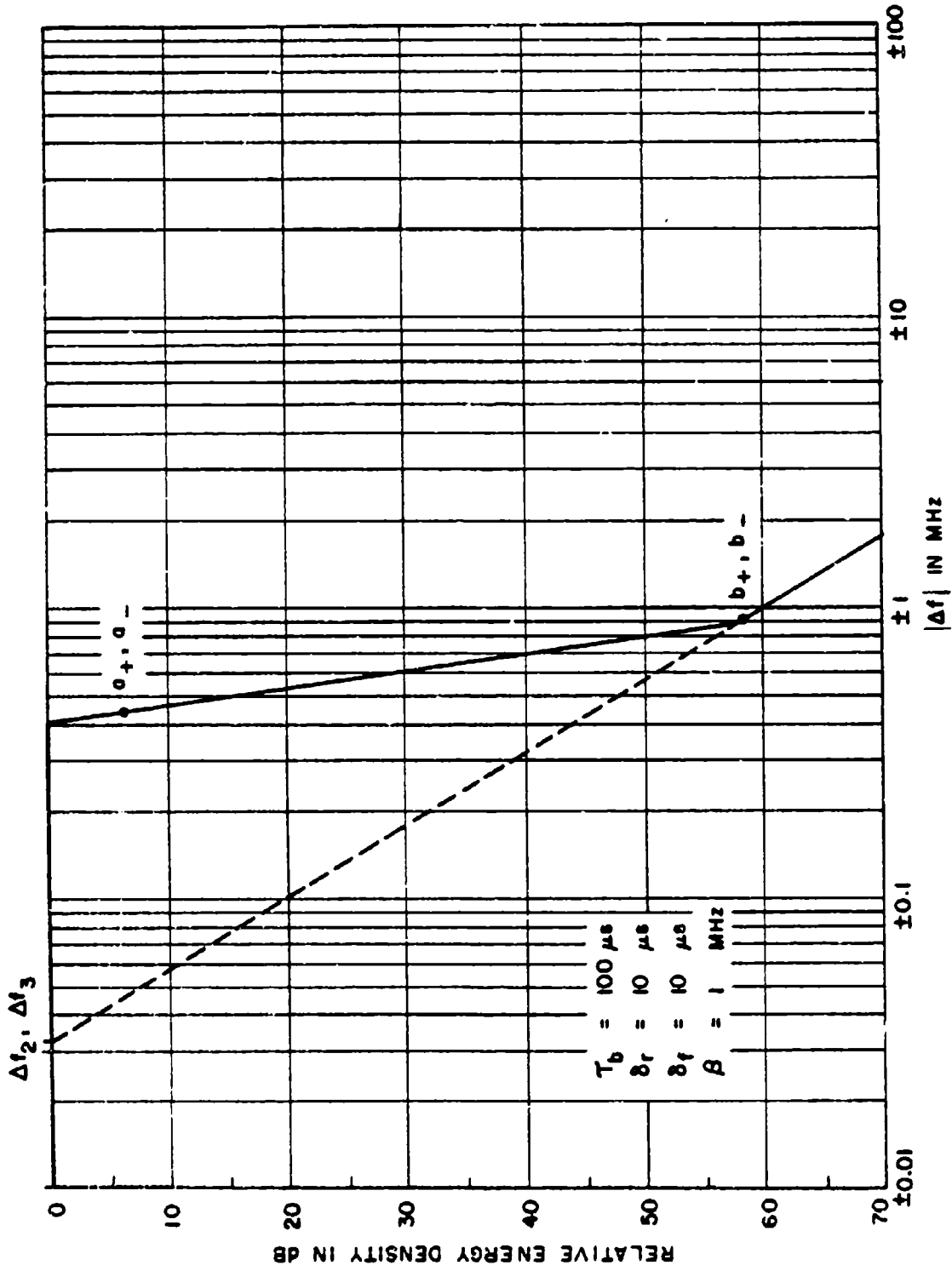


Figure 22. A graph of the spectral bounds for Example 4.

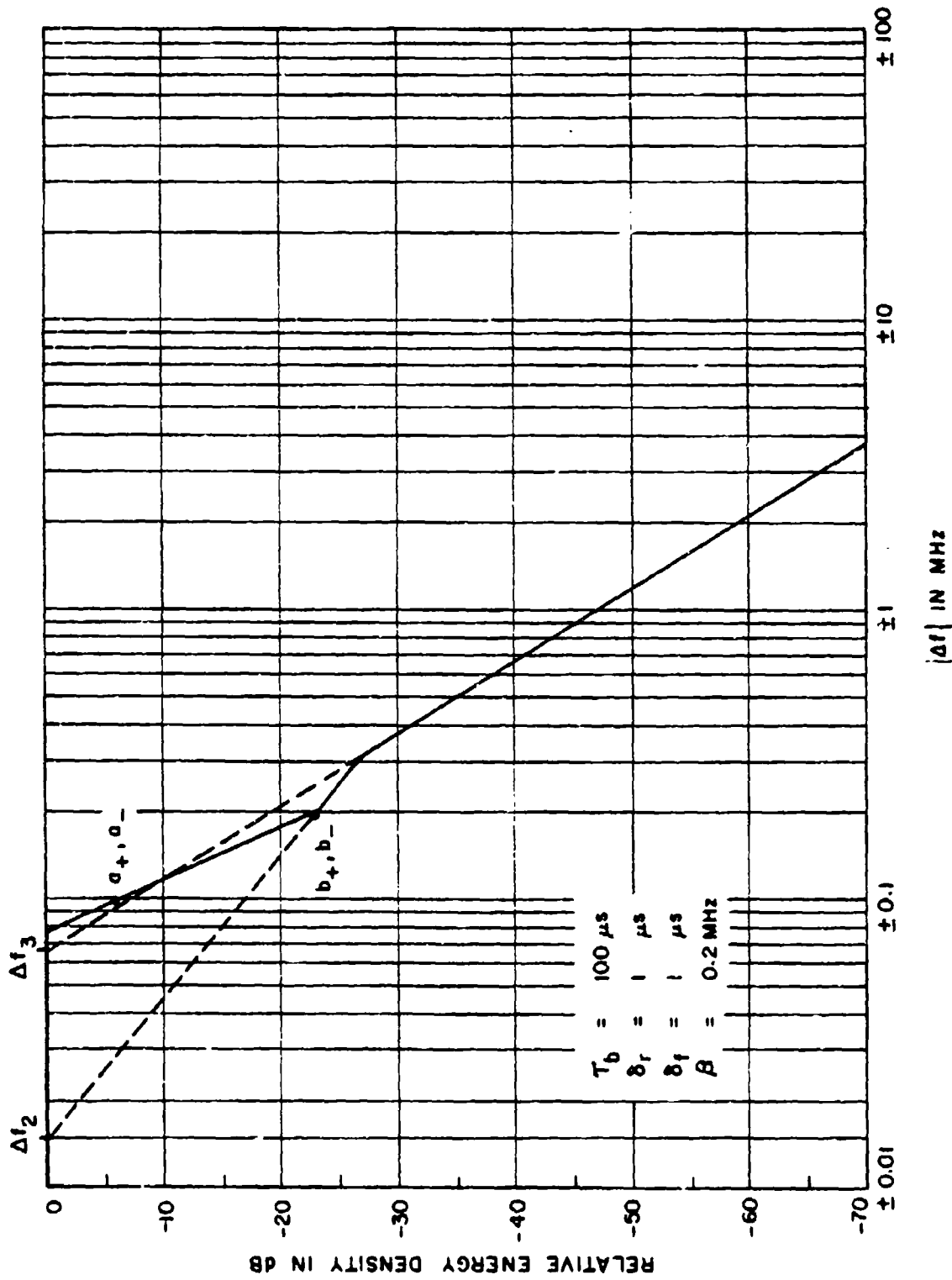


Figure 23. A graph of the spectral bounds for Example 5.

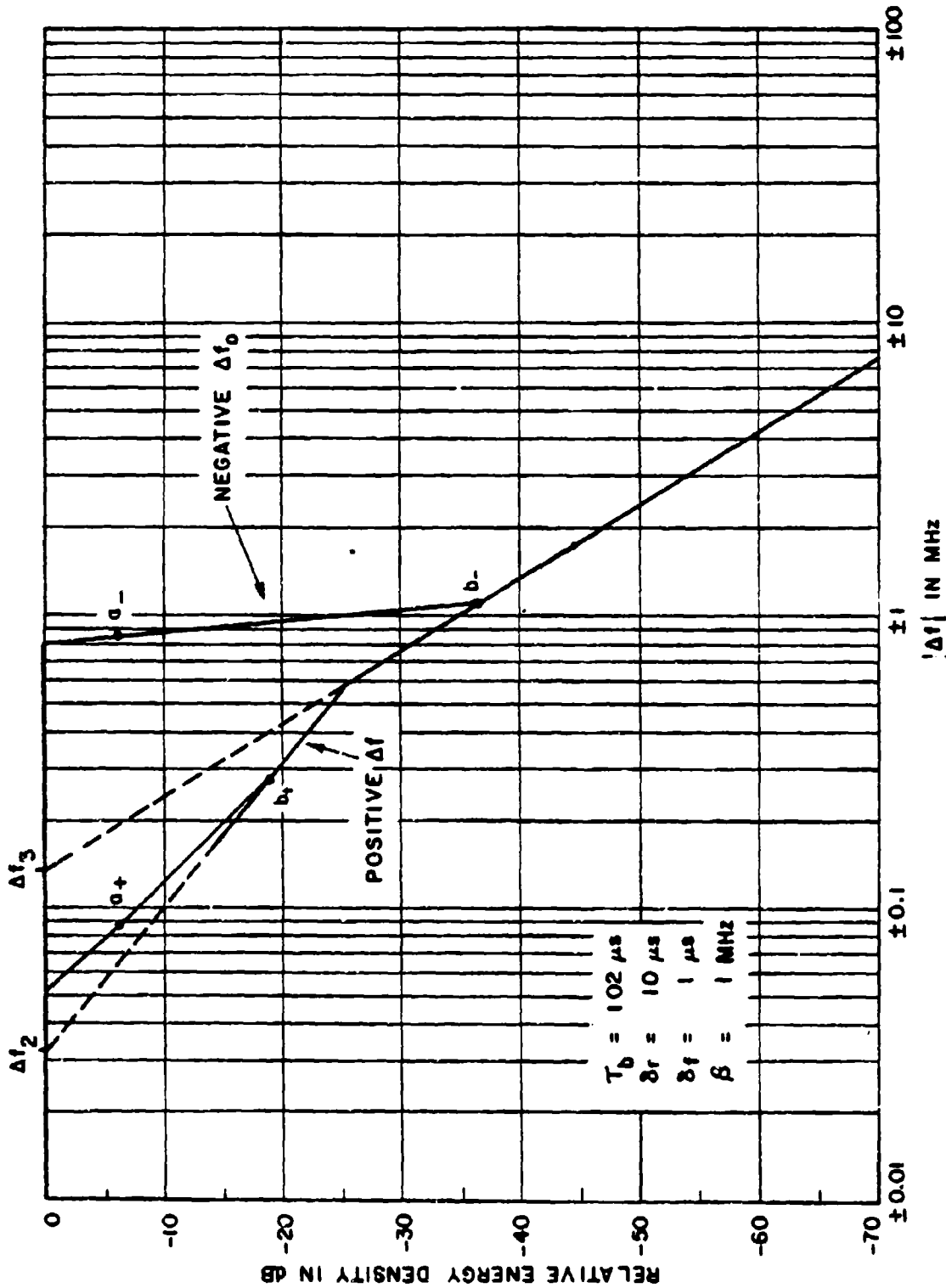


Figure 24. A graph of the spectral bounds for Example 6.

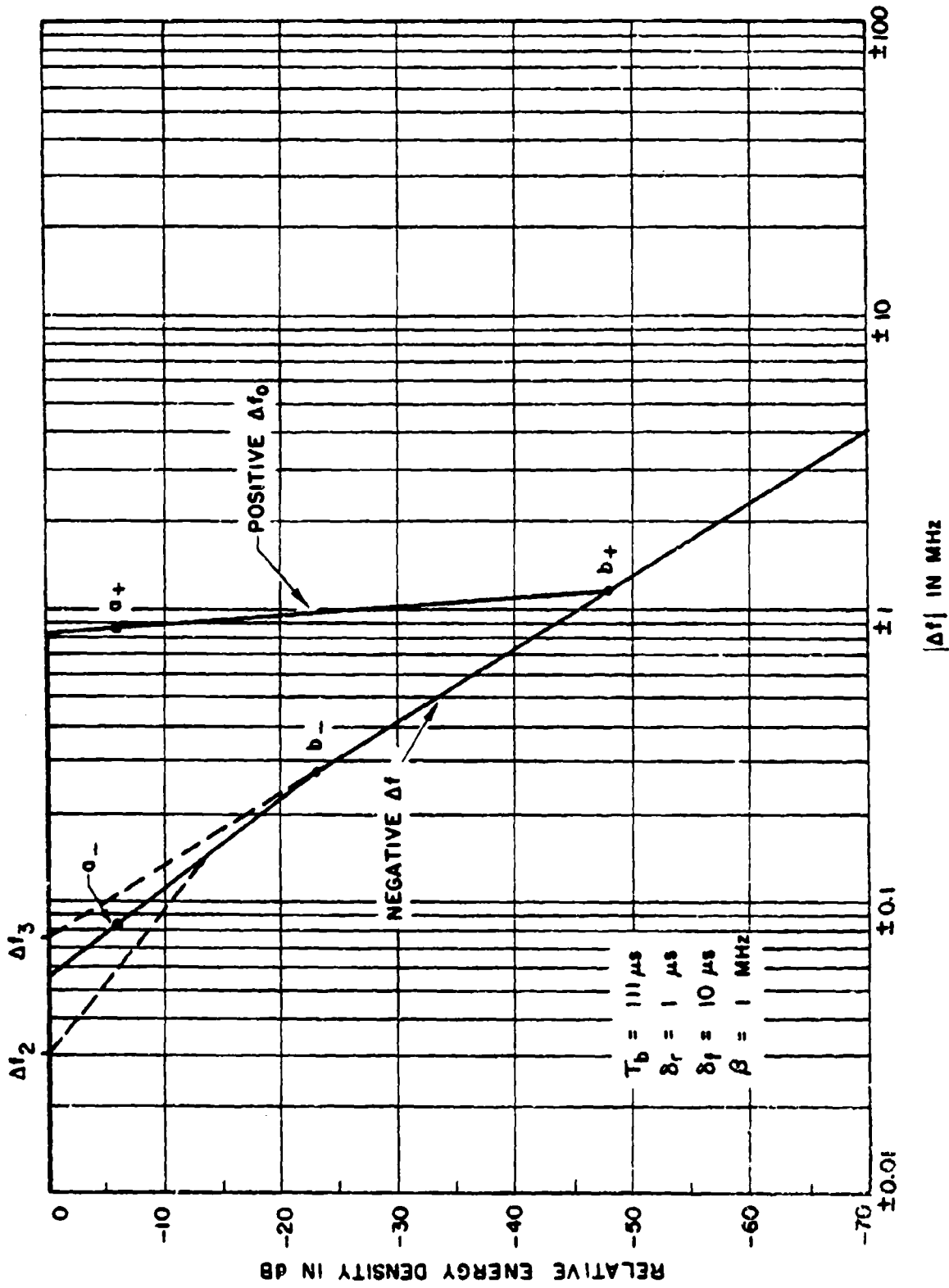


Figure 25. A graph of the spectral bounds for Example 7.

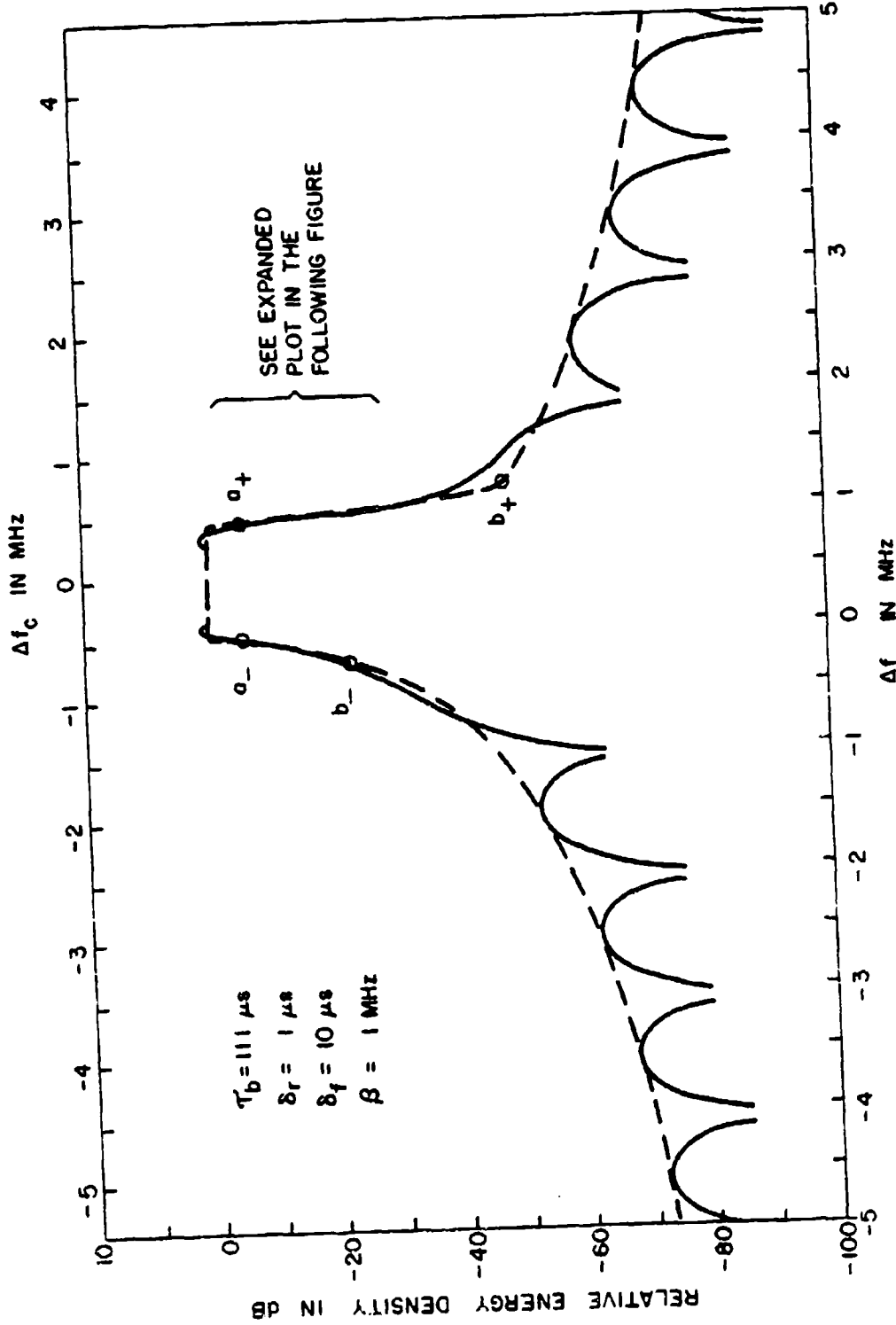


Figure 26. Graphs of the relative energy density function (solid line) and the bounds (dashed line) for Example 7; note that the frequency scale is linear.

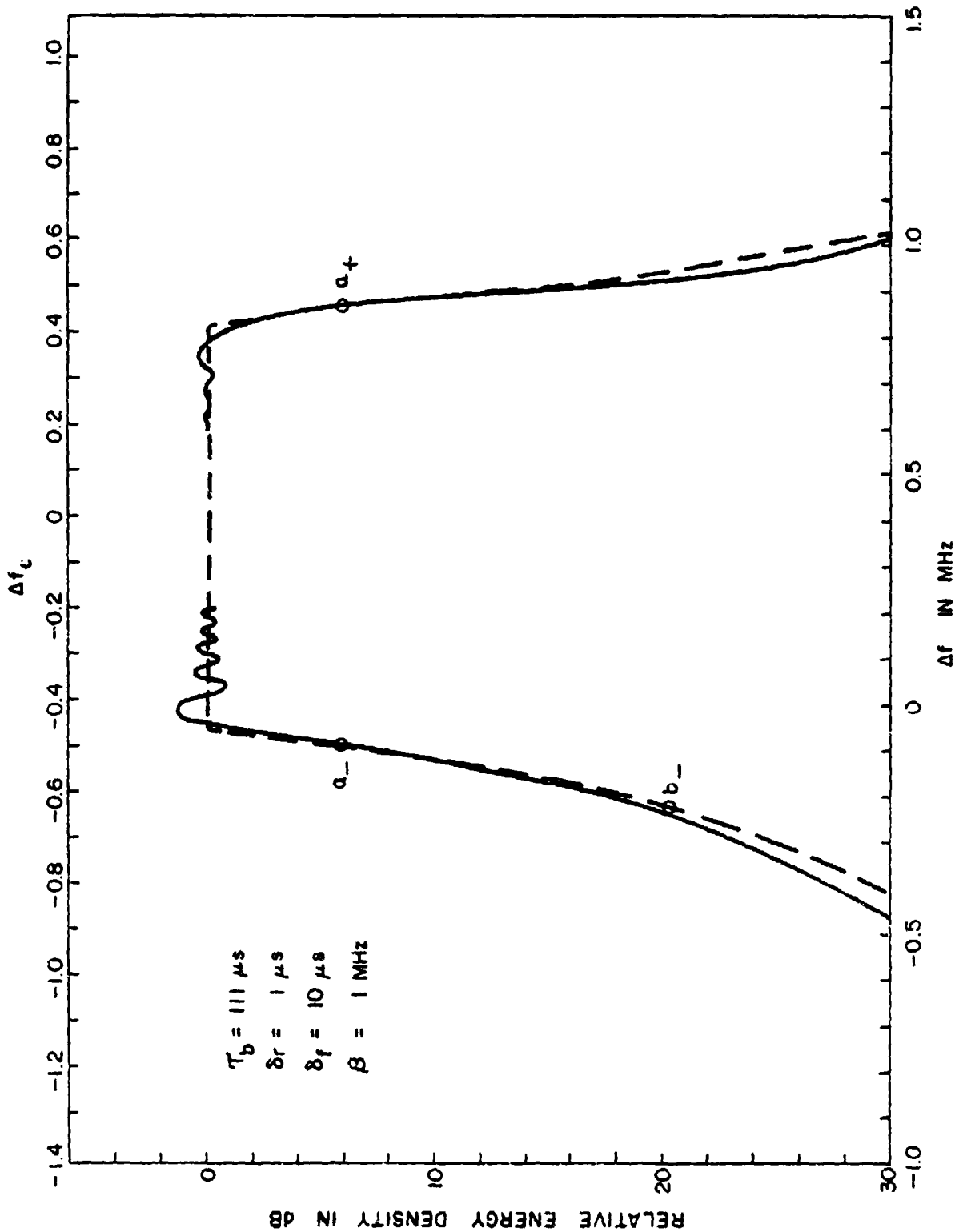


Figure 27. Expanded plots of the relative energy density function (solid line) and the bounds (dashed line) for Example 7.

$f_c$  = carrier frequency of the chirp pulse

$f_o$  = the frequency about which the lower skirts of the spectral bounds are symmetrical.

The relationship between  $f_o$  and  $f_c$  is illustrated graphically in Figure 12. The offset,  $f_o - f_c$ , is given by Equation 5.

As illustrated in Figures 26 and 27, that part of the spectral bounds between point  $a_-$  and  $a_+$  is nearly symmetrical about  $f_c$ ; whereas, the bounds to the left of point  $b_-$  and to the right of point  $b_+$  are symmetrical about  $f_o$ .

The relative energy density function,  $\epsilon(\Delta f)$ , in Figure 26 appears as a smooth curve. Actually, there are minor ripples with an amplitude of about  $\pm 1$  dB and with a period of  $1/\tau_b$ .

APPENDIX A  
TREATMENT OF NEGATIVE FREQUENCIES

(Equations in this appendix that already appeared in the body of the report will be identified by their original numbers.)

The voltage-density spectrum of a linear FM trapezoidal pulse may be expressed in the form:

$$V(f) = \int_{-\infty}^{\infty} v(t) e^{-j2\pi ft} dt$$

where

$$v(t) = A(t) \cos [2\pi(f_0 t + kt^2/2)]$$

$A(t)$  = amplitude of trapezoidal pulse in the interval  $t_1$  to  $t_4$ .

Using Euler's formulas:

$$e^{jy} = \cos y + j \sin y$$

$$e^{-jy} = \cos y - j \sin y$$

we obtain the formulas:

$$F(f) = \frac{1}{2} \int_{t_1}^{t_4} A(t) e^{j2\pi [kt^2/2 + (f_0 - f)t]} dt \quad (30)$$

$$G(f) = \frac{1}{2} \int_{t_1}^{t_4} A(t) e^{-j2\pi [kt^2/2 + (f_0 + f)t]} dt \quad (31)$$

$$V(f) = F(f) + G(f).$$

Thus the voltage-density spectrum consists of the sum of two spectra:  $F(f)$ , which is centered on  $+f_0$  and  $G(f)$ , which is centered on  $-f_0$ . The following

analysis will show that  $|G(f)|$  is approximately 20 dB less than  $|F(f)|$  in the region  $f_0/2 < f < 2f_0$  and  $|F(f)|$  is approximately 20 dB less than  $|G(f)|$  in the region  $-2f_0 < f < -f_0/2$ . Based on these inequalities, we state that:

$$|V(f)| = |G(f)|, \quad -2f_0 < f < -f_0/2 \quad (\text{A-1})$$

$$|V(f)| = |F(f)|, \quad f_0/2 < f < 2f_0 \quad (\text{A-2})$$

These relations permit the bounds on  $V(f)$  in the region  $f_0/2 < f < 2f_0$  to be determined only by considering the bounds on  $|F(f)|$  in that region.

To justify the statement concerning the relations between  $|F(f)|$  and  $|G(f)|$ , consider the expression for the positive part of the spectrum centered on  $+f_0$  of a symmetrical trapezoidal RF pulse having no FM as:

$$F(\Delta f) = \frac{V}{2} \left[ \tau \frac{\sin \pi \tau \Delta f}{\pi \tau \Delta f} \cdot \frac{\sin \pi \delta \Delta f}{\pi \delta \Delta f} \right]$$

where  $\tau$  is the mean pulse length and  $\delta$  is the rise and fall time of the pulse and  $\Delta f = f - f_0$ . For  $f = f_0/2$ , we have:

$$\left| \frac{F(f_0/2)}{G(f_0/2)} \right| = \left( \frac{3}{2} \frac{f_0}{f_0/2} \right)^2 = 9$$

or  $|G(f_0/2)|$  is about 20 dB less than  $|F(f_0/2)|$ . For  $f = 2f_0$ , we have

$$\left| \frac{F(2f_0)}{G(2f_0)} \right| = \left( \frac{3f_0}{f_0} \right)^2 = 9$$

or  $|G(2f_0)|$  is about 20 dB less than  $|F(2f_0)|$ .

These relations also apply to an asymmetrical trapezoidal RF pulse having FM, as can be demonstrated by considering the bounds on the skirts of the spectrum as expressed by Equations 74 and 65 in APPENDIX G and APPENDIX F, respectively. Equations 30 and 31 can be rewritten to show that:

$$F(f) = G^*(-f) \quad (A-3)$$

Thus:

$$|F(f)|^2 = |G(-f)|^2 \quad (A-4)$$

Using Equations A-1, A-2, and A-4, we have:

$$|V(f)|^2 = |V(-f)|^2, \text{ when } f_0/2 < |f| < 2f_0 \quad (A-5)$$

Thus, the energy density at  $f$  is equal to the energy density at  $-f$ . Next, we will use Sakrison's interpretation of energy density.<sup>4</sup>

The energy-density spectrum of the chirp pulse can be expressed as:

$$|V(+f)|^2 + |V(-f)|^2 = 2|F(f)|^2 \quad (A-6)$$

Using this approximation in determining the bounds on the energy-density spectrum causes an error of approximately 1% for the spectral region  $f_0/2 < f < 2f_0$ , since:

$$\left| \frac{G}{V} \right|^2 = \left| \frac{G}{F+G} \right|^2 < \left| \frac{G}{9G+G} \right|^2 = \frac{1}{100}$$

<sup>4</sup>Sakrison, D.J., Communication Theory: Transmission of Waveforms and Digital Information, John Wiley and Sons, Inc., New York, NY, 1968, p.48.

To justify Equation A-6, consider applying  $v(t)$ , the chirp signal, to the input of an ideal bandpass filter which has passbands centered at  $f = \pm f_r$  and each has a bandwidth of  $\Delta$  Hz, as shown in Figure A-1. If the bandwidth,  $\Delta$ , is so small that  $V(f)$  is approximately constant in the interval  $|f \pm f_r| < \Delta/2$ , the Fourier transform of the output,  $y(t)$ , is:

$$Y(f) = \begin{cases} V(+f_r), & \text{when } |f-f_r| < \Delta/2 \\ V(-f_r), & |f+f_r| < \Delta/2 \\ 0, & \text{elsewhere} \end{cases} \quad (\text{A-7})$$

If the output,  $y(t)$ , is the voltage across a 1-ohm resistive load, the energy dissipated in the resistor is:

$$\begin{aligned} \int_{-\infty}^{\infty} y^2(t) dt &= \int_{-\infty}^{\infty} |Y(f)|^2 df & (\text{A-8}) \\ &= \Delta |V(f_r)|^2 + |V(-f_r)|^2 \end{aligned}$$

By using Equations A-1, A-2, and A-4, the above yields:

$$\int_{-\infty}^{\infty} y^2(t) dt = \Delta |F(f_r)|^2 + |G(-f_r)|^2 = 2\Delta |F(f_r)|^2 \quad (\text{A-9})$$

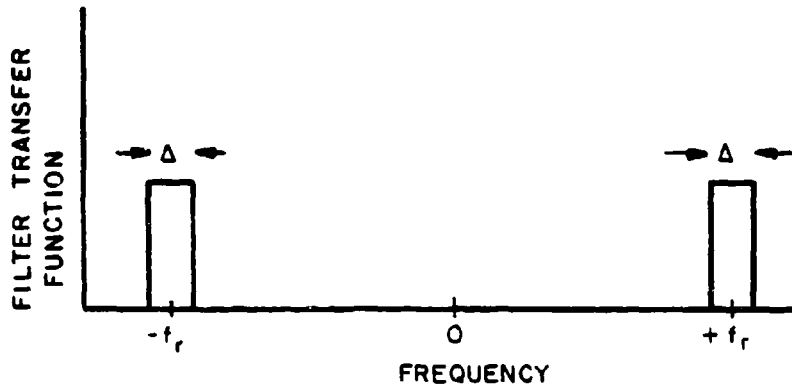


Figure A-1. Band-pass filter used by Sakrison to interpret the energy-density spectrum (see Reference 4).

Thus, the energy-density spectrum of the chirp pulse can be expressed as:

$$|V(+f)|^2 + |V(-f)|^2 = 2 |F(f)|^2 \quad (\text{A-6})$$

APPENDIX B  
DERIVATION OF THE VOLTAGE-DENSITY  
FUNCTION (EQUATION 30)

(Equations in this appendix that have already appeared in the body of the report will be identified by their original numbers.)

Starting with Equation 30:

$$F(f) = 1/2 \int_{t_1}^{t_4} A(t) e^{j 2\pi [kt^2/2 + (f_0 - f)t]} dt$$

we will proceed to derive the solution to this integral. Using Equation 18a, the equation above becomes, by referring to Figure H-1:

$$F(f) = F_{1,2}(f) + F_{2,3}(f) + F_{3,4}(f) \quad (B-1)$$

where

$$F_{1,2}(f) = 1/2 \int_{t_1}^{t_2} \frac{V(t-t_1)}{\delta_r} e^{j2\pi [kt^2/2 + (f_0 - f)t]} dt \quad (B-2a)$$

$$F_{2,3}(f) = 1/2 \int_{t_2}^{t_3} V e^{j2\pi [kt^2/2 + (f_0 - f)t]} dt \quad (B-2b)$$

$$F_{3,4}(f) = 1/2 \int_{t_3}^{t_4} \frac{V(t_4-t)}{\delta_f} e^{j2\pi [kt^2/2 + (f_0 - f)t]} dt \quad (B-2c)$$

Using Reference 4, several general relationships will be used to evaluate these integrals:

$$\int_{t_a}^{t_b} e^{j2\pi [kt^2/2 + (f_0 - f)t]} dt = \frac{1}{\sqrt{2k}} e^{-j\pi(f_0 - f)^2/k} [Z(\chi_b) - Z(\chi_a)] \quad (B-3)$$

Derivation of B-3 using formula 7.438<sup>5</sup> where  $a = \pi k$ ,  
 $2b = 2\pi(f_0 - f)$ , and  $c = 0$ , follows:

---

<sup>5</sup>National Bureau of Standards, Handbook of Mathematical Functions with Formulas, Graphs, and Mathematical Tables, National Bureau of Standards Applied Mathematics Series, June 1964, Equations 7.9.38 - 7.4.41.

$$\int_{t_a}^{t_b} e^{j2\pi \left[ kt^2/2 + (f_o - f)t \right]} dt = \int_{t_a}^{t_b} \cos 2\pi \left[ kt^2/2 + (f_o - f)t \right] dt + \\ + j \int_{t_a}^{t_b} \sin 2\pi \left[ kt^2/2 + (f_o - f)t \right] dt$$

$$\int_{t_a}^{t_b} \cos 2\pi \left[ kt^2/2 + (f_o - f)t \right] dt = \left[ \frac{1}{\sqrt{2k}} \cos \frac{\pi^2 (f_o - f)^2}{\pi k} C \left[ \frac{\sqrt{2}}{\sqrt{k\pi^2}} (\pi kt + \pi (f_o - f)) \right] \right. \\ \left. + \sin \frac{\pi^2 (f_o - f)^2}{\pi k} S \left[ \frac{\sqrt{2}}{\sqrt{k\pi^2}} (\pi kt + \pi (f_o - f)) \right] \right] \Big|_{t_a}^{t_b}$$

$$= \frac{1}{\sqrt{2k}} \left[ \cos \frac{\pi (f_o - f)^2}{k} C(\chi) + \sin \frac{\pi (f_o - f)^2}{k} S(\chi) \right] \Big|_{t_a}^{t_b}$$

$$= \frac{1}{\sqrt{2k}} \left[ \cos \frac{\pi (f_o - f)^2}{k} C(\chi_b) + \sin \frac{\pi (f_o - f)^2}{k} S(\chi_b) \right. \\ \left. - \cos \frac{\pi (f_o - f)^2}{k} C(\chi_a) - \sin \frac{\pi (f_o - f)^2}{k} S(\chi_a) \right]$$

$$j \int_{t_a}^{t_b} \sin 2\pi \left[ \frac{kt^2}{2} + (f_o - f)t \right] dt = j \frac{1}{\sqrt{2k}} \left[ \cos \frac{\pi (f_o - f)^2}{k} S(\chi_b) - \sin \frac{\pi (f_o - f)^2}{k} S(\chi_b) \right. \\ \left. - \cos \frac{\pi (f_o - f)^2}{k} S(\chi_a) + \sin \frac{\pi (f_o - f)^2}{k} S(\chi_a) \right]$$

Therefore:

$$\int_{t_a}^{t_b} e^{j2\pi \left[ \frac{kt^2}{2} + (f_o - f)t \right]} dt = \frac{1}{\sqrt{2k}} e^{-\frac{j\pi (f_o - f)^2}{k}} [Z(\chi_b) - Z(\chi_a)] \quad (B-3)$$

where

$$\begin{aligned}x_1 &= \sqrt{2k} t_1 + \sqrt{2/k} (f_0 - f) \\Z(x_1) &= C(x_1) + j S(x_1)\end{aligned}$$

which is the complex form of the Fresnel integral.

Integrating by parts gives:

$$\begin{aligned}\int_a^b t e^{j2\pi [kt^2/2 + (f_0 - f)t]} dt &= \\ \frac{1}{\sqrt{2k}} e^{-j\pi (f_0 - f)^2/k} &\left\{ t_b Z(x_b) - \frac{1}{\sqrt{2k}} \left[ x_b Z(x_b) - \frac{e^{-j\pi(1 - x_b^2)/2}}{\pi} \right] \right. \\ &\left. - t_a Z(x_a) + \frac{1}{\sqrt{2k}} \left[ x_a Z(x_a) - \frac{e^{-j\pi(1 - x_a^2)/2}}{\pi} \right] \right\} \quad (B-4)\end{aligned}$$

Derivation of B-4.

The left side of B-4 may be rewritten with the aid of Euler's formula as:

$$\begin{aligned}\int_a^b t e^{j2\pi \left[ \frac{kt^2}{2} + (f_0 - f)t \right]} dt &= \int_a^b t \cos 2\pi \left[ \frac{kt^2}{2} + (f_0 - f)t \right] dt \\ &+ j \int_a^b t \sin 2\pi \left[ \frac{kt^2}{2} + (f_0 - f)t \right] dt.\end{aligned}$$

Integrating each term, on the right side, by parts and applying formula 7.438 of Reference 5, we obtain:

$$\begin{aligned}&= \frac{t}{\sqrt{2k}} \left[ \cos \frac{\pi (f_0 - f)^2}{k} C(x) + \sin \frac{\pi (f_0 - f)^2}{k} S(x) \right] \Big|_a^b - \int_a^b \cos \frac{\pi (f_0 - f)^2}{k} \frac{C(x)}{\sqrt{2k}} dx \\ &- \int_a^b \sin \frac{\pi (f_0 - f)^2}{k} \frac{S(x)}{\sqrt{2k}} dx + \frac{jt}{\sqrt{2k}} \left[ \cos \frac{\pi (f_0 - f)^2}{k} S(x) - \sin \frac{\pi (f_0 - f)^2}{k} C(x) \right] \Big|_a^b\end{aligned}$$

$$\begin{aligned}
& -j \left[ t_a \cos \frac{\pi(f_o - f)^2}{k} \frac{S(x)}{\sqrt{2k}} dx + j \left[ t_b \sin \frac{\pi(f_o - f)^2}{k} \frac{C(x)}{\sqrt{2k}} dx \right. \right. \\
& = \frac{1}{\sqrt{2k}} \left\{ t_b \cos \frac{\pi(f_o - f)^2}{k} C(x_b) + t_b \sin \frac{\pi(f_o - f)^2}{k} S(x_b) - t_a \cos \frac{\pi(f_o - f)^2}{k} C(x_a) \right. \\
& - t_a \sin \frac{\pi(f_o - f)^2}{k} S(x_a) + j t_b \cos \frac{\pi(f_o - f)^2}{k} S(x_b) - j t_b \sin \frac{\pi(f_o - f)^2}{k} C(x_b) \\
& - j t_a \cos \frac{\pi(f_o - f)^2}{k} S(x_a) + j t_a \sin \frac{\pi(f_o - f)^2}{k} C(x_a) \\
& - \cos \frac{\pi(f_o - f)^2}{k} x_b \frac{C(x_b)}{\sqrt{2k}} + \frac{\cos \frac{\pi(f_o - f)^2}{k} \sin \frac{\pi}{2} x_b^2}{\pi \sqrt{2k}} \\
& + \frac{\cos \frac{\pi(f_o - f)^2}{k} x_a C(x_a)}{\sqrt{2k}} - \frac{\cos \frac{\pi(f_o - f)^2}{k} \sin \frac{\pi}{2} x_a^2}{\pi \sqrt{2k}} \\
& - \sin \frac{\pi(f_o - f)^2}{k} x_b \frac{S(x_b)}{\sqrt{2k}} - \sin \frac{\pi(f_o - f)^2}{k} \frac{\cos \frac{\pi}{2} x_b^2}{\pi \sqrt{2k}} \\
& + \sin \frac{\pi(f_o - f)^2}{k} x_a \frac{S(x_a)}{\sqrt{2k}} + \sin \frac{\pi(f_o - f)^2}{k} \frac{\cos \frac{\pi}{2} x_a^2}{\pi \sqrt{2k}} \\
& - j \cos \frac{\pi(f_o - f)^2}{k} x_b \frac{S(x_b)}{\sqrt{2k}} - j \cos \frac{\pi(f_o - f)^2}{k} \frac{\cos \frac{\pi}{2} x_b^2}{\pi \sqrt{2k}} \\
& + j \cos \frac{\pi(f_o - f)^2}{k} x_a \frac{S(x_a)}{\sqrt{2k}} + j \cos \frac{\pi(f_o - f)^2}{k} \frac{\cos \frac{\pi}{2} x_a^2}{\pi \sqrt{2k}} \\
& + j \sin \frac{\pi(f_o - f)^2}{k} x_b \frac{C(x_b)}{\sqrt{2k}} - j \sin \frac{\pi(f_o - f)^2}{k} \frac{\sin \frac{\pi}{2} x_b^2}{\pi \sqrt{2k}}
\end{aligned}$$

$$- j \sin \frac{\pi(f_0 - f)^2}{k} x_a \frac{C(x_a)}{\sqrt{2k}} + j \sin \frac{\pi(f_0 - f)^2 \cos \frac{\pi}{2} x_a^2}{k \frac{\pi}{2k}} \Bigg\}$$

These terms correspond term-for-term with the expression of the right side of B-4 when expanded in similar type terms.

Using Equations B-3 and B-4:

$$\begin{aligned}
 F(f) &= \frac{v e^{-j\pi(f_0 - f)^2/k}}{2\sqrt{2k}} \\
 &\left\{ \frac{1}{\delta_r} \left[ \left( t_2 - t_1 - \frac{x_2}{\sqrt{2k}} \right) Z(x_2) - \frac{e^{-j\pi(1 - x_2^2)/2}}{\pi\sqrt{2k}} \right. \right. \\
 &\quad \left. \left. - \left( t_1 - t_1 - \frac{x_1}{\sqrt{2k}} \right) Z(x_1) - \frac{e^{-j\pi(1 - x_1^2)/2}}{\pi\sqrt{2k}} \right] \right. \\
 &\quad \left. + [Z(x_3) - Z(x_2)] \right. \\
 &\quad \left. + \frac{1}{\delta_f} \left[ \left( -t_4 + t_4 + \frac{x_4}{\sqrt{2k}} \right) Z(x_4) - \frac{e^{-j\pi(1 - x_4^2)/2}}{\pi\sqrt{2k}} \right. \right. \\
 &\quad \left. \left. - \left( -t_3 + t_4 + \frac{x_3}{\sqrt{2k}} \right) Z(x_3) + \frac{e^{-j\pi(1 - x_3^2)/2}}{\pi\sqrt{2k}} \right] \right\} \quad (B-5)
 \end{aligned}$$

Derivation of B-5 follows.

The expansion of B-1 by B-2a, B-2b, B-2c, B-3 and B-4 yields:

$$\begin{aligned}
 F(f) &= \frac{v e^{-j\pi(f_0 - f)^2/k}}{2\sqrt{2k}} \left\{ \frac{t_2 Z(x_2)}{\delta_r} - \frac{x_2 Z(x_2)}{\delta_r \sqrt{2k}} + \frac{e^{-j\pi(1 - x_2^2)/2}}{\pi\sqrt{2k} \delta_r} - \right. \\
 &\quad \left. - \frac{t_1 Z(x_1)}{\delta_r} + \frac{x_1 Z(x_1)}{\delta_r \sqrt{2k}} - \frac{e^{-j\pi(1 - x_1^2)/2}}{\pi\delta_r \sqrt{2k}} - \frac{t_1 Z(x_2)}{\delta_r} + \right.
 \end{aligned}$$

$$\begin{aligned}
& + \frac{t_1 z(x_1)}{\delta_r} + z(x_3) - z(x_2) + \frac{t_4 z(x_4)}{\delta_f} - \frac{t_4 z(x_3)}{\delta_f} - \\
& - \frac{t_4 z(x_4)}{\delta_f} + \frac{x_4 z(x_4)}{\delta_f \sqrt{2k}} - \frac{e^{-j\pi(1-x_4^2)/2}}{\pi \sqrt{2k} \cdot \delta_f} + \frac{t_3 z(x_3)}{\delta_f} - \\
& - \frac{x_3 z(x_3)}{\delta_f \sqrt{2k}} + \frac{e^{-j\pi(1-x_3^2)/2}}{\delta_f \pi \sqrt{2k}} \Bigg|
\end{aligned}$$

This expansion corresponds term-for-term with the right side of B-5 when it is expanded in similar type terms.

Derivation of 32 from B-5

From B-5, we have:

$$\begin{aligned}
F(f) &= \frac{V}{2\sqrt{2k}} e^{-j\pi(f_0 - f)^2/k} \left\{ z(x_2) - \frac{x_2 z(x_2)}{\delta_r \sqrt{2k}} + \frac{\phi(x_2)}{\delta_r \sqrt{2k}} + \right. \\
& + \frac{x_1 z(x_1)}{\delta_r \sqrt{2k}} - \frac{\phi(x_1)}{\delta_r \sqrt{2k}} + z(x_3) - z(x_2) + \frac{x_4 z(x_4)}{\delta_f \sqrt{2k}} \\
& \left. - \frac{\phi(x_4)}{\delta_f \sqrt{2k}} z(x_3) - \frac{x_3 z(x_3)}{\delta_f \sqrt{2k}} + \frac{\phi(x_3)}{\delta_f \sqrt{2k}} \right\} \\
F(f) &= \frac{V}{4k} e^{-j\pi(f_0 - f)^2/k} \left\{ \frac{x_1 z(x_1)}{\delta_r} - \frac{\phi(x_1)}{\delta_r} \right. \\
& - \frac{x_2 z(x_2)}{\delta_r} + \frac{\phi(x_2)}{\delta_r} - \frac{x_3 z(x_3)}{\delta_f} \\
& \left. + \frac{\phi(x_3)}{\delta_f} + \frac{x_4 z(x_4)}{\delta_f} - \frac{\phi(x_4)}{\delta_f} \right\} \tag{32}
\end{aligned}$$

## APPENDIX C

## EXPRESSING THE COMPLEX FRESNEL INTEGRAL AS AN ASYMPTOTIC EXPANSION

(Equations in this appendix that have already appeared in the body of the report will be identified by their original numbers.)

The integral in Equation 36:

$$Z(\chi_1) = \int_0^{\chi_1} \cos(\pi t^2/2) dt + j \int_0^{\chi_1} \sin(\pi t^2/2) dt \quad (C-1)$$

is referred to as the complex Fresnel integral. The vector,  $Z(\chi)$ , generates Cornu's spiral, shown in Figure C-1, where  $\chi$  is varied as the independent variable.

Reference 5 gives several types of expansions that can be used to evaluate the Fresnel integral. Using (7.3.9) and (7.3.10) of Reference 5, the integral can be expressed as:

$$Z(\chi) = \frac{u e^{j\pi/4}}{\sqrt{2}} + f(\chi) e^{-j\pi(1 - \chi^2)/2} - g(\chi) e^{j\pi\chi^2/2} \quad (C-2)$$

where

$$u = \begin{cases} -1, & \chi < 0 \\ +1, & \chi > 0 \end{cases} \quad (C-3)$$

$$f(\chi) \sim \frac{1}{\pi\chi} \left\{ 1 + \sum_{m=1}^{\infty} \frac{(-1)^m 1 \cdot 3 \dots (4m-1)}{(\pi\chi^2)^{2m}} \right\} \quad (C-4)$$

$$g(\chi) \sim \frac{1}{\pi\chi} \sum_{m=0}^{\infty} \frac{(-1)^m 1 \cdot 3 \dots (4m+1)}{(\pi\chi^2)^{2m+1}} \quad (C-5)$$

Using the above relationships, the functions within the brackets in Equation 32 can be written in the form:

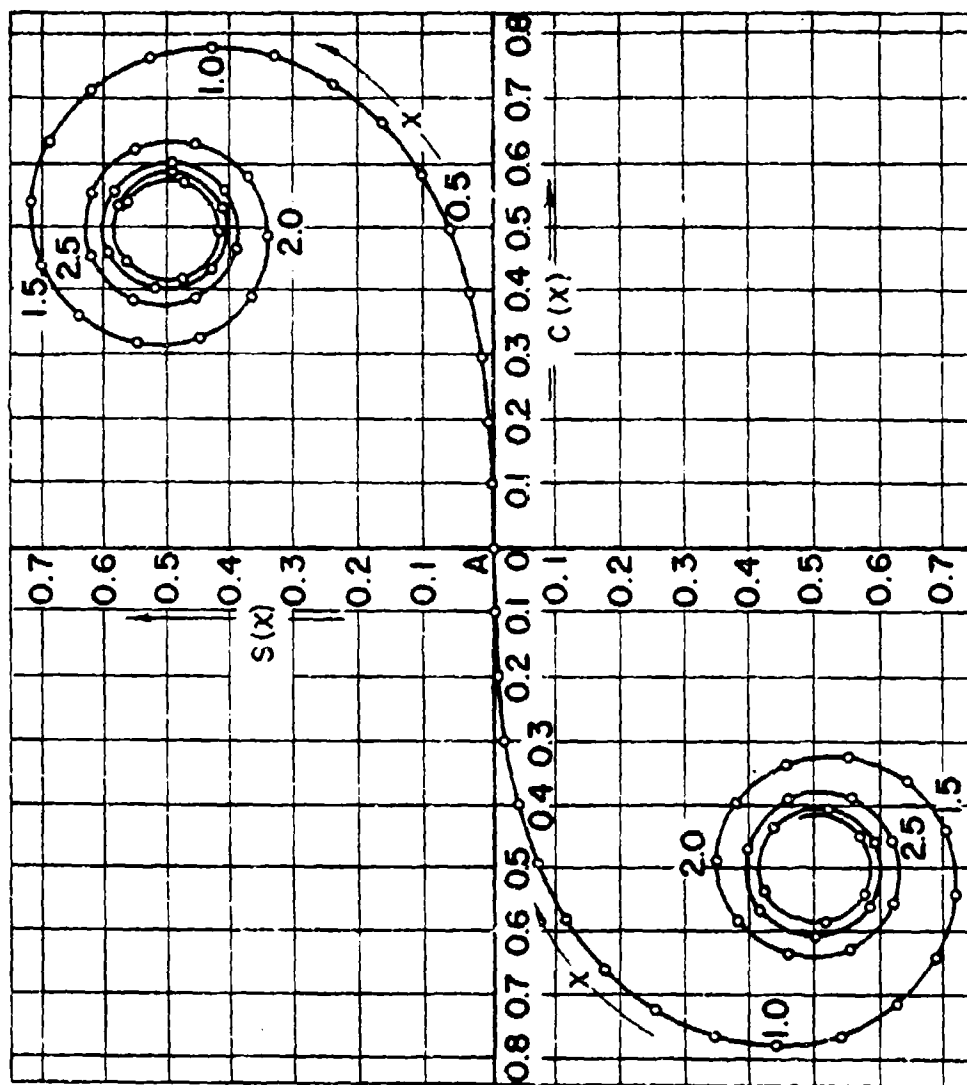


Figure C-1. Cornu's spiral, a plot of the Fresnel integrals.

$$\begin{aligned}
 [X_1 Z(X_1) - \phi(X_1)] &= X_1 u_1 e^{j\frac{\pi}{4}} + [\pi X_1 f(X_1) - 1] \frac{e^{-j\pi(1 - X_1^2)/2}}{\pi} \\
 &\quad - [\pi X_1 g(X_1)] \frac{e^{j\pi X_1^2/2}}{\pi}
 \end{aligned}
 \tag{C-6}$$

where

$$\phi(X_1) = \frac{1}{\pi} e^{-j\frac{\pi}{2}(1 - X_1^2)}
 \tag{37}$$

An approximation of C-6, when  $|X_1| \geq 1$ , may be obtained by deleting the summation in C-4 and including only the first term in summation of C-5 to obtain:

$$[X_1 Z(X_1) - \phi(X_1)] \sim \frac{X_1 u_1 e^{j\frac{\pi}{4}}}{\sqrt{2}} - \frac{e^{j\pi X_1^2/2}}{(\pi X_1)^2}
 \tag{C-7}$$

When  $|X_1| \geq 1$ , the approximation expressed by the right side of (C-7) is in error by less than 0.05 dB when compared with the left side. This is evident by computing the numerical values of these quantities for  $|X_1| = 1$  with the aid of the tables in Reference 5. The results of such a computation are 0.636 and 0.639, respectively, thereby yielding:

$$20 \log \frac{0.639}{0.636} = 0.041 \text{ dB.}$$

## APPENDIX D

APPROXIMATIONS OF  $F(\Delta f)$  AND  $E(\Delta f)$  USING ASYMPTOTIC EXPANSIONS

(Equations in this appendix that have already appeared in the body of this report will be identified by their original numbers.)

The voltage-density spectrum  $F(\Delta f)$  for a trapezoidal chirp pulse is given by Equation 32 as:

$$F(\Delta f) = \frac{V}{4k} e^{-j\pi\Delta f^2/k} \sum_{i=1}^4 \frac{1}{\delta_i} \left[ \chi_i Z(\chi_i) - \Phi(\chi_i) \right] \quad (D-1)$$

A simpler expression is desired so that we can obtain some insight into the behavior of  $F(\Delta f)$ . When the approximation given by C-7 is applied to Equation D-1,  $F(\Delta f)$  can be expressed by:

$$F(\Delta f) = \frac{V}{4k} e^{-j\pi\Delta f^2/k} \sum_{i=1}^4 \frac{1}{\delta_i} \left[ \frac{\chi_i u_i e^{j\pi/4}}{\sqrt{2}} - \frac{e^{j\pi\chi_i^2/2}}{(\pi\chi_i)^2} \right] \quad (D-2)$$

when  $|\chi_i| \geq 1$ , and

$$u_i = \begin{cases} -1, & \chi_i < 0 \\ 1, & \chi_i \geq 0 \end{cases}$$

$$k = \frac{\beta}{\tau_b}, \quad \delta_1 = \delta_r, \quad \delta_2 = -\delta_r, \quad \delta_3 = -\delta_f, \quad \delta_4 = \delta_f$$

$$\Delta f = f - f_0, \quad \chi_i = \sqrt{2k} \tau_i - \sqrt{2/k} \Delta f$$

Figure D-1 depicts graphs of  $\chi_i$  as a function of  $\Delta f$  for  $i = 1, 2, 3$ , and 4. When  $\Delta f$  is in the shaded interval between  $\Omega_1$  and  $\Omega_2$ ,  $|\chi_1|$  and/or  $|\chi_2|$  are less than unity, and when  $\Delta f$  is in the shaded interval between  $\Omega_3$  and  $\Omega_4$ ,  $|\chi_3|$  and/or  $|\chi_4|$  are less than unity; thus, in these two intervals, Equation D-2, which depends upon the approximation given by Equation C-7, is not valid.

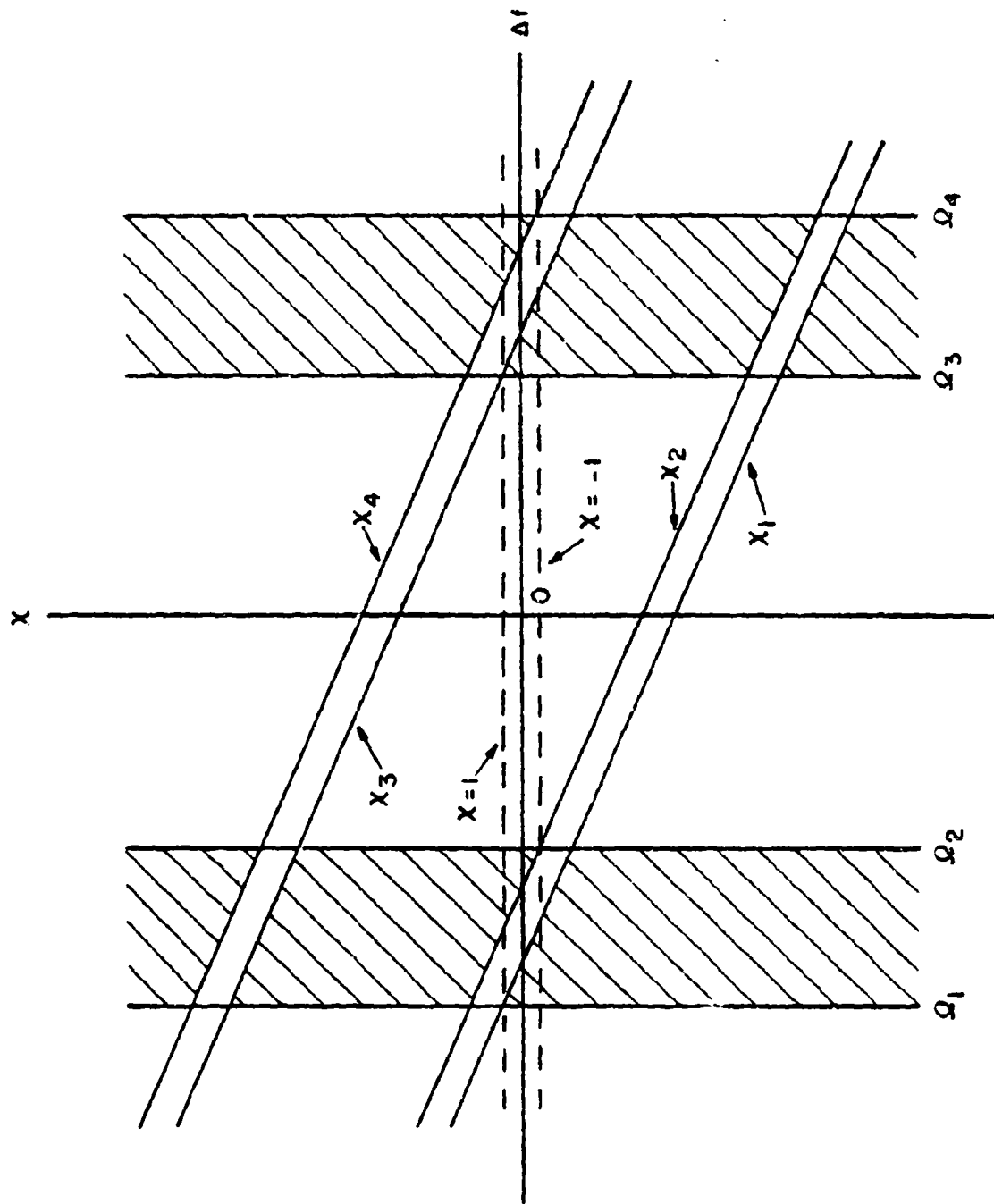


Figure D-1. Graphs of  $X_1$ ,  $X_2$ ,  $X_3$ , and  $X_4$ , as a function of  $\Delta f$ .

By referring to Figure D-1,  $\Omega_1$  is determined by noting that for  $\Omega_1$  the value of  $\chi_1 = +1$ . Likewise,  $\Omega_2$ ,  $\Omega_3$ , and  $\Omega_4$  are defined for  $\chi_2 = -1$ ,  $\chi_3 = +1$ , and  $\chi_4 = -1$ , respectively. Based on these conditions, we have:

$$\Omega_1 = -\frac{\beta \delta_r}{\delta_r + \delta_f} - \sqrt{\frac{\beta}{2\tau_b}} \quad (D-3a)$$

$$\Omega_2 = -\beta \left( \frac{\delta_r}{\delta_r + \delta_f} - \frac{\delta_r}{\tau_b} \right) + \sqrt{\frac{\beta}{2\tau_b}} \quad (D-3b)$$

$$\Omega_3 = \beta \left( \frac{\delta_f}{\delta_r + \delta_f} - \frac{\delta_f}{\tau_b} \right) - \sqrt{\frac{\beta}{2\tau_b}} \quad (D-3c)$$

$$\Omega_4 = \frac{\beta \delta_f}{\delta_r + \delta_f} + \sqrt{\frac{\beta}{2\tau_b}} \quad (D-3d)$$

From Equations 19, 20, and 35 we see that when  $\chi_1$  and  $\chi_2$  are of the same sign:

$$\frac{\chi_1 - \chi_2}{\delta_r} = -\sqrt{2k}, \Delta f < \Omega_1 \text{ or } \Delta f > \Omega_2 \quad (D-4a)$$

Likewise, when  $\chi_3$  and  $\chi_4$  are of the same sign:

$$\frac{\chi_4 - \chi_3}{\delta_f} = \sqrt{2k}, \Delta f < \Omega_3 \text{ or } \Delta f > \Omega_4 \quad (D-4b)$$

The approximation given by Equation D-2 with the aid of Equation D-4a and D-4b can be expressed as:

$$F(\Delta f) = \frac{V}{4k} e^{-j\pi\Delta f^2/k} \left[ \alpha \sqrt{k} e^{j\pi/4} - Y_r(\Delta f) - Y_f(\Delta f) \right] \quad (D-5)$$

where

$$\alpha = 0, \quad \begin{cases} \Delta f < \Omega_1 \\ \Delta f > \Omega_4 \end{cases}$$

$$\alpha = 2, \quad \Omega_2 < \Delta f < \Omega_3$$

$$Y_r(\Delta f) = \frac{e^{j\pi\chi_1^2/2}}{(\pi\chi_1)^2} - \frac{e^{j\pi\chi_2^2/2}}{(\pi\chi_2)^2} \quad (D-5a)$$

$$Y_f(\Delta f) = \frac{e^{j\pi\chi_4^2/2}}{(\pi\chi_4)^2} - \frac{e^{j\pi\chi_3^2/2}}{(\pi\chi_3)^2} \quad (D-5b)$$

The approximation in Equation D-5 is obtained by noting that Equation D-2, with the aid of Equations D-4a and D-4b, can be expressed as:

$$F(\Delta f) = \frac{V}{4k} e^{-j\pi\Delta f^2/k} \left[ \frac{1}{\delta_r} \left[ \left( \frac{\chi_1^{u_1} - \chi_2^{u_2}}{\sqrt{2}} \right) e^{j\pi/4} - \left( \frac{e^{j\pi\chi_1^2/2}}{(\pi\chi_1)^2} - \frac{e^{j\pi\chi_2^2/2}}{(\pi\chi_2)^2} \right) \right] \right. \\ \left. + \frac{1}{\delta_f} \left[ \left( \frac{\chi_4^{u_4} - \chi_3^{u_3}}{\sqrt{2}} \right) e^{j\pi/4} - \left( \frac{e^{j\pi\chi_4^2/2}}{(\pi\chi_4)^2} - \frac{e^{j\pi\chi_3^2/2}}{(\pi\chi_3)^2} \right) \right] \right]$$

when  $\Delta f < \Omega_1$  or  $\Delta f > \Omega_4$ .

(D-5c)

Let  $u_1 = u_2 = u_{12}$  when  $\chi_1$  and  $\chi_2$  are of the same sign.

If  $\chi_1$  and  $\chi_2$  are both positive, then  $u_{12} = 1$ .

If  $\chi_1$  and  $\chi_2$  are both negative, then  $u_{12} = -1$ .

Likewise, let  $u_3 = u_4 = u_{34}$  when  $\chi_3$  and  $\chi_4$  are of the same sign.

If  $\chi_3$  and  $\chi_4$  are both positive, then  $u_{34} = 1$ .

If  $\chi_3$  and  $\chi_4$  are both negative, then  $u_{34} = -1$ .

$$F(\Delta f) = \frac{V}{4k} e^{-j\pi \frac{\Delta f^2}{k}} \left[ (u_{34} - u_{12}) \sqrt{k} e^{j\pi/4} - \gamma_r(\Delta f) - \gamma_f(\Delta f) \right]$$

Let  $\alpha = u_{34} - u_{12}$ , then:

$$F(\Delta f) \sim \frac{V}{4k} e^{-j\pi \frac{\Delta f^2}{k}} \left[ \alpha \sqrt{k} e^{j\pi/4} - \gamma_r(\Delta f) - \gamma_f(\Delta f) \right] \quad (D-5)$$

For  $\Delta f < \Omega_1$ ,  $\alpha = 1 - 1 = 0$

$\Delta f > \Omega_4$ ,  $\alpha = -1 + 1 = 0$

$\Omega_2 < \Delta f < \Omega_3$ ,  $\alpha = +1 + 1 = 2$

For the in-band region of the spectrum where  $\Omega_2 < \Delta f < \Omega_3$ , the term  $|\gamma_r(\Delta f) + \gamma_f(\Delta f)|$  may be neglected since:

$$|\gamma_r(\Delta f) + \gamma_f(\Delta f)| \ll 2\sqrt{k} \quad (D-6)$$

by noting that from APPENDIX C,  $|\chi_1| \geq 1$  and from Equations D-5a and D-5b let  $\delta_r = \delta_f = \delta$ ,  $|\chi_1| = |\chi_2| = |\chi_3| = |\chi_4| = \chi$  in the denominators of Equations D-5a and D-5b and  $|\gamma_r| = |\gamma_f|$ . Then:

$$|\gamma_r(\Delta f) + \gamma_f(\Delta f)| < |\gamma_r(\Delta f)| + |\gamma_f(\Delta f)| < \frac{2 e^{j\pi/2} \chi_2^2}{\pi^2 \delta \chi^2} \left[ e^{j\pi/2} (\chi_1^2 - \chi_2^2) - 1 \right]$$

Since  $x_1 - x_2 = -\delta \sqrt{2k}$ , then :

$$\begin{aligned} |\gamma_r(\Delta f) + \gamma_f(\Delta f)| &<< \left| \frac{2}{\pi^2 \delta \chi^2} \left[ \frac{\pi}{2} (x_1 - x_2) 2\chi \right] \right| \\ &<< \left| \frac{2 \delta \sqrt{2k}}{\pi \delta \chi} \right| = \frac{2\sqrt{2} \sqrt{k}}{\pi |\chi|} < 2 \sqrt{k} \end{aligned}$$

Thus,  $|\gamma_r(\Delta f) + \gamma_f(\Delta f)| << 2\sqrt{k}$  for  $\Omega_2 < \Delta f < \Omega_3$

With the aid of inequality in Equation D-6, D-5 can be expressed for the in-band region of the spectrum as:

$$F(\Delta f) = \frac{V}{2\sqrt{k}} e^{j\pi/4}, \quad \Omega_2 < \Delta f < \Omega_3 \quad (D-7)$$

Thus, the amplitude of the spectrum at  $\Delta f = 0$  is:

$$|F(0)| = \frac{V}{2\sqrt{k}} = \frac{V}{2} \sqrt{\frac{r_b}{B}} \quad (D-8)$$

From Equation D-5, the expression for  $F(\Delta f)$  for the out-of-band region of the spectrum is given by:

$$\begin{aligned} F(\Delta f) = -\frac{V}{4k} e^{-j\pi\Delta f^2/k} & \left\{ \begin{array}{l} \gamma_r(\Delta f) + \gamma_f(\Delta f) \\ \Delta f < \Omega_1 \\ \Delta f > \Omega_4 \end{array} \right\} \quad (D-9) \end{aligned}$$

$$\text{or } F(\Delta f) = -\frac{V}{4k} e^{-j\pi\Delta f^2/k} \sum_{i=1}^4 \frac{1}{\delta_i} \frac{e^{j\pi\chi_i^2/2}}{(\pi\chi_i)^2}$$

$$F(\Delta f) = -\frac{V}{4k} e^{-j\pi\Delta f^2/k} \sum_{i=1}^4 \frac{k}{\delta_i} \frac{e^{j\pi/2 [2kt_i^2 - 4\Delta f t_i + \frac{2}{k}\Delta f^2]}}{2\pi (kt_i - \Delta f)^2}$$

$$F(\Delta f) = -\frac{V}{8\pi^2} \sum_{i=1}^4 \frac{1}{\delta_i} \frac{e^{j2\pi t_i \left( \frac{kt_i}{2} - \Delta f \right)}}{(kt_i - \Delta f)^2} \quad (D-10)$$

for  $\Delta f < \Omega_1$

$\Delta f > \Omega_4$

when  $\Delta f = \Delta f_f = \frac{1}{2} \Omega_3 + \Omega_4$  i.e., when  $\Delta f$  is midway between  $\Omega_3$  and  $\Omega_4$ :

$$\Delta f = \Delta f_f = \frac{\beta\delta_f}{\delta_r + \delta_f} - \frac{\beta\delta_f}{2\tau_b} \quad (D-11)$$

Based upon the definition of  $\chi_i$  and Equation D-11, we have:

$$\chi_3 = -\chi_4, \Delta f = \Delta f_r \quad (D-12)$$

and from the definitions of  $Z(\chi_i)$  and  $\phi(\chi_i)$  we have:

$$\left[ \chi_4 Z(\chi_4) - \phi(\chi_4) \right] - \left[ \chi_3 Z(\chi_3) - \phi(\chi_3) \right] = 0 \quad (D-13)$$

in which case Equation D-1 yields:

$$F(\Delta f_f) = \frac{V}{4k} e^{-j\pi \Delta f_f^2 / k} \sum_{i=1}^2 \frac{1}{\delta_i} \left[ \chi_i Z(\chi_i) - \Phi(\chi_i) \right] \quad (D-14)$$

Using the same procedure for obtaining Equation D-5, the above result can be expressed as:

$$F(\Delta f_f) = \frac{V}{4k} e^{-j\pi \Delta f_f^2 / k} \left[ \sqrt{k} e^{j\pi/4} - \gamma_r(\Delta f_f) \right] \quad (D-15)$$

Since:

$$|\gamma_r(\Delta f)| \ll \sqrt{k}$$

$$F(\Delta f_f) = \frac{V}{4\sqrt{k}} e^{j\pi \left( \frac{1}{4} - \frac{\Delta f_f^2}{k} \right)} \quad (D-16)$$

and then

$$|F(\Delta f_f)| = \frac{V}{4\sqrt{k}} \quad (D-17)$$

From Equations D-8 and D-17 we have:

$$\left| \frac{F(\Delta f_f)}{F(0)} \right| = \frac{1}{2} \quad (D-18)$$

In a similar manner, it can be shown that when  $\Delta f = \Delta f_r = \frac{1}{2} (\Omega_1 + \Omega_2)$ , i.e., when  $\Delta f$  is midway between  $\Omega_1$  and  $\Omega_2$ ,  $\chi_1 = -\chi_2$  so that:

$$F(\Delta f_r) = \frac{V}{4\sqrt{k}} e^{j\pi \left( \frac{1}{4} - \frac{\Delta f_r^2}{k} \right)} \quad (D-19)$$

and

$$\frac{F(\Delta f_r)}{F(0)} = \frac{1}{2} \quad (D-20)$$

From Equations D-7, D-8, D-9, D-18, and D-20 the relative energy density, defined by:

$$E(\Delta f) = \left| \frac{F(\Delta f)}{F(0)} \right|^2 \quad (D-21)$$

is expressed by:

$$E(\Delta f) = 1, \quad \Omega_2 < \Delta f < \Delta f_3 \quad (D-22)$$

$$E(\Delta f) = \frac{k}{16\pi^4} \left| \sum_{i=1}^4 \frac{e^{j2\pi t_i \left( \frac{kt_i}{2} - \Delta f \right)}}{\delta_i (kt_i - \Delta f)^2} \right|^2 \quad (D-23)$$

for  $\Delta f < \Omega_1$

$$\Delta f > \Omega_4$$

Then:

$$E(\Delta f_r) = \frac{1}{4} \quad (D-24)$$

and

$$E(\Delta f_f) = \frac{1}{4} \quad (D-25)$$

A tabulation identifying the approximating equations for  $E(\Delta f)$  is given by:

Region of $\Delta f$	Applicable Equations
$\Omega_1 < \Delta f < \Omega_2$	(D-22)
$\Delta f < \Omega_1$ or $\Delta f > \Omega_4$	(D-23)
$\Delta f_r = \frac{1}{2} (\Omega_1 + \Omega_2)$	(D-24)
$\Delta f_f = \frac{1}{2} (\Omega_3 + \Omega_4)$	(D-25)

An example of an application of the approximations derived in this appendix is shown in Figure D-2. The points on the graph are values of  $E(\Delta f)$  accurately calculated by evaluating the integrals in Equations B-2a, B-2b, and B-2c with the aid of a computer algorithm involving double precision. The solid curves were obtained by applying the approximations derived in this appendix. Curve 1 was obtained using Equation D-22 with the results expressed in dB. Curve 2 was obtained using Equation D-23. Curve 3 was obtained by plotting:

$$20 \log \left| \frac{Y_r(\Delta f) + Y_f(\Delta f)}{2\sqrt{k}} \right|$$

and clearly depicts the inequality in Equation D-6. Point 4 was obtained using Equation D-25, expressed in dB.

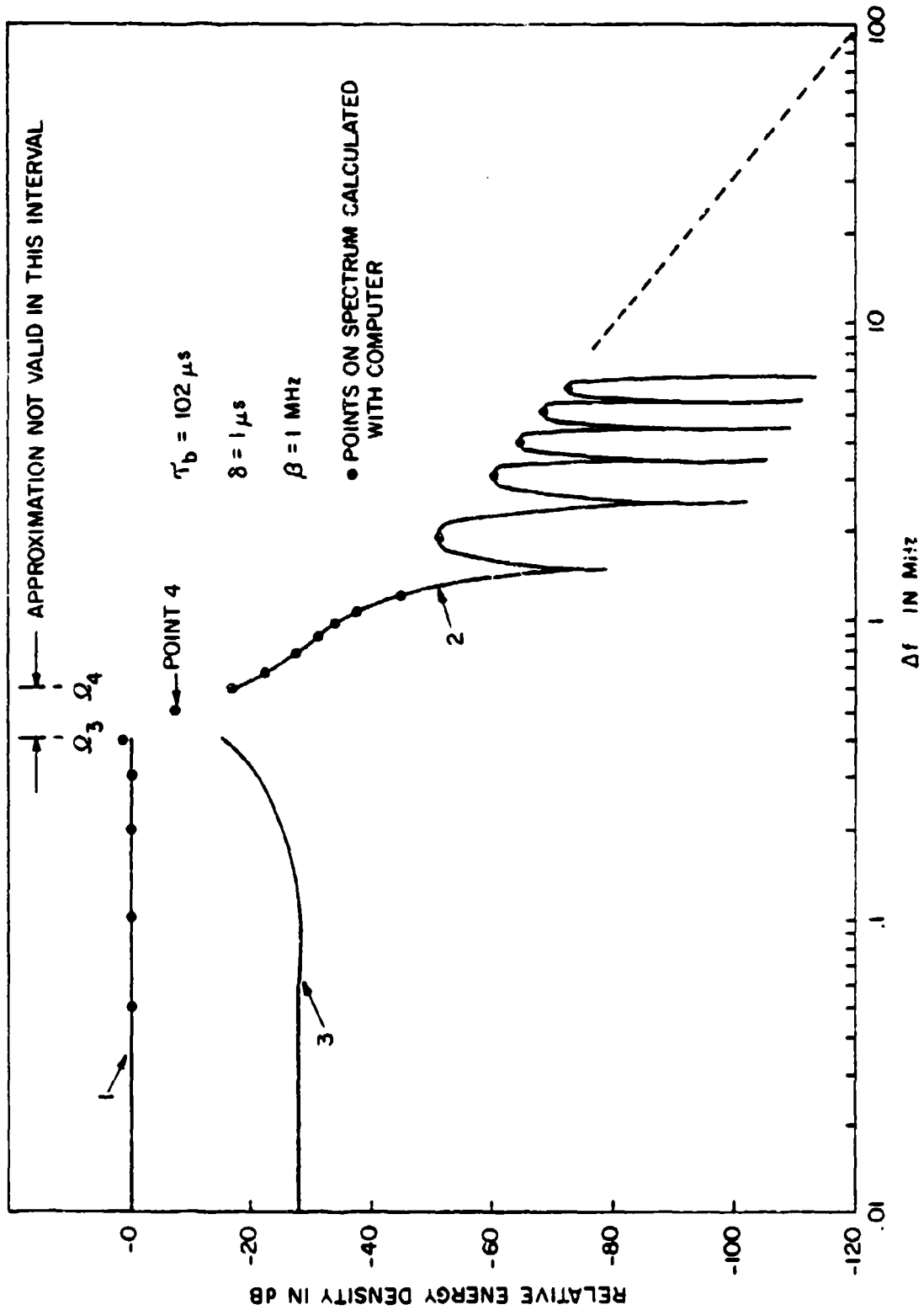


Figure D-2. An example of a graph of the relative energy density obtained with Equation D-22 (Curve 1) and Equation D-23 (Curve 2). Curve 3 confirms Equation D-6.

## APPENDIX E

F( $\Delta f$ ) FOR SKIRTS OF SPECTRUM (DERIVATION OF EQUATION 59)

(Equations in this appendix that have already appeared in the body of the report will be identified by their original numbers.)

Starting with Equation 58, we will derive Equation 59, which is used to determine the bounds on the skirts of the spectrum:

$$F(\Delta f) = -\frac{V}{8\pi} \sum_{i=1}^4 \frac{e^{j2\pi t_i (kt_i/2 - \Delta f)}}{\delta_i (kt_i - \Delta f)^2} \quad (58)$$

where  $\delta_1 = \delta_r$ ,  $\delta_2 = -\delta_r$ ,  $\delta_3 = -\delta_f$ ,  $\delta_4 = \delta_f$

From Equations 19-27 we have:

$$t_1 = t_r - \delta_r/2 \quad (E-1a)$$

$$t_2 = t_r + \delta_r/2 \quad (E-1b)$$

$$t_3 = t_f - \delta_f/2 \quad (E-1c)$$

$$t_4 = t_f + \delta_f/2 \quad (E-1d)$$

$$\text{Let } \phi_i = 2\pi t_i (kt_i/2 - \Delta f) \quad (E-2)$$

Using the above equations, we can get:

$$\phi_1 = 2\pi t_1 \left( \frac{kt_1}{2} - \Delta f \right) = 2\pi \left( t_r - \frac{\delta_r}{2} \right) \left[ \frac{k \left( t_r - \frac{\delta_r}{2} \right)}{2} - \Delta f \right]$$

$$\phi_1 = \pi t_r^2 k - \pi \delta_r t_r k - \pi k \frac{\delta_r^2}{4} - 2\pi t_r \Delta f + \pi \delta_r \Delta f$$

$$\phi_1 = \pi k \left( t_r^2 - \frac{\delta_r^2}{4} \right) - \pi \delta_r (k t_r - \Delta f) - 2\pi \Delta f t_r$$

$$\phi_2 = 2\pi t_2 \left( \frac{kt_2}{2} - \Delta f \right) = 2\pi \left( t_r + \frac{\delta_r}{2} \right) \left[ \frac{k \left( t_r + \frac{\delta_r}{2} \right)}{2} - \Delta f \right]$$

$$\phi_2 = \pi t_r^2 k + \pi \delta_r t_r k + \pi k \frac{\delta_r^2}{4} - 2\pi t_r \Delta f - \Delta \delta_r \Delta f$$

$$\phi_2 = \pi k \left( t_r^2 + \frac{\delta_r^2}{4} \right) + \pi \delta_r (k t_r - \Delta f) - 2\pi t_r \Delta f$$

$\phi_3$  is the same expression as  $\phi_1$  except subscript r is replaced by subscript f.

$\phi_4$  is the same expression as  $\phi_2$  except subscript r is replaced by subscript f.

Then:

$$\phi_1 = \pi k \left( t_r^2 + \frac{\delta_r^2}{4} \right) - 2\pi \Delta f t_r - \pi \delta_r (k t_r - \Delta f) \quad (E-3a)$$

$$\phi_2 = \pi k \left( t_r^2 + \frac{\delta_r^2}{4} \right) - 2\pi \Delta f t_r - \pi \delta_r (k t_r - \Delta f) \quad (E-3b)$$

$$\phi_3 = \pi k \left( t_f^2 + \frac{\delta_f^2}{4} \right) - 2\pi \Delta f t_f - \pi \delta_f (k t_f - \Delta f) \quad (E-3c)$$

$$\phi_4 = \pi k(t_f^2 + \delta_f^2/4) - 2\pi \Delta f t_f - \pi \delta_f (kt_f - \Delta f) \quad (\text{E-3d})$$

We will now examine the case where the leading and trailing edges of the pulses are steep, as in most chirp pulses, i.e.,

$\delta_r \ll |t_r|$  and  $\delta_f \ll |t_f|$ , so that

$t_r \approx t_1 \approx t_2$ ,  $t_f \approx t_3 \approx t_4$  and  $\delta = \delta_r \approx \delta_f$ . Then :

$$(kt_1 - \Delta f) \approx (kt_2 - \Delta f) \approx (kt_r - \Delta f) \quad (\text{E-4a})$$

$$(kt_4 - \Delta f) \approx (kt_3 - \Delta f) \approx (kt_f - \Delta f)$$

With these approximations, Equation 58 is rewritten to give:

$$F(\Delta f) = \frac{v}{8\pi^2} \left\{ -\frac{e^{j\phi_1}}{\delta_1 (kt_1 - \Delta f)^2} - \frac{e^{j\phi_2}}{\delta_2 (kt_2 - \Delta f)^2} - \frac{e^{j\phi_3}}{\delta_3 (kt_3 - \Delta f)^2} - \frac{e^{j\phi_4}}{\delta_4 (kt_4 - \Delta f)^2} \right\}$$

$$F(\Delta f) = \frac{v}{8\pi^2} \left\{ -\frac{e^{j\pi k(t_r^2 + \delta_r^2/4)} \cdot e^{-j2\pi \Delta f t_r} \cdot e^{-j\pi \delta_r (kt_r - \Delta f)}}{\delta_r (kt_r - \Delta f)^2} \right. \\ \left. - \frac{e^{j\pi k(t_r^2 + \delta_r^2/4)} \cdot e^{-j2\pi \Delta f t_r} \cdot e^{j\pi \delta_r (kt_r - \Delta f)}}{-\delta_r (kt_r - \Delta f)^2} \right. \\ \left. - \frac{e^{j\pi k(t_f^2 + \delta_f^2/4)} \cdot e^{-j2\pi \Delta f t_f} \cdot e^{-j\pi \delta_f (kt_f - \Delta f)}}{-\delta_f (kt_f - \Delta f)^2} \right\}$$

$$\left. - \frac{e^{j\pi k(t_f^2 + \delta_f^2/4)} \cdot e^{-j2\pi\Delta f t_f} \cdot e^{j\pi\delta_f(kt_f - \Delta f)}}{\delta_f(kt_f - \Delta f)^2} \right\}$$

$$F(\Delta f) = \frac{V}{8\pi^2} \left\{ e^{j\pi k(t_r^2 + \delta_r^2/4)} \cdot e^{-j2\pi t_r \Delta f} \left[ - \frac{e^{-j\pi\delta_r(kt_r - \Delta f)} - e^{j\pi\delta_r(kt_r - \Delta f)}}{\delta_r(kt_r - \Delta f)^2} \right] \right.$$

$$\left. + e^{j\pi k(t_f^2 + \delta_f^2/4)} \cdot e^{-j2\pi t_f \Delta f} \left[ \frac{e^{-j\pi\delta_f(kt_f - \Delta f)} - e^{j\pi\delta_f(kt_f - \Delta f)}}{\delta_f(kt_f - \Delta f)^2} \right] \right\}$$

or

$$F(\Delta f) = \frac{V}{8\pi^2} \left\{ e^{j\pi k(t_r^2 + \delta_r^2/4)} \frac{e^{-j2\pi t_r \Delta f}}{(kt_r - \Delta f)} \right.$$

$$\cdot \left[ (-1) \frac{e^{-j\pi\delta_r(kt_r - \Delta f)} - e^{j\pi\delta_r(kt_r - \Delta f)}}{\delta_r(kt_r - \Delta f)} \right]$$

$$+ e^{j\pi k(t_f^2 + \delta_f^2/4)} \frac{e^{-j2\pi t_f \Delta f}}{(kt_f - \Delta f)}$$

$$\cdot \left[ (+1) \frac{e^{-j\pi\delta_f(kt_f - \Delta f)} - e^{j\pi\delta_f(kt_f - \Delta f)}}{\delta_f(kt_f - \Delta f)} \right] \left. \right\}$$

Further reduction yields:

$$F(\Delta f) = \frac{V}{4} e^{j\pi/2} \left[ e^{j\pi k(t_r^2 + \delta_r^2/4)} \frac{e^{-j2\pi t_r \Delta f}}{\pi(k t_r - \Delta f)} \right] \quad (59)$$

$$\cdot \left[ \frac{\sin \pi \delta_r (k t_r - \Delta f)}{\pi \delta_r (k t_r - \Delta f)} \right]$$

$$- e^{j\pi k(t_f^2 + \delta_f^2/4)} \frac{e^{-j2\pi t_f \Delta f}}{\pi(k t_f - \Delta f)} \left[ \frac{\sin \pi \delta_f (k t_f - \Delta f)}{\pi \delta_f (k t_f - \Delta f)} \right]$$

This concludes the derivation of Equation 59, however, we will check to see if the equation degenerates into the conventional equation for a pulse having no FM when we let  $k = 0$ .

If the pulse is symmetrical, from Figure 12 and Equations 23 - 27, we have  $\delta_r = \delta_f$ ,  $t_r = -\tau/2$ , and  $t_f = \tau/2$ . Equation 59 becomes:

$$F(\Delta f) = \frac{V}{4} e^{j\pi[k(\tau^2 + \delta^2/4) + 1/2]} \quad (E-5)$$

$$\cdot \left[ \frac{e^{j\pi\tau\Delta f}}{\pi(-k\tau/2 - \Delta f)} \cdot \frac{\sin \pi \delta (-k\tau/2 - \Delta f)}{\pi \delta (-k\tau/2 - \Delta f)} \right. \\ \left. - \frac{e^{-j\pi\tau\Delta f}}{\pi(k\tau/2 - \Delta f)} \cdot \frac{\sin \pi \delta (k\tau/2 - \Delta f)}{\pi \delta (k\tau/2 - \Delta f)} \right]$$

Letting  $k = 0$ , Equation E-5 can be written:

$$F(\Delta f) = \frac{V}{2} \left[ \frac{\tau \sin \pi \tau \Delta f}{\pi \tau \Delta f} \cdot \frac{\sin \pi \delta \Delta f}{\pi \delta \Delta f} \right] \quad (\text{E-6})$$

which is the conventional expression for the positive part of the spectrum (centered on  $+f_0$ ) of a symmetrical trapezoidal RF pulse with no FM.

## APPENDIX F

## BOUNDS ON SKIRTS OF SPECTRUM WHEN

$$\beta < \frac{1}{\pi\delta} \text{ and } \delta = \delta_r = \delta_f < \tau_b, \tau_r = \tau_1 = \tau_2, \tau_f = \tau_3 = \tau_4$$

(Equations in this appendix that have already appeared in the body of the report will be identified by their original numbers.)

Using Equation 59, we can write the inequality:

$$|F(\Delta f)| \leq \frac{V}{4\pi} \left\{ \left| \frac{1}{(kt_r - \Delta f)} \frac{\sin \chi_r}{\chi_r} \right| + \left| \frac{1}{(kt_f - \Delta f)} \frac{\sin \chi_f}{\chi_f} \right| \right\} \quad (F-1)$$

where

$$\chi_r = \pi\delta_r (kt_r - \Delta f)$$

$$\chi_f = \pi\delta_f (kt_f - \Delta f)$$

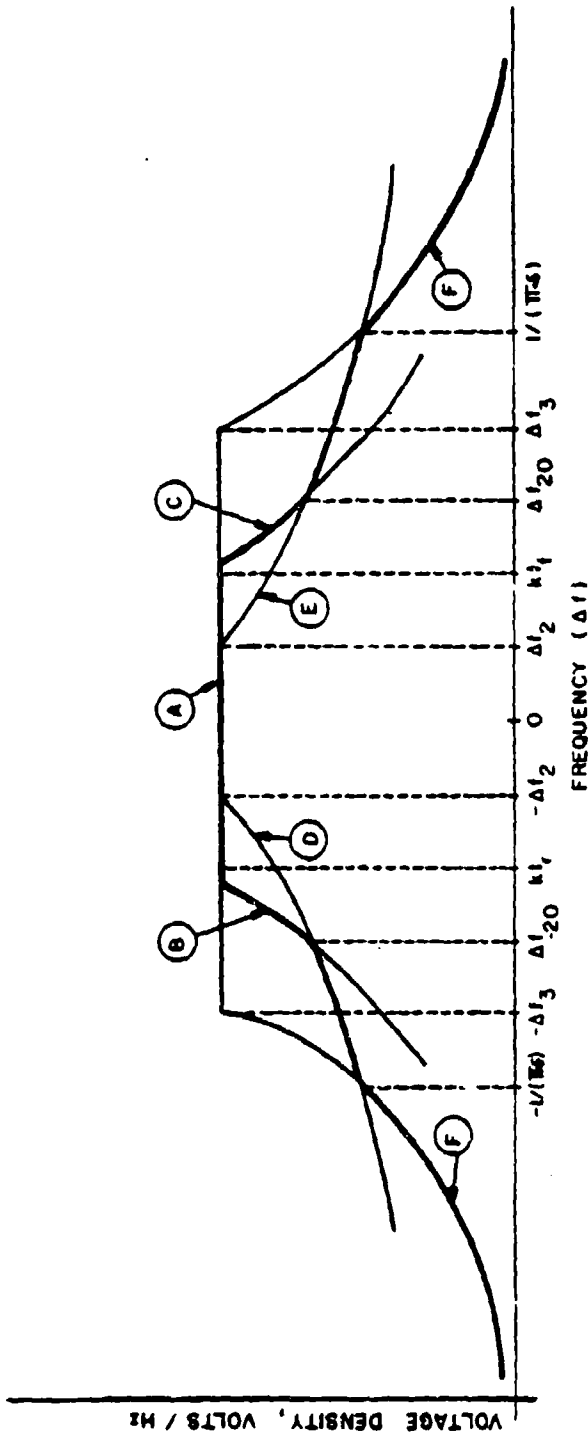
The bound on the skirts of the spectrum determined from Equation F-1 may be divided into three regions of  $\Delta f$  for convenience of graphical construction.

(1) If  $\Delta f$  is slightly more positive than  $kt_f$ , we shall refer to the bound as  $\hat{F}_C(f)$ , which is depicted by curve C in Figure F-1 and determined from Equation F-1 by:

$$\hat{F}_C \leq \frac{V}{4\pi} \frac{1}{|kt_f - \Delta f|} \quad (62)$$

If  $\Delta f$  is slightly more negative than  $kt_r$ , we shall refer to the bound as  $\hat{F}_B(f)$ , which is depicted by curve B in Figure F-1 and determined from Equation F-1 by:

$$\hat{F}_B \leq \frac{V}{4\pi} \frac{1}{|kt_r - \Delta f|} \quad (61)$$



Curve	Equation No.	Critical Freq.	Equation No.
A	51	$\Delta f_2$	66
B	61	$\Delta f_3$	67
C	62	$\Delta f_{-20}$	68
D	63	$\Delta f_{+20}$	69
E	64		
F	65		

Figure F-1. The curves that approximate the bounds on the voltage-density spectrum,  $\hat{F}(\Delta f)$ , when  $\beta < \frac{1}{10}$ .

(2) Because  $\left| \frac{\sin X}{X} \right| \leq 1$ , another bound on the spectrum is given by:

$$|F(\Delta f)| \leq \frac{V}{4\pi} \left\{ \left| \frac{1}{(kt_f - \Delta f)} \right| + \left| \frac{1}{(kt_f + \Delta f)} \right| \right\} \quad (F-2)$$

If  $\Delta f$  is considered to be sufficiently greater than  $kt_f$ , then the bound can be estimated from Equation F-2 by:

$$\hat{F}_E(\Delta f) \leq \frac{V}{2\pi\Delta f} \quad (64)$$

where  $\hat{F}_E(\Delta f)$  is depicted as curve E in Figure F-1.

The range of  $\Delta f$  where:

$$\hat{F}_E(\Delta f) \geq \hat{F}_C(\Delta f)$$

is approximately determined by noting that in this range:

$$\frac{V}{2\pi\Delta f} \geq \frac{V}{4\pi} \frac{1}{(\Delta f - kt_f)}$$

$$\text{or } \Delta f \geq 2 kt_f = \beta$$

Thus, when  $\Delta f \geq 2kt_f = \beta$ ,  $\hat{F}_E(\Delta f) \geq \hat{F}_C(\Delta f)$  and Equation 64 should be used as the bound.

If  $\Delta f$  is considered to be sufficiently less than  $kt_f$ , then the bound can be

If  $\Delta f$  is considered to be sufficiently less than  $kt_r$ , then the bound can be estimated from Equation F-2 by:

$$\hat{P}_D(f) \leq - \frac{V}{2\pi\Delta f} \quad (63)$$

where  $\hat{P}_D(\Delta f)$  is depicted as curve D in Figure F-1.

The range of  $\Delta f$  where:

$$\hat{P}_D(\Delta f) \geq \hat{P}_B(\Delta f)$$

is approximately determined by noting that in this range:

$$\frac{V}{2\pi\Delta f} \leq \frac{V}{4\pi} \frac{1}{(\Delta f - kt_r)}$$

or

$$\Delta f \leq 2 kt_r = \beta$$

Thus, when  $\Delta f \leq 2kt_r = \beta$ ,  $\hat{P}_D(\Delta f) \geq \hat{P}_B(\Delta f)$  and Equation 63 should be used as the bound.

(3) When  $\left| \frac{\sin X}{X} \right| \leq \frac{1}{|X|}$ , a bound on the spectrum is given by:

$$|F(\Delta f)| \leq \frac{V}{4\pi^2} \left\{ \frac{1}{\delta_r(kt_r - \Delta f)^2} + \frac{1}{\delta_f(kt_f - \Delta f)^2} \right\} \quad (F-3)$$

for a certain range of  $\Delta f$ .

If  $\Delta f$  is sufficiently greater than  $2kt_f$ , then the bound determined from Equation F-3 will be:

$$\hat{F}_F(\Delta f) = \frac{V}{2\pi^2 \delta \Delta f^2} \quad (65)$$

where  $\hat{F}_F(\Delta f)$  is depicted as curve F in Figure F-1. For this  $\Delta f$ , the inequality:

$$\hat{F}_F(\Delta f) \leq \hat{F}_E(\Delta f)$$

will be satisfied, and the lower bound on  $\Delta f$ , for this condition, is determined by noting that:

$$\frac{V}{2\pi^2 \delta \Delta f^2} \leq \frac{V}{2\pi \Delta f}$$

or

$$|\Delta f| \geq \frac{1}{\pi \delta}$$

Thus when  $\beta < \frac{1}{\pi \delta}$ :

$$\hat{F}_B(\Delta f) \text{ is the bound on the spectrum for } kt_r > \Delta f > 2 kt_r \quad (61)$$

$$\hat{F}_C(\Delta f) \text{ is the bound on the spectrum for } kt_f < \Delta f < 2 kt_f \quad (62)$$

$$\hat{F}_D(\Delta f) \text{ is the bound on the spectrum for } 2 kt_r > \Delta f > -\frac{1}{\pi \delta} \quad (63)$$

$$\hat{F}_E(\Delta f) \text{ is the bound on the spectrum for } 2 kt_f < f < \frac{1}{\pi \delta} \quad (64)$$

$$\hat{F}_F(\Delta f) \text{ is the bound on the spectrum for } |\Delta f| > \frac{1}{\pi\delta}. \quad (65)$$

These bounds are depicted in Figure F-1. The frequencies at which these bounding curves intersect are defined as critical frequencies. The critical frequencies are determined by solving simultaneously the equations that represent the corresponding bounding curves. Thus to obtain  $\Delta f_2$ , solve Equations 51 and 64, simultaneously, and obtain:

$$\Delta f_2 = \frac{1}{\pi} \sqrt{\frac{\beta}{\tau_b}} \quad (66)$$

In a similar manner, the critical frequencies  $\Delta f_3$ ,  $\Delta f_{-20}$ , and  $\Delta f_{+20}$  are found to be expressed by:

$$\Delta f_3 = \frac{1}{\pi} \left(\frac{\beta}{\tau_b}\right)^{1/4} \left(\frac{1}{\delta}\right)^{1/2} \quad (69)$$

$$\Delta f_{-20} = 2k\tau_r \quad (67)$$

and

$$\Delta f_{+20} = 2k\tau_f \quad (68)$$

## APPENDIX G

BOUNDS ON SKIRTS OF SPECTRUM WHEN  $\beta > \frac{1}{\pi\delta}$ 

(Equations in this appendix that have already appeared in the body of the report will be identified by their original numbers.)

By referring to Figure F-1, we observe that the point of intersection of curves F and E occurs at  $\Delta f = \frac{1}{\pi\delta}$ . In APPENDIX F, the inequalities:

$$kt_f < 2 kt_f < \frac{1}{\pi\delta}$$

were obtained for the condition that the leading and trailing edges of the chirp pulse were "steep." Under these conditions:

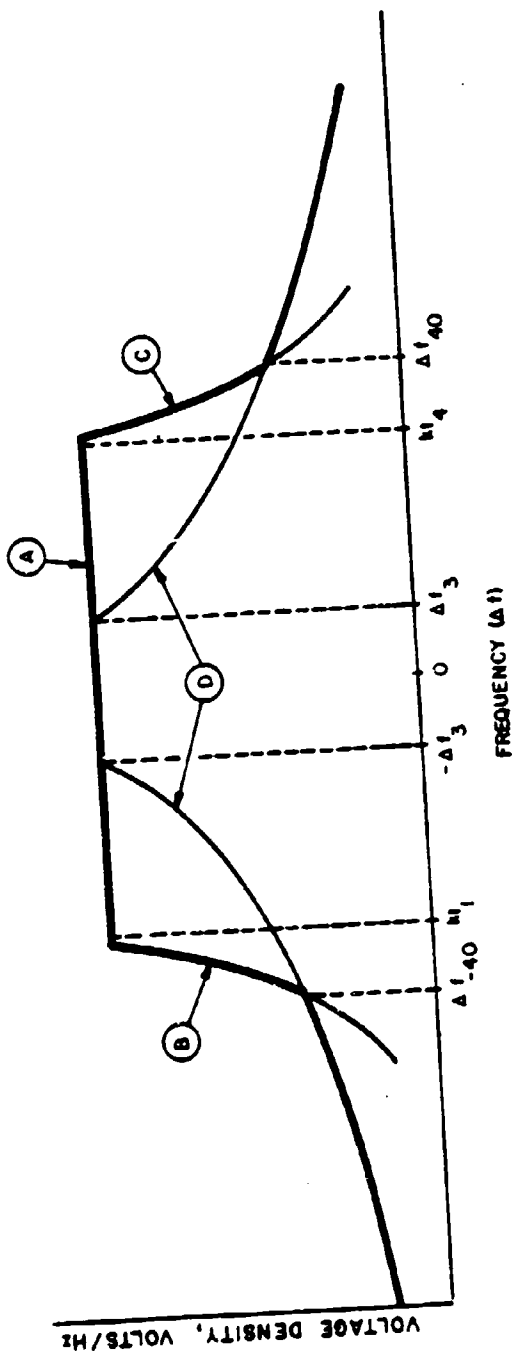
$$kt_f = \frac{\beta}{\tau_b} \frac{(t_3 + t_4)}{2} = \frac{\beta}{2}$$

which means that

$$\beta < \frac{1}{\pi\delta}$$

and is depicted in Figure F-1.

One method of visualizing a necessary change in Figure F-1 when considering the condition  $\beta > \frac{1}{\pi\delta}$  is to assume that the point of intersection of curves F and E shifts to the left due to an increase in the value of  $\delta$  until  $\frac{1}{\pi\delta} < \beta$ , while curve E is maintained as fixed. With the removal of the restriction on the pulse edges being "steep," Equation 58 may be used to determine the bounds of the spectrum for the condition  $\frac{1}{\pi\delta} < \beta$ , which are depicted in Figure G-1 and obtained in the following presentation.



Curve	Equation No.	Critical Freq.	Equation No.
A	51	$\Delta f_3$	75
B	72	$\Delta f_{-40}$	76
C	73	$\Delta f_{+40}$	77
D	74		

Appendix G

Figure G-1. The curves that approximate the bounds on the voltage-density spectrum,  $F(\Delta f)$ , when  $\beta > 1/\pi\delta$ .

From Equation 58 we have:

$$F(\Delta f) = -\frac{V}{8\pi^2} \sum_{i=1}^4 \frac{1}{\delta_i} \frac{e^{j2\pi t \left( \frac{kt_i}{2} - \Delta f \right)}}{(kt_i - \Delta f)^2}$$

The bounds on  $F(\Delta f)$  are expressed as:

$$\begin{aligned} \hat{F}(\Delta f) = \frac{V}{8\pi^2} & \left\{ \frac{1}{\delta_r} \left| \frac{1}{(kt_1 - \Delta f)^2} + \frac{1}{(kt_2 - \Delta f)^2} \right| \right. \\ & \left. + \frac{i}{\delta_f} \left| \frac{1}{(kt_3 - \Delta f)^2} + \frac{1}{(kt_4 - \Delta f)^2} \right| \right\} \end{aligned} \quad (71)$$

When  $\Delta f$  is slightly more negative than  $kt_1$ , the bound becomes curve B and is expressed by:

$$\hat{F}_B(\Delta f) = \frac{V}{8\pi^2} \frac{1}{\delta_r} \frac{1}{(kt_1 - \Delta f)^2} \quad (72)$$

When  $\Delta f$  is slightly more positive than  $kt_4$ , the bound becomes curve C and is expressed by:

$$\hat{F}_C(\Delta f) = \frac{V}{8\pi^2} \frac{1}{\delta_f} \frac{1}{(kt_4 - \Delta f)^2} \quad (73)$$

When  $\Delta f \ll kt_1$  or  $\Delta f \gg kt_4$ , the bound becomes curve D and is expressed by:

$$\hat{F}_D(\Delta f) = \frac{V}{4\pi^2 \Delta f^2} \left( \frac{1}{\delta_r} + \frac{1}{\delta_f} \right) = \frac{V}{2\pi^2 \Delta f^2 \delta} \quad (74)$$

For sufficiently large  $|\Delta f|$  where  $\Delta f \ll kt_1$ , the range of  $\Delta f$  such that:

$$\hat{F}_D(\Delta f) > \hat{F}_B(\Delta f)$$

is determined by setting:

$$\frac{V}{2\pi^2 \Delta f^2 \delta} > \frac{V}{8\pi^2 \delta_r (kt_1 - \Delta f)^2}$$

Then:

$$\pm \frac{1}{2} \Delta f \sqrt{\frac{\delta}{\delta_r}} < kt_1 - \Delta f$$

or

$$\Delta f \left(1 \pm \frac{1}{2} \sqrt{\frac{\delta}{\delta_r}}\right) < kt_1$$

Since  $t_1 < 0$  and  $\Delta f < 0$ , then  $1 \pm \frac{1}{2} \sqrt{\frac{\delta}{\delta_r}}$  should be small but positive.

That is:

$$\Delta f \left(1 - \frac{1}{2} \sqrt{\frac{\delta}{\delta_r}}\right) < kt_1$$

Then:

$$\Delta f < \frac{kt}{1 - \frac{1}{2} \sqrt{\frac{\delta}{\delta_r}}} = - \frac{\beta \delta_r}{\delta_r + \delta_f} \cdot \frac{1}{1 - \sqrt{\frac{\delta_f}{2(\delta_r + \delta_f)}}}$$

and

$$\Delta f < \Delta f_{-40} = -\frac{\beta \delta_r}{\delta_r + \delta_f} \cdot \frac{1}{1 - \sqrt{\frac{\delta_f}{2(\delta_r + \delta_f)}}} \quad (76)$$

Thus, for  $\Delta f < \Delta f_{-40}$ :

$$\hat{F}_D(\Delta f) > \hat{F}_B(\Delta f)$$

In a similar manner, the range of  $\Delta f$  may be determined for  $\Delta f \gg kt_4$ , such that:

$$\hat{F}_D(\Delta f) > \hat{F}_C(\Delta f)$$

by setting

$$\frac{v}{2\pi^2 \Delta f^2 \delta} > \frac{v}{8\pi^2 \delta_f (kt_4 - \Delta f)^2}$$

Then:

$$\pm \frac{1}{2} \Delta f \sqrt{\frac{\delta}{\delta_f}} < kt_4 - \Delta f$$

Since  $\Delta f \gg kt_4 > 0$ , the left side of the inequality cannot be negative, as that would bound the magnitude of  $\Delta f$  from above. Thus,  $-(kt_4 - \Delta f) > 0$  and:

$$\frac{1}{2} \Delta f \sqrt{\frac{\delta}{\delta_f}} < -(kt_4 - \Delta f) = -kt_4 + \Delta f$$

or

$$kt_4 < \Delta f \left(1 - \frac{1}{2} \sqrt{\frac{\delta}{\delta f}}\right)$$

$$\Delta f > \frac{kt_4}{1 - \frac{1}{2} \sqrt{\frac{\delta}{\delta f}}} = \frac{\beta \delta_f}{\delta_r + \delta_f} \cdot \frac{1}{1 - \sqrt{\frac{\delta_r}{2(\delta_r + \delta_f)}}}$$

and

$$\Delta f > \Delta f_{40} = \frac{\beta \delta_f}{\delta_r + \delta_f} \cdot \frac{1}{1 - \sqrt{\frac{\delta_r}{2(\delta_r + \delta_f)}}} \quad (77)$$

Thus, for  $\Delta f > \Delta f_{40}$ :

$$\hat{F}_D(\Delta f) > \hat{F}_C(\Delta f)$$

Thus, when  $\beta > \frac{1}{\pi \delta}$ :

$$\hat{F}_B(\Delta f) \text{ is the bound on the spectrum for } kt_1 > \Delta f > \Delta f_{-40} \quad (72)$$

$$\hat{F}_C(\Delta f) \text{ is the bound on the spectrum for } kt_4 < \Delta f < \Delta f_{40} \quad (73)$$

$$\hat{F}_D(\Delta f) \text{ is the bound on the spectrum for } \Delta f > \Delta f_{40} \quad (74)$$

$$\hat{F}_D(\Delta f) \text{ is the bound on the spectrum for } \Delta f < \Delta f_{-40} \quad (74)$$

These bounds are depicted in Figure G-1.

The intersection of curves determined by Equations 51 and 74 is denoted as the critical frequency,  $\Delta f_3$ , and is given by:

$$\Delta f_3 = \frac{1}{\pi} \left( \frac{\beta}{\tau_b} \right)^{1/4} \left( \frac{1}{\delta} \right)^{1/2} \quad (75)$$

Likewise, the critical frequencies  $\Delta f_{-40}$  and  $\Delta f_{+40}$  are given by Equations 76 and 77, respectively, and are depicted in Figure G-1.

## APPENDIX H

## CHOOSING A LOCATION FOR THE ORIGIN ON THE TIME SCALE

(Equations in this appendix that have already appeared in the body of the report will be identified by their original numbers.)

Equation 74 is used as an approximation of Equation 71 when  $|\Delta f|$  is large, compared to  $kt_1$  or  $kt_4$ . The error in the approximation depends upon the location of the origin.

When the pulse shape is symmetrical ( $\delta_r = \delta_f$ ), the approximation is best when the origin is located midway between  $t_1$  and  $t_4$ . When the pulse shape is asymmetrical,  $\delta_r \ll \delta_f$  for example, the terms containing  $\delta_r$  in Equation 71 have more influence on  $F(\Delta f)$  than the terms containing  $\delta_f$ ; for this case the approximation given in Equation 74 is better when the origin is located closer to  $t_1$  than to  $t_4$ . On the other hand when  $\delta_r \gg \delta_f$ , the approximation is better when the origin is located closer to  $t_4$ . Thus, the origin should be located closer to the steeper edge of the pulse.

Although an optimum method for locating the origin on the time scale was not found, the approximation given by Equation 74 appears to be best when the origin is located such that:

$$t_1 = \frac{-\delta_r \tau_b}{\delta_r + \delta_f} \quad (19)$$

$$t_2 = \frac{-\delta_r \tau_b}{\delta_r + \delta_f} + \delta_r \quad (20)$$

$$t_3 = \frac{\delta_f \tau_b}{\delta_r + \delta_f} - \delta_f \quad (21)$$

$$t_4 = \frac{\delta_f \tau_b}{\delta_r + \delta_f} \quad (22)$$

$$t_r = \frac{t_1 + t_2}{2} = \frac{-\delta_r \tau_b}{\delta_r + \delta_f} + \frac{\delta_r}{2} \quad (23)$$

$$t_f = \frac{t_3 + t_4}{2} = \frac{\delta_f \tau_b}{\delta_r + \delta_f} - \frac{\delta_f}{2} \quad (24)$$

These relations are obtained from Figure H-1 by noting that:

$$\frac{v'}{-t_1} = \frac{v}{\delta_r} \quad \frac{v'}{t_4} = \frac{v}{\delta_f}$$

$$v' = \frac{-t_1 v}{\delta_r} = \frac{t_4 v}{\delta_f} \quad t_1 \delta_f = -t_4 \delta_r$$

$$t_1 \delta_r + t_1 \delta_f = t_1 \delta_r - t_4 \delta_r$$

$$t_1 (\delta_r + \delta_f) = -(t_4 - t_1) \delta_r = -\tau_b \delta_r$$

$$t_1 = -\frac{\tau_b \delta_r}{\delta_r + \delta_f} \quad (19)$$

$$t_2 = t_1 + \delta_r \quad (20)$$

$$t_3 = t_4 - \delta_f \quad (21)$$

$$t_4 = -t_1 \frac{\delta_f}{\delta_r} = \frac{\tau_b \delta_f}{\delta_r + \delta_f} \quad (22)$$

$$t_r = \frac{t_1 + t_2}{2} = t_1 + \frac{\delta_r}{2} \quad (23)$$

$$t_f = \frac{t_3 + t_4}{2} = t_4 - \frac{\delta_f}{2} \quad (24)$$

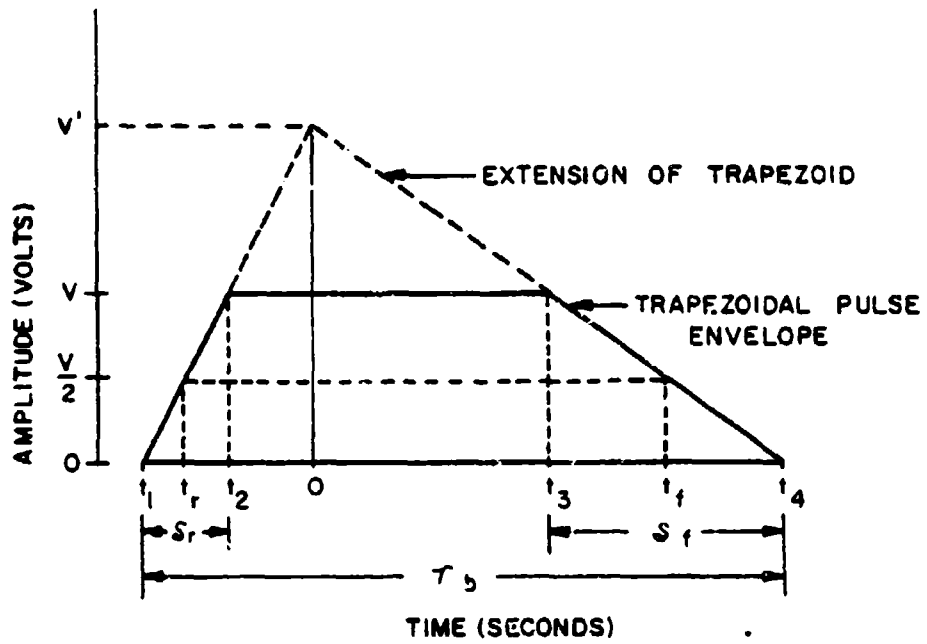


Figure H-1. Geometry associated with location of the origin.

APPENDIX I  
DISPLACEMENT BETWEEN  $f_o$  AND  $f_c$

As shown in Figure 12,  $f_o$  is the instantaneous frequency at  $t = 0$ , and  $f_c$  is the instantaneous frequency at the center of the pulse. The bounds on the skirts of the spectrum are symmetrical about  $f_o$ , whereas the peak of the spectrum tends to be centered about  $f_c$  (see Figure 4). As explained in Section 3,  $f_o$  and  $f_c$  are displaced when the pulse shape is asymmetrical. Using the relationships shown in Figure 12 the displacement is determined to be:

$$f_c - f_o = k(\tau_b/2 + t_1) \quad (\text{I-1})$$

Using Equation 19 to express  $t_1$ , we can rewrite Equation I-1 as:

$$f_c - f_o = \frac{\beta}{\tau_b} \left[ \frac{\tau_b}{2} - \frac{\delta_r \tau_b}{\delta_r + \delta_f} \right] \quad (\text{I-2})$$

$$f_o = f_c + \frac{\beta}{2} \left[ \frac{\delta_r - \delta_f}{\delta_r + \delta_f} \right] \quad (\text{I-3})$$

From this we get Equations 88 and 89.

DISTRIBUTION LIST FOR  
A SIMPLIFIED METHOD FOR CALCULATING THE BOUNDS ON THE  
EMISSION SPECTRA OF CHIRP RADARS (REVISED EDITION)  
ESD-TR-81-100

<u>External</u>	<u>No. of copies</u>
CDR, USACECOM ATTN: DRSEL-COM-RY-3 FORT MONMOUTH NJ 07703	1
USAAMSA ATTN: E BARTHEL ABERDEEN PROVING GROUND MD 21005	1
CDR, USACECOM ATTN: DRSEL-SEI-A (S SEGNEK) FORT MONMOUTH NJ 07703	1
HQDA DAMO-C4Z-S (PAUL PHILLIPS) WASHINGTON DC 20310	1
CDR USARRADCOM ATTN: DRCPM-ADG-E (CHRISTENSON) PICATINNY ARSENAL DOVER NJ 07801	1
COMMANDER US ARMY FORCES COMMAND ATTN: AFCE (F HOLDERNESS) FORT MCPHERSON GA 30330	1
CDR, USATECOM ATTN: DRSTE-EL (MAJ ANGEL) ABERDEEN PROVING GROUND MD 21005	1
USACC CH, C-E SERVICES DIVISION ATTN: CC-OPS-CE-P ALEXANDRIA VA 22333	1
CHIEF OF NAVAL OPERATIONS (OP-941F) NAVY DEPARTMENT WASHINGTON DC 20350	1
DIRECTOR NAVAL ELECTROMAGNETIC SPECTRUM CENTER 4401 MASSACHUSETTS AVL NW WASHINGTON DC 20390	1

DISTRIBUTION LIST FOR PSD-TR-81-100 (Continued)

<u>External</u>	<u>No. of copies</u>
DIRECTOR NATIONAL SECURITY AGENCY ATTN: W36/MR. V. MCCONNELL FT. GEORGE G. MEADE MD 20755	1
FEDERAL AVIATION ADMINISTRATION FOB 10A/RM 736D ATTN: ARD-450 800 INDEPENDENCE AVE SW WASHINGTON DC 20591	1
NATIONAL AERONAUTICS & SPACE ADMINISTRATION GODDARD SPACE FLIGHT CENTER ATTN: CODE 801/JIM SCOTT GREENBELT MD 20771	1
NATIONAL TELECOMMUNICATIONS & INFORMATION ADMINISTRATION ATTN: STAN COHN 1325 G. ST., N.W. WASHINGTON DC 20005	1
COMMANDING OFFICER NAVAL RESEARCH LABORATORY WASHINGTON DC 20375	1
COMMANDER NAVAL OCEAN SYSTEMS CENTER SAN DIEGO, CA 92152	1
JEWC/TAE SAN ANTONIO, TX 78243	1
FTD/TQE ATTN: J. WISE WRIGHT-PATTERSON AFB, OH 45433	1
NATIONAL TELECOMMUNICATIONS & INFORMATION ADMINISTRATION ATTN: MR. ROBERT MAYHER 179 ADMIRAL COCHRANE DRIVE ANNAPOLIS, MD 21401	35

DISTRIBUTION LIST FOR ESD-TR-81-100 (Continued)

Internal

No. of copies

CCN/J. Atkinson  
XM/J. Janoski  
CA  
CF  
CJ  
CN  
DRD/P. Newhouse  
DRD/A. Fitch  
DQT/R. Whiteman  
DIL  
DIL

2  
1  
2  
1  
1  
5  
1  
1  
10  
Camera-Ready